Dissertation

Molecular analysis of oral biofilm

submitted by

Mag.rer.nat. Barbara **Schinagl** (formerly **Klug**), Bakk.biol.

for the Academic Degree of

Doctor of Medical Science

(Dr. scient. med.)

at the

Department of Dentistry and Maxillofacial Surgery

Medical University of Graz

under the supervision of

Sen.-Scientist Mag.phil. Dr.med.univ. Dr.med.dent. Elisabeth Santigli
Univ.-Ass. Priv.-Doz. Dr.med.univ. Gernot Wimmer
Univ.-Prof. Mag. Dr.rer.nat. Martin Grube

Graz, 2019

For my family

thank you!

Declaration

I hereby declare that this thesis is my own original work and that I have fully acknowledged by name all of those individuals and organisations that have contributed to the research for this thesis. Due acknowledgement has been made in the text to all other material used.

Throughout this thesis and in all related publications I followed the "Standards of Good Scientific Practice and Ombuds Committee at the Medical University of Graz ".

Graz, October 2019

Acknowledgment

First, I would like to thank my supervisors, Gernot Wimmer and Martin Grube for the possibility to write this thesis and their expertise and especially Elisabeth Santigli whose consistent support made this work possible.

This thesis was financially supported the Land Steiermark initiative “Human technology interface”, Projektnummer: A3-22.H-2/2011-42, Projekt: „Interface Mundraum: Analyse und in vitro Simulation oraler Bakteriengemeinschaften auf natürlichen und künstlichen Materialien – OraSim“. The 454-Pyrosequencing was done at the Center for Medical Research, Medical University of Graz. Persons I would like to thank are: Michael Bozic from the Diagnostic & Research Institute of Hygiene, Microbiology and Environmental Medicine, Medical University of Graz who performed the DNA extractions. Slave Trajanoski from the Center for Medical Research helped with problems during the data exploration in QIIME. Katharina Eberhard from the Center for Medical Research, Medical University of Graz did the statistical analysis for the comparison on different taxonomic levels. Dr. Christian Westendorf, University of Graz (Current address: MPI for Dynamics and Self-Organization, Göttingen) wrote the Matlab script for the interpretation of the bacterial survival data and helped with the data interpretation. Dr. Stefan Tangl (Medical University of Graz) and his team prepared the standardized dentin-enamel slabs. My colleagues at the Institute of Botany, University of Graz, Theodora Gößler, Lucia Muggia, Philipp Resl and Christian Westendorf for the technical support, the inspiring discussions and their friendship.

1. Table of Contents

Abbreviations and Definitions

PFA	Paraformaldehyde
PBS	Phosphate buffered saline
CLSM	Confocal laser scanning microscopy
FISH	Fluorescence *in situ* hybridization
NGS	Next generation sequencing
BHI	Brain heart infusion
OTU	Operational taxonomic unit
AEP	Acquired enamel pellicle
ITS	Internal transcribed spacer
CPR	Candidate phyla radiation
HMP	Human microbiome project
PI	Propidium Iodide
PCoA	Principal coordinate analysis
MSA	Multiple sequence alignment
RDP	Ribosomal Database Project
PTFE	Polytetrafluorethylen
DTT	Dithiothreitol
SSCP	Single Strand Conformation Polymorphism
DGGE	Denaturing Gradient Gel Electrophoresis
PCA	Principal component analysis
CA	Correspondence analysis
SSCP	Single strand conformation polymorphism
DGGE	Denaturing gradient gel electrophoresis

List of Figures

List of Tables

Abstract

Aim: The aim of this study was to create a combined *in vivo – in vitro* biofilm model system. We hypothesized that with our set-up, oral bacterial biofilms can be grown under defined *in vivo* conditions, that these biofilms can be transferred into an *in vitro* test system and kept alive in its natural composition for 48 hours.

Such, different materials as well as microbiological and molecular methods were adapted in order to analyze native oral biofilms on the one hand and be able to handle this biofilm for research applications without distortion on the other hand.

Materials und Methods: First, a FISH and CLSM method was developed enabling the analysis of oral microbiota grown on orthodontic appliances. Secondly, an *in vivo - in vitro* biofilm model was set up and tested. Therefore, a dental splint for research containing six standardized human enamel-dentin slabs as a surface to grow native oral biofilm on intraorally for 48 hours was developed. These slabs could then be clipped out and transferred into an *in vitro* test-system. Microbiota survival and compositional changes over time were then tested in a biofilm reactor using 454-pyrosequencing and exploring the data with QIIME and R. Live/dead staining and CLSM were used to monitor bacterial survival *in vitro* and stack data evaluated with a self-written Matlab®-script and Python. FISH was used for the visualization of bacteria down to genus level. In parallel two temperature loggers were embedded in these research splints and oral temperatures monitored over 48 hours in the oral cavity.

Results: FISH and CLSM can be used to analyze native oral biofilm grown on orthodontic appliances. A strong dominance of Firmicutes was found as well as the periodontopathogen *Porphyromonas gingivalis*. In the *in vitro – in vivo* biofilm model microbiota stayed alive and in a stable composition on phylum level over 48 hours *in vitro*. Firmicutes (*Streptococcus* and *Veillonella)* dominated making up almost 90% of the microbiota. On genus level significantly higher numbers of *Rothia, Prevotella, Granulicatella* and *Haemophilus* were found after 48 hours. The live/dead ratio approximated initial values after 48 hours *in vitro*.

Discussion: The newly developed *in vivo – in vitro* biofilm model allows for native oral biofilm growth intraorally, its transfer to *in vitro* settings and monitoring its survival over 48 hours. The research splint developed extends conventional splints through the incorporation of temperature loggers.

Zusammenfassung

Ziel: Das Ziel dieser Arbeit war es ein *in vivo* und *in vitro* kombinierendes Biofilm Model System zu etablieren. Die Hypothese hierzu war, dass das neue Setup eine intraorale – *in vivo* - Biofilmanzucht erlaubt, dieser dann in ein *in vitro* System transferiert und in seiner nativen Zusammensetzung für 48h am Leben erhalten werden kann. Hierfür wurden verschiedene Materialen wie auch mikrobiologische und molekulare Methoden adaptiert.

Material und Methode: Als erstes wurde hierfür eine FISH und CLSM Methode entwickelt, die es erlaubte Biofilm, der auf Zahnspangen gewachsen war, zu analysieren. Zweitens wurde eine kombiniertes *in vivo – in vitro* Testsystem entwickelt. Mit diesem kann Biofilm auf humanen Enamel-Dentin-Plättchen, die in speziell entwickelten Analysezahnspangen eingebettet waren, in 48h intraoral gezüchtet werden um dann in einen Biofilmreaktor transferiert und dort unter *in vitro* Bedingungen kultiviert zu werden. Die bakterielle Zusammensetzung wurde mittels 454-Pyrosequenzierung analysiert, das Überleben der Bakterien mittels Lebend-Tot-Färbung und CLSM. Die Datenanalyse wurde mit QIIME und R gemacht. Die Überlebensraten wurden aus den 2D Stack-Daten der CLSM mit einem im Haus geschriebenen Matlab®-Skript und Python errechnet. FISH wurde für die Visualisierung einzelner Phyla, aber auch Genera verwendet. In die Zahnspangen wurden auch zwei Temperaturlogger eingebaut, die die intraoralen Temperatur-schwankungen in den 48h aufzeichneten.

Resultate: FISH und CLSM können für die Analyse von Biofilm auf Zahnspangen verwendet werden. Firmicutes dominierten diesen, aber auch Parodontopathogene Stämme wie *Porphyromonas gingivalis* wurden gefunden. Im *in vivo – in vitro* Biofilm model können Mikrobiota für 48h stabil in ihrer Zusammensetzung und am Leben erhalten werden. Firmicutes (*Streptococcus* und *Veillonella)* dominierten mit fast 90% den Biofilm. Auf Genuslevel stiegen *Rothia-, Prevotella-, Granulicatella-* und *Haemophilus-* Zahlen signifikant nach 48h. Die Überlebensrate pendelte sich im Ausgangslevel ein nach den 48h.

Diskussion: Das neue *in vivo – in vitro* Biofilmmodel erlaub intraorale Anzucht von nativem oralem Biofilm, dessen Transfer in ein *in vitro* Testsystem und ein Beobachten seiner Überlebensrate. Die hier entwickelte Analysezahnspange ist eine Erweiterung zu herkömmlichen Spangen, da sie auch zwei Temperaturlogger enthält.

1. Introduction

1.1. The oral microbiome

1.1.1. Inhabitants of the oral cavity

More than 700 bacterial species are so far known to inhabit a single oral cavity (Aas et al. 2005). Estimations on the overall diversity meanwhile exceed the number of several thousand species making them our inhabitants with the biggest diversity (Gomez and Nelson 2016). In the mouth, different soft and hard tissues (like teeth, mucosa or the tongue) offer surfaces for bacteria to colonize on. Saliva inhabits a broad range of bacteria. Even artificial materials as dental splints or implants are habitats. They all have in common that the bacteria there live in biofilms. First believing that bacteria float around as single cells, researchers very quickly found out, that the biofilm lifestyle seems to be the “normal” condition (Watnick and Kolter 2000; Costerton et al. 1999; Costerton et al. 1978).

This work mainly focuses on the exploration of the diversity and the spatial arrangement of oral bacterial biofilms (*in vivo*) as well as their survival under laboratory conditions and in artificial environments (*in vitro*). However, to complete the picture of oral microorganism latest knowledge on the lifestyles and influences of the non-bacterial microbes and their interactions are shortly summarized in the following.

Many researchers have investigated life in the oral cavity since Antonie van Leeuwenhoek first described the Animalcules in the dental plaque in 1683 (Gest 2004). We now know that the oral microbiome comprises a huge variety of organisms. This complex ecosystem inhabits not only bacteria and the candidate phyla radiation (CPR) group of ultrasmall bacteria but also fungi, archaea, viruses, phages, micro-eukaryotes (Hug et al. 2016; Baker et al. 2017).

Oral fungi, for example, have been neglected as important players in the oral microbiome for a long time. Ghannoum et al. found over 74 culturable and 11 non-culturable fungal genera already in 2010 in healthy subjects (Ghannoum et al. 2010). They identified them using the internal transcribed spacer region (ITS) - a region lying between the small-subunit ribosomal RNA and the large-subunit rRNA genes - for pyrosequencing. Candida there were shown to be the most frequent species followed by *Cladosporium*, *Aureobasidium*, *Saccharomycetales*, *Aspergillus*, *Fusarium* and *Cryptococcus*. Some of them are also known to be pathogens in humans (Dupuy et al.

2014). pyrosequenced saliva from healthy volunteers also using ITS1 in 2014. They extended the list of genera found by Ghannoum adding *Mallassezia*, *Lenzites*/*Trametes*, *Irpex*, *Cytospora*/*Valsa*, and *Sporobolomyces*/ *Sporidiobolus* (Dupuy et al. 2014). Most of them had been described as soil and/or plant pathogens before. The last three had also been identified as causative agents in infections in immunocompromised persons. Most genera found in these two studies have also been identified via cultivation studies as reviewed by Diaz et al. (Diaz et al. 2016). The ones found common to all studies were *Alternaria*, *Aspergillus*, *Aureobasidium*, *Candica*, *Cladosporium*, *Cryptococcus*, *Fusarium*, *Penicillium*, *Saccharomyces* and *Trichosporon*. Krom et al. reviewed fungal and bacterial interactions in the oral microbiome. They state that fungi and bacteria interact physically over co-adhesion and repulsion (exclusion) and chemically including metabolic dependencies, quorum sensing and the production of antimicrobial agents (Krom et al. 2014).

Another big but understudied player in the oral microbiome are viruses and phages. Ly et al. compared samples of healthy subjects to those with periodontal disease in different oral sites (Ly et al. 2014). They found *Siphoviridae* as the most abundant in healthy subjects. *Podoviruses* were equally distributed while the relative abundance of *Myoviruses* considerably varied by site and disease state. The later were found significantly more abundant in saliva from healthy subjects. Still, *Siphoviruses* exhibited the highest relative abundance in both healthy and diseased. *Myoviruses* however were significantly more abundant in subgingival plaque of periodontally diseased subjects. Generally, completely novel viral sequences encoding proteins with no known homology challenge the researchers. Annotations and further analysis thus are extremely arduous (Bikel et al. 2015).

The “Candidate Phyla Radiation” (CPRs) have only recently been found as a new branch in the tree of life (Hug et al. 2016). So far it is assumed that the more than 35 phyla found in this group are obligate symbionts. Their ultra-small cell size and presence of several characteristics of bacteria and archaea make them an interesting research object. Challenging cultivation makes it difficult to find out more about their lifestyle. The HMP showed that *Gracilibacteria* (GN02), *Absconditabacteria* (SR1) and *Saccharibacteria* (TM7), three phyla of the CPR were also found in different body sites including the oral cavity (Segata et al. 2012; Zhou et al. 2013). For a simplification in

the following “oral biofilm” will stand for the bacterial fraction of the oral microbial community.

1.1.2. Microbial biofilm formation

Generally, bacteria in a biofilm live together in multispecies associations in a so-called matrix. Biofilm formation occurs everywhere in the mouth. Soft and hard tissues are equally inhabited by bacteria as is saliva. Mager et al. identified three communities that can mainly be correlated to certain regions in the mouth (Mager et al. 2003). The teeth are the first, saliva together with dorsal/lateral surfaces of the tongue the second and other epithelial surfaces are the third. Saliva though is generally not seen as having its own biofilm but further inhabiting bacteria removed from other oral tissues. Saliva is a very poor medium for bacterial growth and the time between its generation and the swallowing is too short for biofilm to really grow in it.

For dental plaque, the formation of this biofilm and the matrix are very well investigated. Neither supragingival nor subgingival surfaces shed biofilms. Thus, they present a stable location for long-term biofilm formation. The acquired enamel pellicle (AEP), being a film of different proteins, builds the docking station for bacteria on the tooth surface (Lee et al. 2013). The AEP is never completely removed with normal dental hygiene and regenerates immediately after tooth brushing. Already after five minutes first bacteria, the so-called primary colonizers, attach to this pellicle over adhesion-receptor interactions (Nobbs et al. 2011).

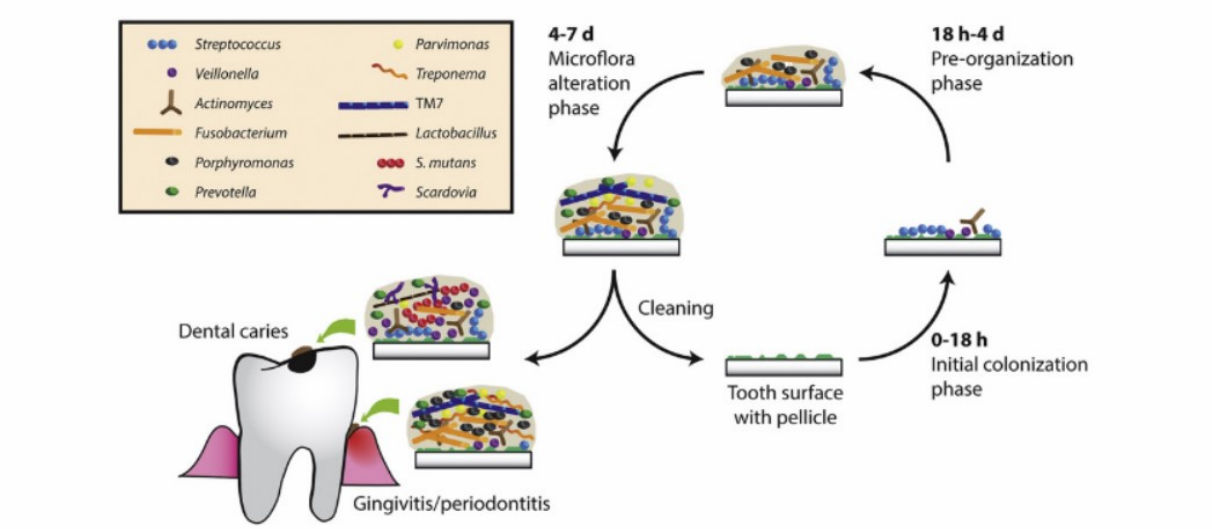

Figure 1: Biofilm formation on tooth surfaces. *Reproduced from Jakubovics N., 2015 with permission (Elsevier)*.

During this first phase of colonization primarily *Streptococcus* such as *Streptococcus mitis* and *Streptococcus oralis* are found (Diaz et al. 2006). Other genera as *Gemella*, *Neisseria*, *Veillonella* or *Actinomyces* quickly join the first bacterial layers during the first 18 hours as summarized by Jakubovics in Figure 1 and shown by several other groups (Zijnge et al. 2010; Jakubovics 2015; Segata et al. 2012). After this first phase, diversity increases and *Fusobacteria*, *Prevotella*, *Porphyromonas* and *Capnocytophaga* gain in relative abundance depending also on host factors and the human life style (diet, oral hygiene, smoking, alcohol, stress). In daily routine, tooth brushing would now perturbate the biofilm maturation and remove the plaque. If this does not happen overgrowth of acidogenic and aciduric bacteria can occur. This can further lead to gingivitis or periodontitis (Kistler et al. 2013).

1.1.3. Oral biofilm in health and disease

For over 20 years, oral biofilm investigation was mainly based on the analysis of up to 20 species found with commercially available kits (Santigli et al. 2017). Checkerboard analysis increased the number to 48 species in one run (do Nascimento et al. 2006). This widened the horizon of oral microbiome research. This development is described in detail in 1.4.2.

Around fifteen years ago, next generation sequencing technologies started coming up. These methods allowed a more detailed analyses of the microbiome given in a sample than before. With these huge data sets, also the pictures of microbiomes in health and disease changed immensely. Some bacteria that had been seen as pathogens could now be related to health as for example in the study of Griffen et al. comparing healthy subjects to periodontitis patients (Griffen et al. 2011). *Streptococcus*, *Acinetobacter*, *Haemophilus* and *Aggregatibacter* were found in high relative abundance and high numbers. Also, *Graniculatella*, *Gemella*, *Moraxella*, *Actinomyces*, *Rothia* and *Arthrobacter* were found related to health. *Prevotella*, *Treponema* and *Fusobacteria* instead were genera with high relative abundance and high numbers associated with disease. In the overall picture, Clostridia were the class highly associated with disease while Gamma- and Betaproteobacteria seem to be more associated with health. Segata et al. analyzed then samples from the Human Microbiome Project from seven mouth surfaces in a healthy cohort (Segata et al. 2012). They found three groups of bacteria in the different oral habitats. Group 1 (buccal mucosa, keratinized gingiva and

hard palate) consisting mainly of *Firmicutes*, *Proteobacteria*, *Bacteroidetes* and *Actinobacteria* or *Fusobacteria*, group 2 (saliva, tongue, tonsils and throat) inhabiting less *Firmicutes* but an increased level of *Bacteroidetes*, *Fusobacteria*, *Actinobacteria* and *TM7*, and group 3 (sub- and supra-gingival plaque) showing a decreased number of *Firmicutes* compared to group 1 and 2 and an increased relative abundance of *Actinobacteria* (Segata et al. 2012). Interestingly, clades of known oral pathogens were found in representative numbers in this disease-free cohort. Pathogens as normal inhabitants of the oral cavity were also found in a study performed in our laboratory sampling the subgingival compartment of healthy children (Santigli et al. 2017). On family level *Porphyromonadaceae*, *Prevotellaceae* and also *Staphylococaceae* were found in these children. Seeing pathogens in the normal flora of the oral cavity alters the picture of a pathogenic biofilm. Knowing that the sole presence of some pathogens does not coercively mean that the biofilm also harms the human carrier, more research on biofilm variations is needed. Most clinical studies so far investigated the effects of e.g. a new treatment on the biofilms of all subjects tested together. These studies often left out analysis of the basic microbiome compositions and changes in the single subjects. But these differences might give us further clues to health and disease states in future.

1.1.4. Inter- and intra-individual differences in the oral biofilm diversity

The data mass created with next generation sequencing methods brought up new challenges in comparing different samples and different individuals with each other. A strong need for a baseline, being a core microbiome of identical bacterial genera in all individuals and over time appeared. Quite fast it became evident that such a baseline is hard to find as the oral microbiota show a strong inter- and intra-individual diversity. Even more complicated, the microbiome composition depends on various factors like age, general health, stress, the immune system, gender and ethnicity but also oral hygiene, smoking habits or alcohol consumption lead to changes over time. Probably more factors will arise as we learn more about the oral microbial metabolom. The oral biofilm formation starts at birth and during the first years the biofilm composition changes significantly. Crielaard et al. investigated children at different developmental stages (Crielaard et al. 2011). They showed that for example the salivary microbiome has reached high complexity by the age of 3. But the microbiome composition in

adolescents is still different to the microbiome in adults. This study also revealed that the deciduous dentition varies from the other groups analyzed. In the youngest healthy group, also *Pseudomonadaceae*, *Moraxellaceae* and *Enterobacteriaceae* were found that had so far not been related to health. Regarding the individuality of the samples, this study showed that members of the same family have individual microbiome patterns but shared the same genotypes of certain bacteria.

Huse et al. compared 18 body sites of 200 subjects (Huse et al. 2012). They found that even the most abundant core OTUs highly vary across subjects. The relative abundance of the respective OTUs spans multiple orders of magnitude. Individuality of the subjects' microbiota seems to be preconditioned state looking at the richness in the oral sites of up to 11,501 OTUs (Huse et al. 2012).

These strong variations both in one individual over time and between several subjects makes it hard to find a baseline microbiome composition for health and for disease.

1.2. Artificial biofilm habitats in the oral cavity

Oral biofilms form on every surface in the oral cavity, also on artificial surfaces. Bacteria can attach to dental implants as well as orthodontic appliances (de Waal et al. 2014; Größner- Schreiber et al. 2009; Busscher et al. 2010; Apel et al. 2009; Veerachamy et al. 2014). But colonization of these new habitats may vary drastically from the original oral flora. This can lead to diseases as dental caries or periodontitis. Peri-implantitis and implant failures due to biofilm formation is a very well investigated field in dentistry (Rams et al. 2014; Sbordone and Bortolaia 2003; Größner- Schreiber et al. 2009; Buser et al. 2017; Veitz-Keenan and Keenan 2017; Howe 2017; de Waal et al. 2014). However, less is known about the influence of orthodontic appliances and the respective biofilm colonizing them.

1.2.1. Oral biofilm on orthodontic appliances

Fixed orthodontic appliances are the most common method to correct tooth displacement. Only very few studies have so far examined the changes in the oral biofilm with respect to these artificial habitats. They all found changes in the subgingival microbiome (Kim et al. 2010; Ren et al. 2014; Ireland et al. 2014; Pan et al. 2017). In addition, most studies also show, that this effect is not or not fully resolved after up to

3 months after completion of the treatment and removal of the appliance. The levels of periodontopathogens like *Porphyromonas gingivalis*, *Prevotella intermedia* or *Tannerella forsythia* were still significantly elevated three months after removal of the appliance compared to the control groups (de Freitas et al. 2014; Ren et al. 2014; Ireland et al. 2014; Pan et al. 2017). Seeing a possible health risk, we also wanted to find out what happens on palatal expanders that are regularly used in dental practices. Therefore, biofilm on these appliances was analyzed with Fluorescence *In Situ* Hybridization (FISH) and Confocal Laser Scanning Microscopy (CLSM) in this thesis.

1.3. Oral biofilm models

Two different approaches are used in biofilm research. Bottom up assays mainly investigate single species or small groups of single species set together under laboratory conditions. This reductionism was the most prominent way to study the oral microbiome as all factors in the system can easily be controlled. A second way of studying oral biofilm is to make a top down assay. These assays aim in snapshotting the whole picture of the native biofilm. This allows analysis of biofilm composition over time, spatial arrangement and interactions but also metabolic states of bacterial groups.

For both approaches, different test systems were and are in use that can mainly be grouped in "*in vivo*", "*in vitro*" models and a combination of both.

1.3.1. *In vitro* models

In vitro cultivation of bacterial strains was for a long time the gold standard for the analysis of bacterial behavior and their interactions. Also, susceptibilities to e.g. antibiotics or mouth washes can be tested in such systems (Exterkate et al. 2014; Lee et al. 2011; Hansen et al. 2000; Rath et al. 2017; Lamfon et al. 2005; Guggenheim et al. 2001; Belibasakis and Thurnheer 2014). The *in vitro* systems are mainly classified in three groups: a) open systems (dynamic), b) closed systems (static) and c) microcosms (more complex) (Lebeaux et al. 2013). In the open models the medium the bacteria grow in is constantly replaced. Thus, fresh nutrients are added and waste products are removed. Biofilm growth, reaction on substances or shear forces can be

monitored in these systems. Closed or static models e.g. in microtiter plates have limited nutrients and do not last as long as open ones. The advantage of such systems is, that high throughput analysis is simplified and technical efforts more basic than in the open systems. Biofilm mass and colony forming can here quickly and easily be monitored. The third and more sophisticated models are the microcosms. In such systems, several bacterial species are combined (Rudney et al. 2012). They also include biomaterials or natural substances as saliva. These environmental factors make them more complex mimicking natural conditions in a more holistic way.

Different surfaces are used in *in vitro* assays to grow biofilms on. The most prominent are hydroxyapatite disks, mimicking the tooth surface, Polytetrafluorethylen (PTFE) or dental composite but also other synthethic materials are in use (Santos et al. 2010; Rogers et al. 2001; Takeshita et al. 2015; Schwartz et al. 2010; Rath et al. 2017; Veerachamy et al. 2014). The biofilm can then be cultivated in different systems. Biofilm reactors as e.g. the drip flow reactor, Modified Robbins Device, Microfermentors, CDC biofilm reactors, rotating disc reactors or flow cells are the most prominent ones (Goeres et al. 2009; Schwartz et al. 2010; Klug et al. 2016; Rudney et al. 2012; Salek et al. 2009; Elvers et al. 2002). Biofilm reactors and related systems here can mainly be used for big assays with a huge biofilm mass. Flow cells instead offer the possibility to watch biofilm growth or reaction on substances directly under the microscope. For this thesis, a drip flow reactor was used (Klug et al. 2016). To feed the bacteria, artificial media but also sterilized saliva can be used depending on the bacterium cultivated and the questions posed. Saliva as medium is gained from volunteers by spitting and is then mostly sterile filtrated and supplemented with dithiothreitol (DTT). Tian et al. have tested several media and found SHI in a pyrosequencing assay as a medium suitable to grow also uncultivable oral bacteria derived from saliva (Tian et al. 2010). In this study brain heart infusion (BHI) was used to grow anaerobes and aerobes. This medium has been shown to nourish anaerobes and aerobes equally well in several studies (Chen et al. 2011; Tian et al. 2010; Lee et al. 2011; Rath et al. 2017). A further factor in the growth of oral bacteria is always temperature. Most studies used temperatures between 34 °C and 37 °C (Mei et al. 2009; Eckert et al. 2006; Foster and Kolenbrander 2004). No long-term information existed on the natural temperature oscillations in the oral cavity. The *in vitro* systems provide a wide range of possible setups. Though, the number of bacteria tested and

the exclusion of environmental factors limit *in vitro* approaches. Complex interactions of the microbiota here cannot sufficiently be analyzed. Also, complex interactions of different organisms, as for example bacteria and fungi, can only be investigated in very basal traits *in vitro* analysis.

1.3.2. *In vivo* models

This thesis includes *in vivo* models where native oral biofilm is grown in the oral cavity and is subsequently analyzed in *in vitro* settings. The *in vivo* models use retrievable chips/slabs of different materials as biofilm carriers. These slabs are inserted in the oral cavity for a certain time and then removed and analyzed. Slabs are either directly glued onto to teeth or are fixed in e.g. dental splints. The biofilm formed on their surface is then analyzed with different methods as are further described in chapter 1.4. The most prominent slab substances chosen are: enamel, dentin and hydroxyapatite (Jung et al. 2010; Al-Ahmad et al. 2009; Svendsen and Lindh 2009; Obata et al. 2014). *In vivo* models also include all dental materials used in daily clinical routine. This includes different metals as implants or orthodontic brackets, bonding material, PTFE and dental composite (de Freitas et al. 2014; Garcez et al. 2011; Mei et al. 2009; Darrene and Cecile 2016). Also, pieces of human and animal bones and teeth are used for slab production (Jung et al. 2010). Two types of assays are performed. On the one hand, biofilm on artificial materials is tested in the case of disease due to biofilm formation (e.g. implant failure), on the other hand, biofilm growth, spatial arrangement and composition are monitored on specifically fixed slabs in healthy and diseased subjects. In the first case a reduction of implant failures due to inflammation is aimed using different materials and also different implant shapes. Biofilm growing on and surrounding the implant are characterized in such *in vivo* assays (Howe 2017; Veitz-Keenan and Keenan 2017; Größner- Schreiber et al. 2009; Busscher et al. 2010).

In the second case, researchers try to find out more about biofilm formation in the oral cavity in general and about changes over time or due to inflammatory events. Leaving the slabs inside the oral cavity for days or weeks allows them to monitor biofilm formation over time. During disease, such slabs can even be positioned right in a periodontal pocket to gain information about the biofilm there.

1.3.3. Combined biofilm models

Biofilm models using only *in vitro* or *in vivo* assays always loses information. Both attempts have their advantages and disadvantages. Lately combined models try to fill this gap. Walker et al. tried to cultivate biofilm sampled in the gingival sulcus on sterile ceramic calcium hydroxyapatite disks (Walker and Sedlacek 2007). These disks were coated with 10% sterile saliva overnight. Sonically dispersed biofilm was then added. Biofilm formation was monitored at 37 °C for 10 days. Comparing 15-20 species over this time they found 81% similarity in species and 70% similarity in proportions in healthy subjects. In diseased the respective percentages were 69% and 57%. Rudney et al. grew saliva and plaque biofilms on hydroxyapatite and dental composite discs in CDC biofilm reactors (Rudney et al. 2012). They used the “Human Oral Microbe Identification Microarray” (HOMIM®) for the analysis of 272 species in their microcosm. Around 60% of the original inoculum were regained after 72 hours of incubation.

To keep native oral biofilm alive under laboratory conditions in its native composition was one aim of this thesis. Methods used to analyze survival and composition over time are described in the following.

1.4. Molecular analysis of the oral biofilm: from Animalcules to -Omics

For several decades cultivating bacteria on solid and in liquid media was the gold standard for the identification and characterization of new species. Since the 1980s, molecular analysis methods have started to take over. Greatly improved and refined, these techniques now allow visualization of the biofilm structure and spatial composition. Further, detailed information on species composition and their lifestyles and interactions is gained. The methods used in this thesis will be described in the following.

1.4.1. Visualizing biofilm diversity

FISH

A lot of different methods have been developed to analyze biofilms so far. Not only the biofilm composition regarding bacterial species but also its spatial arrangement and

changes over time or due to influences from the outside can be assessed. Fluorescence *In Situ* Hybridization (FISH) used in Confocal Laser Scanning Microscopy (CLSM), for example, allows for staining of specific structures and certain bacteria or bacterial groups (Moter and Göbel 2000; Sunde et al. 2003; Diaz et al. 2006; Zijnge et al. 2010). For FISH, biofilm samples are fixed with Paraformaldehyde to preserve the cells. Then lysozyme treatment enables specific oligonucleotide probes to penetrate the cell walls. These oligonucleotide probes target the bacterial rRNA at very specific positions. If used to find certain species, these probe sequences are often targeting highly variable regions of the 16S rRNA gene. Nucleotide changes during evolution have led to quite unique sequence regions in this gene for the respective bacterial species or phylum. Identifying them can then easily be performed over this unique sequence. In contrary to that, if wanting to stain for example all bacteria, as is done with probe EUB338, a position in the 16S rRNA sequence is chosen that has been highly conserved over time and thus exists in most bacteria. The oligonucleotide probes are synthetically produced and have fluorochromes attached to the 3'-, or the 5'- end or both. This labelling later enables us to find the respective bacteria in the CLSM. For this thesis, up to 3 oligonucleotide probes with 3 different fluorochromes were used to distinguish between all bacteria, certain phyla, and certain species in one sample. After several wash-steps the samples are fixed for CLSM with antifade reagents protecting it from bleaching of the fluorochromes through the laser. Using an Argon and a Helium/Neon- laser possible excitation wavelengths for the fluorochromes included 488nm, 555nm and 633nm. The respective emission spectra used lay at 520nm, 565nm and 647nm.

Live/dead staining

A different way of staining bacteria relies on the fact that cell walls of living and dead bacteria show a different permeability with respect to certain substances. A lot of different dyes for this purpose exist and are more or less controversial in staining only one of the two groups. The assay used in this work is called LIVE/DEAD® BacLight™ Bacterial Viability Kit. It uses Syto9 and propidium iodide (PI) to stain living and dead bacteria respectively. Syto9 is a green fluorescent stain, able to penetrate and stain living and dead bacteria. Propidium Iodide in contrast can only enter and stain dead bacteria causing a reduction in the signal of Syto9 if used together. The emission

maxima of these two stains lie at 500nm (Syto9) and 635nm (PI). Staining biofilms with this kit allows for quantification of living and dead bacteria but also for qualitative analysis of biofilm structure and spatial arrangement as all bacteria are stained. No fixation of the sample is needed for live/dead staining making it a quick and easy procedure. A negative point for the handling of this staining is the untested toxicity of Syto9 and PI.

1.4.2. Analyzing microbial diversity

From single species to whole sample sequence patterns

PCR and realtime-PCR were used to identify and also quantify certain bacterial species in the oral biofilms. For a long time, they were the gold standard for the identification of specific bacterial species. Different groups developed primer pairs matching certain bacteria seen as periodontopathogens. Also, commercially available kits for clinicians relied on these methods to identify up to 20 periodontopathogens (Santigli et al. 2016). For research use, Socransky et al. established the checkerboard DNA-DNA hybridization method in 1994 (Socransky et al. 1994). This method allowed a parallel analysis of up to 43 single species which revolutionized oral biofilm research. The hybridization technologies were then further developed and in 2008 the Human Oral Microbe Identification Microarray (HOMIM®) was presented (Paster et al. 2006). This microarray allowed quick identification of 270 bacterial species. For the differentiation of communities Single Strand Conformation Polymorphism (SSCP) and Denaturing Gradient Gel Electrophoresis (DGGE) were established. In SSCP, the typical secondary structure of single strand DNA is used to identify sequence patterns specific for a sample (Schwieger and Tebbe 1998; Größner- Schreiber et al. 2009; Cardinale et al. 2008). In DGGE an electrophoretic gel containing a salt gradient progressively denatures the nucleic acids which also leads to specific patterns on the gel (Tian et al. 2010; Ling et al. 2010; Watanabe et al. 2001). But, also in the field of sequencing, developments continued and next generation sequencing methods appeared around the year 2000.

Next generation sequencing - 454 Pyrosequencing

Measurements of bacterial diversity have only recently been extended to highly complex microbiome studies. Due to advanced sequencing techniques, the analysis of

the microbiome down to even species level was facilitated immensely. We used here 454-pyrosequencing, a next generation sequencing method (Roche 454 Life Sciences). Pyrosequencing is a “sequencing by synthesis” method where a pyrophosphate is released during nucleotide incorporation. The bacterial DNA is therefore hybridized to a special sequencing primer as a single-strand. A DNA polymerase is then added together with ATP sulfurylase, luciferase and apyrase. APS and luciferin are added as substrates. For the sequencing, deoxynucleotide triphosphates (dNTPs) are then added for the incorporation in the second strand. This process releases a pyrophosphate. The ATP sulfurylase converts it to an ATP in the presence of APS. The luciferase can then use this ATP as substrate for the conversion of luciferin to oxyluciferin. During this step light is emitted proportional to the amount of ATP used. This light is detected by a camera and analyzed with the respective software. The Apyrase finally degrades all unincorporated nucleotides and the ATP. This enables the reaction to restart with another nucleotide. The development of an array-based pyrosequencing technology has led to an immense increase in possible reads (sequences) per run. The FLX technology used here can generate 400 Mb (megabases) in a 10-hour run with a single machine.

Analysing the pyrosequencing data

Next generation sequencing results in an enormous amount of sequences (reads) per sample. New bioinformatic tools were created to analyze the bulk of data. In this thesis, ACACIA and the open-source pipeline QIIME (Quantitative Insights Into Microbial Ecology) were used (Bragg et al. 2012; Caporaso et al. 2010). In the following, a short overview on the functions of these two tools are given. Pyrosequencing sequences contain false reads resulting from the sequencing method as for example sequences with the wrong length or wrong base calls. In a first analysis step all potentially error-containing sequences thus have to be removed using e.g. ACACIA. Also, primer and adaptor sequences from the pyrosequencing are cut off. Finally, sequences are trimmed to a maximum and minimum length. The adjusted dataset is then further processed in QIIME. Here, chimeric sequences where two sequences from different species align and form an artificial sequence are removed. For an easier handling of the huge datasets generated, groups of sequences are defined before further analyses. These groups are called Operational Taxonomic Units (OTUs). One OTU

then reflects one reference sequence representing a group of species having more than 97% sequence similarity. Using only this reference sequence instead of all sequences in this group eases and accelerates computational efforts. In ecological studies, also 99% and 95% similarities are used. For pyrosequencing, the 97% became established. As laboratory and bioinformatic analysis can only minimize a certain error rate but not completely exclude them, 99% similarity are not seen as valid for this kind of analysis. The 95% border is less common as the phylogenetic resolution is not high enough to gain information on lower phylogenetic levels. All OTUs found are then aligned using PyNAST against the Greengenes database (Bragg et al. 2012; Caporaso, Kuczynski, et al. 2010). PyNAST is a tool for the alignment of sequences also removing gaps common to all sequences. Greengenes is a 16S rRNA gene database consisting of a multiple-sequence alignment (MSA) of bacterial and archaeal 16S rRNA genes. A phylogeny is then created using the Ribosomal Database Project (RDP) classifier (Cole et al. 2005; Cole et al. 2009). Based on these steps an OTU table can be created. This OTU table needs to be cleaned from singletons, sequences that are only found once. Due to methodological inaccuracy in the laboratory handling those values cannot be taken for granted and are thus excluded from further analyses. The generated microbiome data is then ready for statistical analysis of the diversity. Two terms of diversities need to be explained for a better understanding. The alpha-diversity (α-diversity) measuring the diversity within a sample and the beta-diversity (β-diversity) comparing diversities of different samples with each other (Whittaker 1972; Whittaker 1960).

1) Alpha diversity

The alpha diversity can be calculated in several taxa. First the **Richness** of a sample is calculated, giving the number of different species found in a sample. The **Eveness** then shows how evenly distributed the taxa are – the closer the numbers, the higher the Eveness. Finally, the phylogenetic relationships can be included in diversity measures using e.g. the index PD (Faith 1992). Including not only species counts but also their phylogenetic relation, a more realistic picture on the distribution of taxa can be calculated. The diversity metrics used in this thesis were: **observed_species** (measuring the richness), **Chao1**, **Shannon** and **Simpson** (all three using richness and eveness) and **PD_whole_tree** (this one includes also the phylogeny). To visualize

alpha-diversity, rarefaction curves can be used. They show the number of individuals sampled (at a particular depth) versus the alpha diversity. These curves are calculated generating random samples for each biological sample. The alpha diversity is then calculated for each random sample. A sufficient sequencing depth (enough sequences for the respective sample sequenced) is reached, when the curve starts to level off. If it is still increasing, the sequencing depth was not high enough to reflect the whole estimated diversity.

2) Beta diversity

The beta diversity is used to compare microbiome samples of different subjects, habitats or sites with each other. The distance and dissimilarity of two samples can herewith be assessed. Beta-diversity can also be used to compare the diversity of several samples with each other. Therefore, so-called distance matrices are generated. There, every pair of samples is compared with each other. Different metrics are used to calculate such matrices. The most commonly applied are: **unweighted** (uses OTUs and phylogeny) and **weighted** (uses abundance of OTUs and phylogeny) **UniFrac** and **Bray-Curtis** (uses only abundances without phylogeny) (Bray and Curtis 1957; Lozupone et al. 2010). Plotting the results of beta diversity analysis new ways had to be found. Group level differences cannot be explained by single numbers anymore. The previously used contingency tables listing up three different bacteria had to be extended to several hundreds or even thousands and with that 3-dimensional analysis became multidimensional. Plotting this data is challenging and needs previous reduction of the complexity of the data. This can e.g. be performed by **Principal coordinate analysis** (PCoA). It allows the comparison of several thousand sequences found in several samples not only calculating Euclidian distance values but also plotting the data in 3-dimensional plots. This enables the search for patterns that cannot be found in the Euclidian values alone giving only numbers. **Heat maps**, presenting the relative abundances at the respective phylogenetic levels, are another way to compare samples with each other. Using a color code showing high abundance in lighter colors and a lower abundance in darker colors makes it easier to compare samples visually. Patterns due to certain treatments or the difference between treatment and placebo group can such easily be found without going through the respective numbers.

Principal component analysis (PCA) is a multivariate analysis. As Ramette describes, it should be used when objects cover very short gradients (i.e. when samples mostly differ in species abundances) and species linearly respond to environmental gradients (Ramette 2007). Eigenvalues calculated here account for the amount of variance. If the most variance is given in the first two or three groups, PCA is the method of choice.

Correspondance analysis (CA) allows to differentiate communities according to environmental factors. Kent et al. have used CA to compare community-level dynamics among phytoplankton and bacteria in six north temperate humic lakes (Kent et al. 2007). In contrast to other methods, CA maximizes the correspondence between species scores and sample scores. CA is used when species display unimodal (bell-shaped or Gaussian) relationships with environmental gradients (ter Braak 1985).

For a better understanding of the changes over time **log2fold changes** were calculated. Log-transformed analysis will model proportional changes typical to biological processes. The log2 scales present a doubling or reduction of 50% change in the unit of +1 or -1. Such biologically relevant changes can often better be displayed as when using a log10.

All these methods were applied in this thesis to create a new combined *in vivo* - *in vitro* biofilm model for the analysis of native oral biofilm. The specimens and subjects sampled and the methods used therefore are described in the following.

2. Material and Methods

2.1. Study design

In this thesis, biofilm material from two setups was used for the analysis of native oral biofilms (Figure 2). Panel A shows the palatal expander from which native oral biofilm was derived from. These palatal expanders were worn by children for 4 weeks during a regular orthodontic treatment. The aim of this study was to create a method to analyze the biofilm grown on them with FISH and Confocal Laser Scanning Microscopy (CLSM).

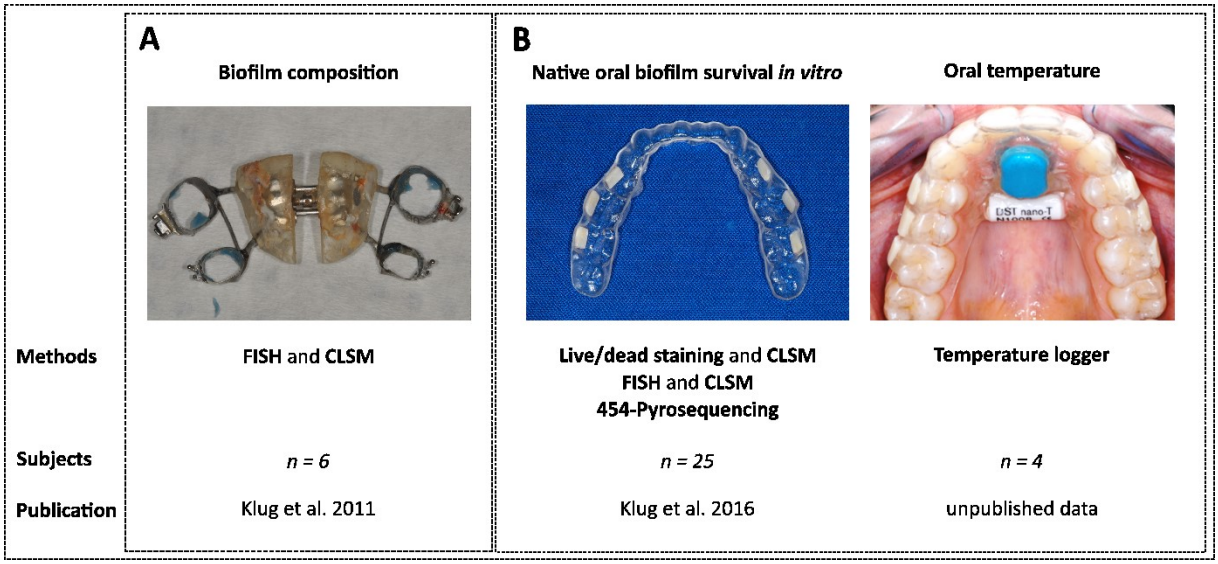

Figure 2: Study setup. A: Biofilm derived from palatal expanders worn for 4 months analyzed with FISH and CLSM. B left: Biofilm survival on enamel-dentin slabs analyzed with live/dead staining and CLSM, FISH and CLSM and 454-Pyrosequencing. B right: Oral temperature measured with 2 temperature loggers over 48 hours.

In panel B the research splints developed for the second part of this study can be found. It aimed in growing oral biofilm *in vivo*, transferring it to the laboratory and keeping it there alive in its native constitution. Biofilm from this study was imaged with FISH and live/dead staining and subsequent CLSM. Biofilm composition was investigated with 454-Pyrosequencing. For further information on the biofilm surrounding, two temperature loggers were integrated in this research splint. They allowed monitoring of temperature oscillations in the oral cavity.

2.2. Study subjects

The palatal expanders in the first study were worn by female and male children, aged 12, due to orthodontic treatment. In the second study female and male adult volunteers wore individually fitted dental research splints. They had an age of 22-30 years and were healthy non-smokers. All procedures were approved by the ethics committee of the Medical University of Graz (EK-numbers: 25-117 ex 12/13, 26-357 ex 13/14, 26-358 ex 13/14 and 27-126 ex 14/15).

Written informed consent was obtained from all volunteers in accordance with the Declaration of Helsinki. Inclusion criteria for the second study were: non-smoker, good general health, no present medication and no antibiotic intake three months prior to the study.

2.3. Timelines

The children due to orthodontic implication, continuously wore the palatal expanders for four months in the first study. After the four months, the expander was removed carefully and transferred into a transport vial. This vial was then frozen at -80 °C until further use.

In the second study, healthy volunteers wore individually fitted dental splints for 48 hours (Figure 3A). They were not allowed to drink alcohol, brush their teeth or go swimming in chlorinated water in order not to influence biofilm growth during this time. After 48 hours, the volunteers came to the laboratory where the splint was taken out and enamel-dentin slabs were clipped out and transferred to a biofilm reactor immediately (Figure 3B).

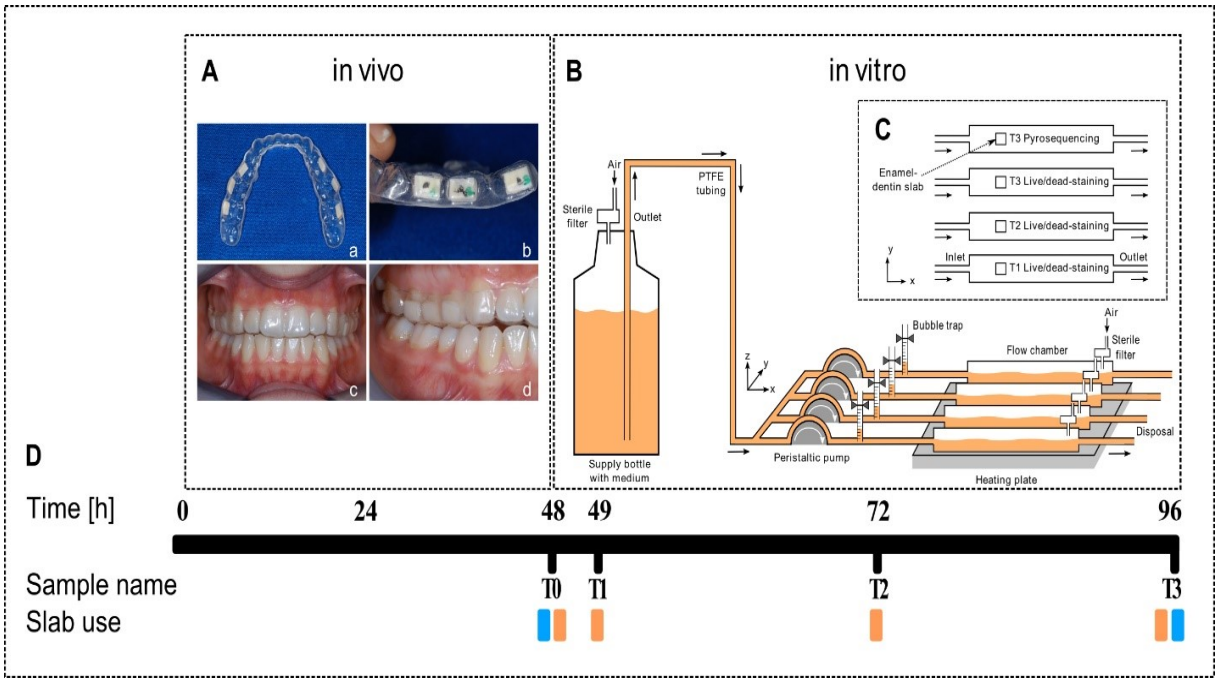

Figure 3: Timeline biofilm on enamel-dentin slabs. A: Native oral biofilm growth on six enamel-dentin slabs in a research splint; a and b show the slabs in the splint, c and d wearing of the splint. B: Biofilm reactor setup. Enamel-dentin slabs were transferred into biofilm reactors where they were nourished with BHI medium at 34 °C. C: Use of the enamel-dentin slabs for the respective analyses. D: Timeline presenting the different points in time where biofilm was sampled and which method was used for the respective analysis. *Reproduced from Klug et al. 2016 with permission of Frontiers*.

The slabs with the biofilm on top were then incubated in the biofilm reactor for another 48 hours. Brain Heart Infusion (BHI) medium with a flow velocity of 0.2 ml/min and a temperature of 34 °C nourished the biofilm (Figure 3C). Measurements were performed at the points in time described in Figure 3D: T0 – directly after removal from the mouth, T1 – after a one-hour incubation *in vitro*, T2 – after 24 hours incubation *in vitro*, T3 – after 48 hours incubation *in vitro*. Slabs were either stained of fixed immediately or frozen at -80 °C for further use at the respective points in time.

2.4. Dental splints used in this study

Two different types of dental splints were used in this study. First, palatal expanders used for regular orthodontic treatment of children, and second, special research splints were developed by Santigli and Klug to grow native oral biofilm and transfer it for further analysis to the laboratory. The development and production of these splints is subsequently described.

2.4.1. Orthodontic appliances – tooth and tissue borne palatal expanders

Palatal expanders used in this study were Haas expanders. Their design allows lateral forces on both palate tissue and teeth. An acrylic plate is lying in the palate. This plate consists of two pieces connected via an acrylic borne screw. Turning this screw widens a splint in the expander along the patient's midline. Metallic bands around the patient's posterior teeth fix the expander. These expanders were fixed in the upper jaw of children for 4 months continuously with the goal to expand the maxilla transversally. Biofilm growing on the expander was untouched during this time.

2.4.2. Research splints

Research splints were worn in two runs. Splints for the lower jaw were worn by 25 male volunteers. Splints for the upper jaw were worn by four female volunteers. Both groups wore the splints for 48 hours continuously omitting alcohol drinking, mouth hygiene (including also tooth brushing) and swimming in chlorinated water. Human enamel-dentin slabs were inserted into the research splints as biofilm carriers enabling quick biofilm transfer into the laboratory. Functions of the research splints for the upper jaw were extended integrating two standardized sensors as described below.

Research splints for the lower jaw

A special splint made from a deep drawing template was used for the lower jaw. This splint inherited six enamel-dentin slabs of a standardized size each (Figure 4, A).

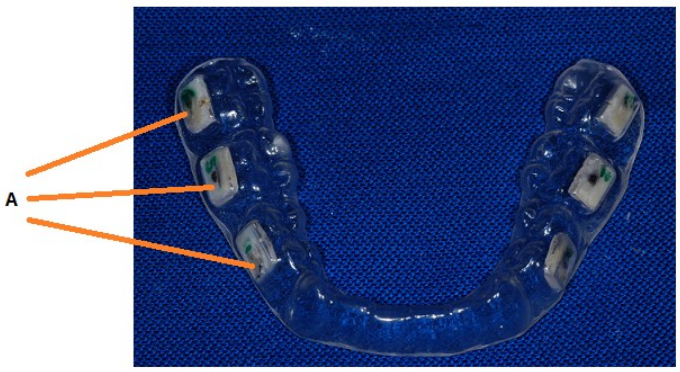

Figure 4: Research splint for the lower jaw including human enamel-dentin slabs. A: standardized enamel-dentin slabs with a size of 6 x 4 mm integrated in a deep-drawing template.

Research splints for the upper jaw

As the upper jaw offers more space, two sensors were added in two different designs to the deep drawing template (Figure 5).

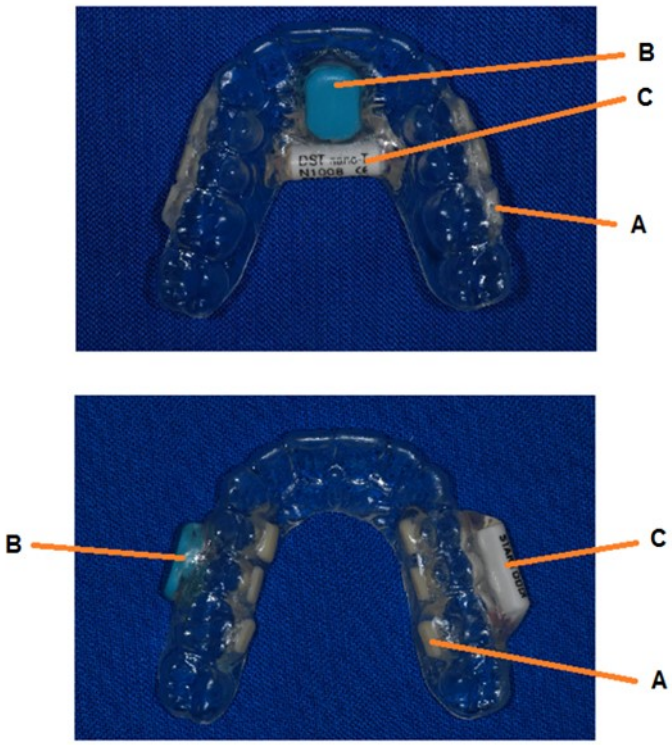

Figure 5: Research splint design for the upper jaw. Deep drawing splint containing A) standardized human enamel-dentin slabs, B) TheraMon® Microsensor, C) Star Oddi® DST nano-T). The upper design was finally chosen for further experiments.

Enamel-dentin slabs were inserted buccally and palatinally (Figure 5, A). The two sensors were fixed in the upper jaw (Figure 5, B and C).

For all research splints the space between the enamel-dentin slabs and the teeth was big enough to allow the development of native oral biofilm. The slabs were bathed in saliva as the teeth usually are. This also allowed nourishment of the biofilm on the slabs and evacuation of waste products. Due to more comfort for the carriers, the design on top in Figure 4, having the sensors palatially, was chosen for further studies.

Microsensors

The microsensors used were 1) the TheraMon® Microsensor (TheraMon, Handelsagentur Gschladt) and 2) the Star Oddi® DST nano-T (Star Oddi®, Iceland). The blue TheraMon® Microsensor has a rectangular form (9x13 mm) and is usually used for compliance testing in orthodontics. It measured and logged the temperature

in 15-minute intervals. Data was then read out via RFID read-out station connected to a normal PC.

The Star Oddi® DST nano-T has a cylindric form (17x6 mm) and is usually used in animal research. It measured and logged temperature in the time scale varied by the us. The communication box and the software (Mercury, Star-Oddi®) provided facilitated data retrieval. A five minutes' measurement interval was used for this sensor.

Enamel-dentin slab preparation

Human teeth freshly extracted for dental treatment were collected at the oral-surgical ambulance and the septic OR at the Department of Dentistry and Maxillofacial Surgery, Medical University of Graz. All donors signed an informed consent. All procedures were approved by the ethics committee, Medical University of Graz (EK 26-357 ex 13/14).

Inclusion criteria for tooth collection:

- Natural teeth
- Minimum 50% intact crown

Exclusion criteria for tooth collection:

- Fang rests
- Deeply destroyed crowns (>50%)
- Tooth crown or prosthetical tooth treatment

Teeth were collected in plastic tubes containing 80 ml physiological saline (Meditrade) to prevent them from desiccation (Figure 6). Sterilization was performed for 20 min at 134 °C and 2.1bar. Periodontal ligaments, tartar and bone sequesters were removed and teeth rinsed again with sterile saline.

Figure 6: Teeth collection in physiological saline

Teeth were then sent to the Karl Donath laboratory for hard tissue and biomaterial research, Vienna. Stefan Tangl and Christian Schuh performed the final enamel-dentin slab production. Therefore parts suitable for slab production were marked on the pristine tooth. Then these pieces were cut off with a diamond band saw as shown in Figure 5 (EXAKT Advanced Technologies GmbH).

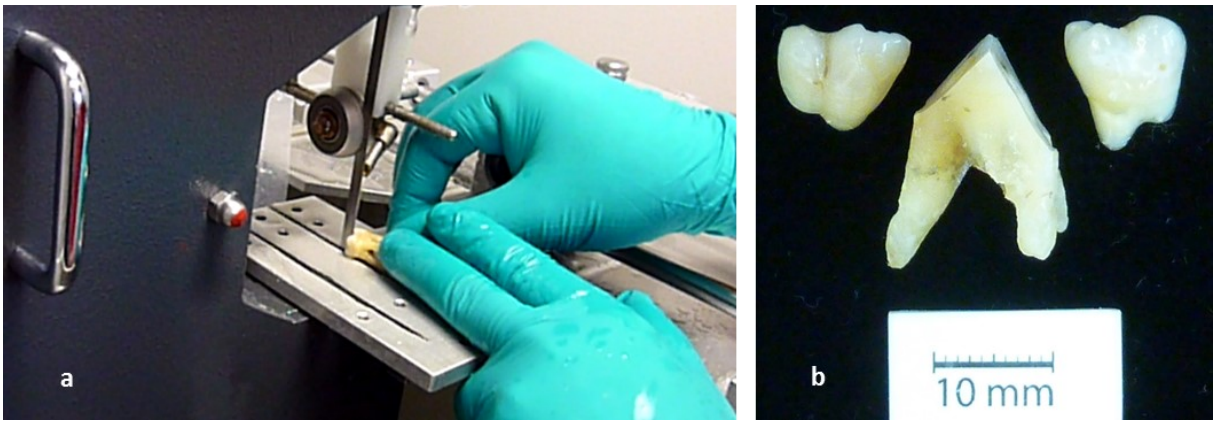

Figure 7: Cutting of teeth: a) diamond band saw, b) tooth pieces suitable for slab production

Pieces were then ground on a rotary disc sander (Buehler MetaServ® 250 Grinder-Polisher) with a grit of 1200 first and then polished with a very fine grit of 4000 (Figure 8).

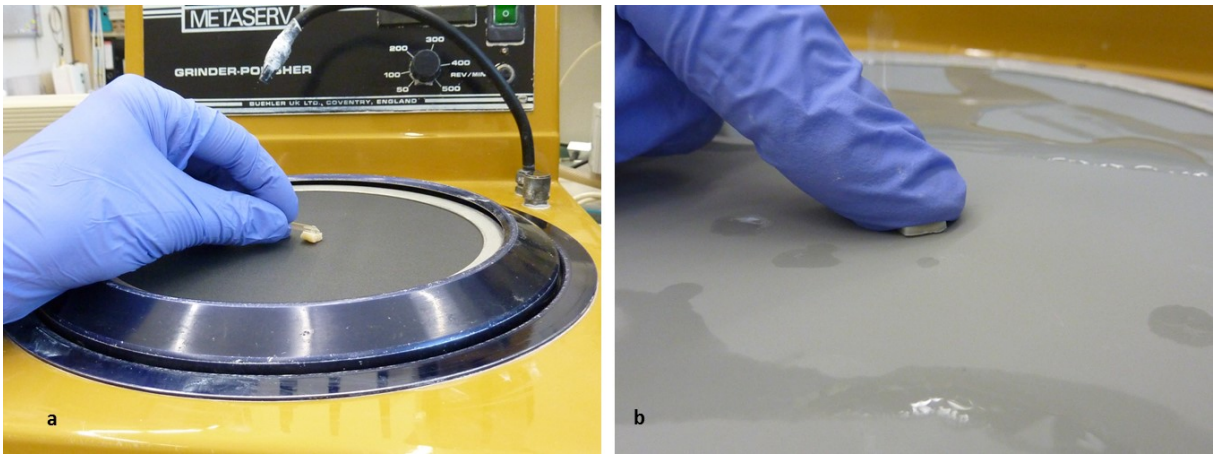

Figure 8: Grinding of the tooth pieces: a) rough grinding (1200), b) polishing (4000)

Standardized slabs with a size of 2 x 4 x 6 mm were produced having the enamel surface on top (Figure 9).

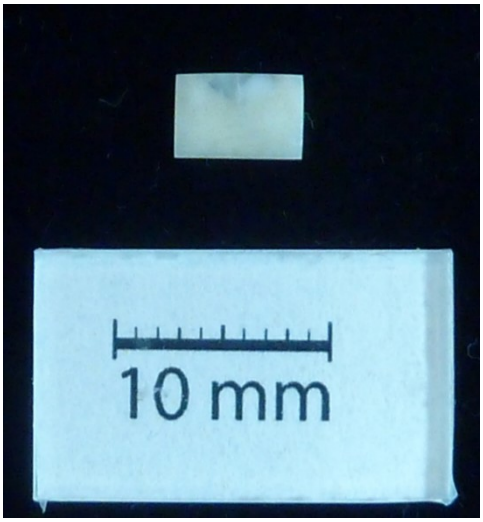

Figure 9: Standardized enamel-dentin slab (2 x 4 x 6 mm)

For safety reasons slabs were sterilized again and freed from DNA and RNA under UV light for 30 minutes.

Splint fabrication

Alginate impressions were made and grouted with dental stone (class II) for individual splints for each volunteer. For deep drawing the splint, the six enamel-dentin slabs were fixed bucally to the cement model. For the insertion of the Star Oddi® DST nano-T a dummy was used as the Sensor does not resist the heat during the deep drawing

process (Figure 10). Complete research splints were DNA and RNA sterilized with UV light before wearing them.

Figure 10: Integration of enamel-dentin slabs and sensor dummy before deep drawing. A: six enamel-dentin slabs, B: dummy for the Star Oddi® DST nano-T. *Image taken from the diploma thesis Heidrun Frankl, Medical University of Graz.*

Following deep drawing was performed like described by the producer (SCHEU-DENTAL GmbH, Germany). After hardening, the TheraMon® Microsensor was added on the outside of the deep drawing film with the acrylic resin Paladur (Heraeus Kulzer GmbH, Germany). Figure 11 shows the complete research splint including the six enamel-dentin slabs and the two sensors (blue: TheraMon® Microsensor completely covered in acrylic resin, white: Star Oddi® DST nano-T).

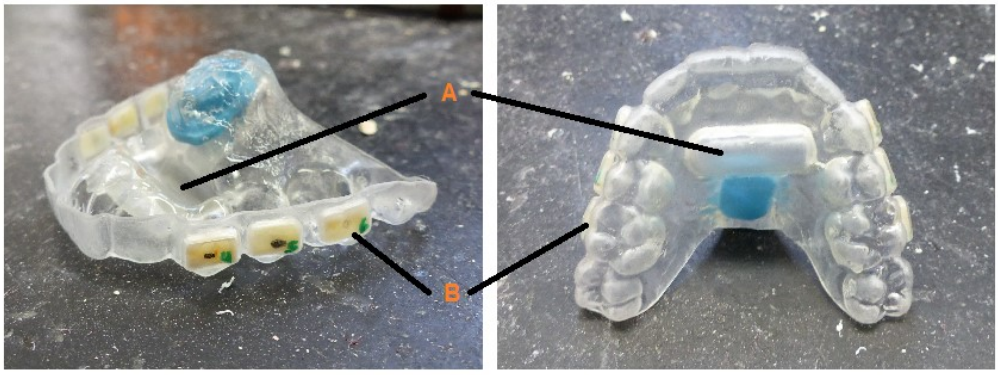

Figure 11: Research splint completion. A: the sensor dummy is replaced by the real Star Oddi® DST nano-T sensor. B: the six enamel-dentin slabs inserted. Blue: TheraMon® Microsensor.

The Star Oddi® DST nano-T was activated via the communication box using a measurement interval of 34 seconds. The TheraMon® Microsensor was activated via

RFID holding it close to the readout device. A UV-irradiation was subsequently performed in the PCR Workstation Pro (Peqlab, Germany) to remove DNA and RNA on the completed research splints. The storage in an also UV irradiated box avoided contamination until the start of the wearing.

To read out the Star Oddi® DST nano-T data the sensor was removed from the dental appliance, washed and sterilized in 70% Ethanol for 30 minutes, bevor washing it again and sterilizing it for another 10 minutes in 70% Ethanol. After that a UV-irradiation was performed like described above. Then the Star Oddi® communication box and the Mercury computer software supplied were used to read out the data. The data was transferred to an excel file and values equalized to three minutes intervals to calculate temperature curves.

The TheraMon® Microsensor was read out via the supplied read out device directly after the end of the respective measurement. Temperature curves were again calculated in Excel adjusting the 15 minutes intervals measured to three minutes values by using the same value 5 times.

2.5. Preparation of the biofilm reactor

The biofilm reactor setup used in this study is shown in Figure 12 and as a scheme in Figure 3D. A two-liter bottle filled with sterile BHI medium was connected to the Ismatec IPC peristaltic pump (Cole-Palmer GmbH, Germany). This pump allowed a drip free flow of the medium. A flow rate of 0.2 ml/min was used to ensure minimal shear forces on the biofilm. To collect gas bubbles from the influent supply, a four-valve bubble trap (Biosurface Technologies Corp., Montana, USA) was interconnected between peristaltic pump and biofilm reactor. The biofilm reactor used in this study was the DFR110 (Biosurface Technologies Corp., Montana, USA). It consists of four chambers (25 x 75 x 1 mm). All chambers are sealed with rubber O rings forming tight air seals. The medium was inserted over syringes through a mini nert valve. Through a positioning of the biofilm reactor horizontally without inclination the medium was retained in the chamber.

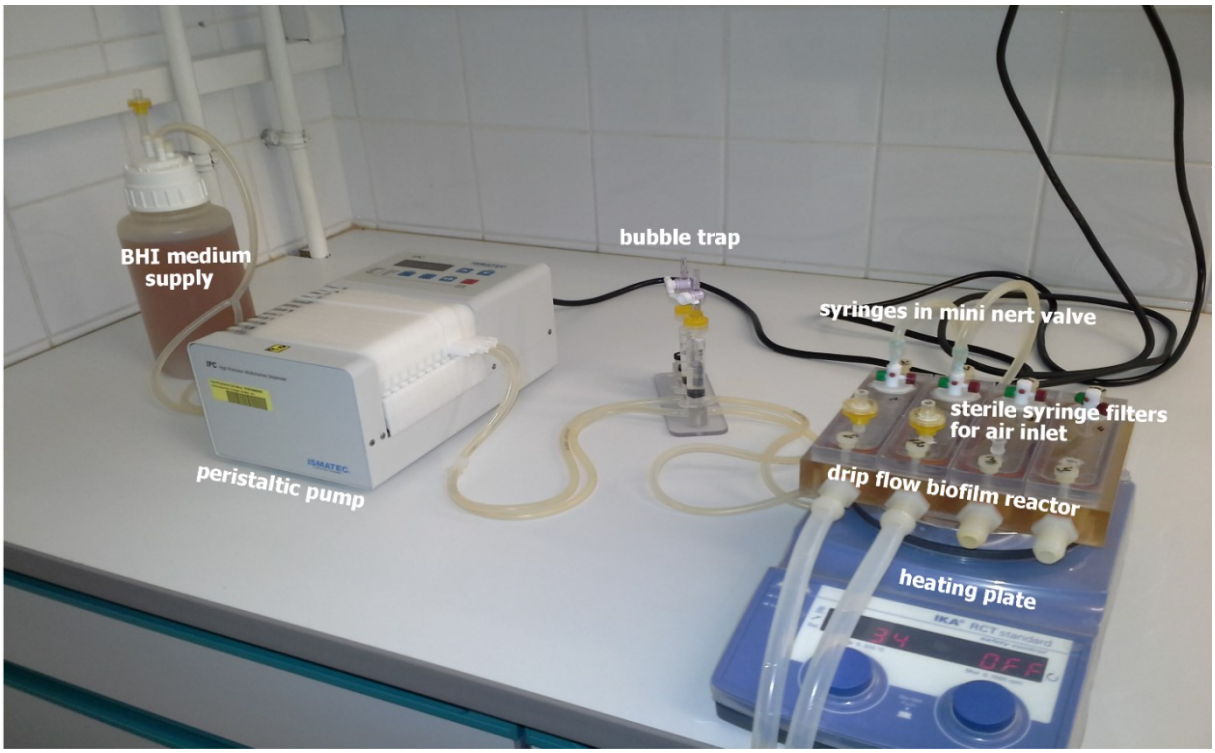

Figure 12: Test setup. BHI medium supply, peristaltic pump, bubble trap, mini nert valve inlet for syringes, drip flow biofilm reactor and heating plate (from left to right). Not visible: waste bottle below. Sterile syringe filters (yellow) for the air inlet are fixed on the medium flask, bubble trap and biofilm reactor.

The enamel-dentin slabs carrying the biofilm were so covered completely with BHI all the time. Sterile syringe filters with a pore size of 0.2 µm (Bartelt, Austria) were used for air inlets on the bubble trap and the biofilm reactor. All parts in the setup were fully autoclavable and the biofilm reactor was UV irradiated to exclude DNA contamination in the pyrosequencing assays. The biofilm reactor setup was connected using a Bunsen burner to keep the air around sterile. Sterilization was performed with a 0.5% sodium hypochlorite solution using a flow rate of 3 ml/min for 30 minutes. Then the setup was thoroughly rinsed with sterile water. One chamber was used empty as sterile control.

2.6. Oral biofilm staining for confocal laser scanning microscopy

Oral biofilm samples were stained with two different methods: FISH and LIVE/DEAD staining with SYTO 9 and Propidium Iodide (Klug et al. 2011; Klug et al. 2016).

2.6.1. Fluorescence *in situ* hybridization

Sample preparation

The thick biofilm grown on the palatal expanders was scraped of carefully with a sterile scalpel as shown in Figure 13.

Figure 13: Scraping off biofilm flakes (red circle) with a sterile scalpel.

Biofilm flakes (Figure 13, red circle) were collected in a Petri dish. A new scalpel was used for every expander in order to avoid disruption of the biofilm through cutting or mashing.

For the second study, enamel-dentin slabs sampled directly after removal of the research splint were immediately fixed as described below.

Sample fixation

Oral biofilm from the palatal expanders and on the enamel-dentin slabs and was fixed with ice-cold 4% PFA solution (ratio of 3: 1; PFA: sample). Samples were incubated at 4 °C for 3-12 hours. Then PFA was removed and samples were washed 3 times with ice-cold 1xPBS. For long term storage at -20 °C a 1:1 mixture of 1xPBS and 96% ethanol was applied ice cold covering the samples completely.

For FISH staining of very small biofilm pieces, samples were fixed on polysine® coated slides (VWR). For bigger pieces and the enamel-dentin slabs FISH was performed in 1.5 ml reaction tubes. Volumes of buffers and other liquids were multiplied respectively.

Cell wall lysis and dehydration

To facilitate probe penetration bacterial cell walls were partially digested with lysozyme (1mg/ ml) for 10 minutes at room temperature. Then samples were dehydrated in an

ethanol series, 50%, 80% and 96% for 3 minutes each. Finally, samples were dried at room temperature or 46 °C for a couple of minutes to remove ethanol residues.

Fluorescence *in situ* hybridization

Fluorescence *in situ* hybridization (FISH) was performed using a modification of the method described by Cardinale et al. (Cardinale et al. 2008; Klug et al. 2011; Klug et al. 2016). Hybridization buffers containing 5M NaCl, 1M Tris-HCl (pH 8), 2% SDS and formamide in a concentration according to those needed by the respective oligonucleotide probes were prepared in advance and pre-warmed at 46 °C. Oligonucleotide probes (100 mM) were added to the hybridization buffer just before application. Oligonucleotide probe sequences shown in Table 1 were derived from probeBase (Loy et al. 2007).

Table 1: Fluorescence *in situ* hybridization probes used in this study.

Oligonucleotide probe	Target organism	Sequence [5'-3']	Position	Formamide [%]
EUB388	most bacteria	GCT GCC TCC CGT AGG AGT	338-355	0-50
EUB388 II	Planctomycetales	GCA GCC ACC CGT AGG TGT	338-355	0-50
EUB388 III	Verrucomicrobiales	GCT GCC ACC CGT AGG TGT	338-355	0-50
LGC354A	Firmicutes (Gram-positive bacteria with low G+C content)	TGG AAG ATT CCC TAC TGC	354-371	35
LGC354B	Firmicutes (Gram-positive bacteria with low G+C content)	CGG AAG ATT CCC TAC TGC	354-371	35
LGC354C	Firmicutes (Gram-positive bacteria with low G+C content)	CCG AAG ATT CCC TAC TGC	354-371	35
Bac303	most Bacteroidaceae and Prevotellaceae, some Porphyromonadaceae	CCA ATG TGG GGG ACC TT		0

Hybridization was performed at 46 °C for 1.5 to 2 hours. After hybridization samples were washed in washing buffer containing 5M NaCl, 1M Tris-HCl (pH 8), and 0.5M EDTA in concentrations according to the formamide concentration used for hybridization buffers. Washing was performed for 10-15 minutes at 48 °C. If more than one oligonucleotide probe was used with different formamide concentrations, two steps were made. The probe needing a higher formamide concentration was applied first followed by direct hybridization with the second oligonucleotide probe after the first washing buffer. After the last hybridization, all reactions were stopped adding ice-cold water for 3 seconds. Then samples were either air dried and covered with ProLong® Antifade Reagents (lifetechnologies, Thermo Fisher Scientific Inc., Germany) or covered with water for confocal laser scanning microscopy.

2.6.2. LIVE/DEAD staining

LIVE/DEAD staining was performed with the LIVE/DEAD® BacLight™ Bacterial Viability Kit (Molecular Probes®) according to the protocol. Enamel–dentin slabs were stained for 20 minutes in a volume of 500 µl containing 1.5 µl of component A (SYTO 9) and B (propidium iodide) each. Samples were then rinsed twice with ddH_2O. For CLSM enamel–dentin slabs were covered completely with ddH_2O in a small Petri dish.

2.7. Confocal laser scanning microscopy

Confocal laser scanning microscopy (CLSM) was performed with a Leica TCS SP. Objectives used for CLSM analysis were: HCX PL APO 63x/1.2, HCX APO L 20x /0.5 W UVI/D 3.5 and an HCX APO L 63x/0.90W. Three lasers were used for excitation at wavelengths 488, 543 and 633 nm were used. Emission measuring ranges were fitted to the respective fluorophores and their intensities in the respective samples. Image stacks with voxel sizes of 0.155010 µm x 0.155010 µm x 0.407034 µm and a resolution of 1024x1024 were made and saved. At least five stacks were made for each sample at each point in time.

2.8. CLSM data analysis

2.8.1. Processing of the CLSM maximum projections

For the visual analysis of the maximum projections produced with the respective Leica software a MATLAB® R2010b (© 1994-2014 The MathWorks, Inc.) script was written (Figure 14).

```
function Bilderzuschnitt_BK (arglist)
Foldername = arglist{1};
Rows = arglist{2};

% Bilderzuschnitt
% © Barbara Klug
% path information and plotting parameters
loadpath1 = 'J:\Barbara Sicherungen\HTI\'
savepath1 = 'D:\Users\klugba\Desktop\Data_analysis\Bilderzuschnitt';
loadpath2 = [loadpath1,Foldername,'\'];
savepath2 = [savepath1,Foldername,'\'];
if exist (savepath2,'dir') == 0
```

```
 mkdir (savepath2)
end

% scalebar info
pxpro20mu = 124;

% open, crop and save pictures
sIR = size (Rows);
for l = 1:sIR (2)
 Rowname = Rows{l};
 display (['Processing: -Sna- ',Foldername,' -Row- ',Rowname])
 A = dir ([loadpath2,'*Sna*',Rowname,'*.tif*']);
 sIA = size (A);
 for j = 1:sIA (1)
 imname = A (j).name;
 I = imread ([loadpath2,imname]);
 Snapshot = imname (end-5:end-4);
 I2 = imcrop (I, [379 3 974 1350]);
 imagesc (I2);
 imwrite (I2,[savepath2,imname (1:end-4),'.tif']);
 I2 (850:860,800:800+pxpro20mu-1,:) = 255;
 imwrite (I2,[savepath2,imname (1:end-4),'_s.tif'])
 end
end
```

Figure 14: MATLAB script for cropping maximum projections and inserting a 20 µm scale bar.

Running this script opened all pictures automatically, cut off all grey frames produced by the Leica software, inserted a scale bar of 20 µm and saved them with a new name. The original scale bar of 31.75 µm inserted directly by the program was not used due to the unsuitable value.

2.8.2. AMIRA® – 3D reconstruction

3D reconstructions of the 2D confocal stacks were made with AMIRA® 5.6 software (FEI Visualization Science Group). Files were loaded directly from the .lei files. A resample using the Mitchel filter was performed. Isosurfaces were then created using a threshold around 20 – varying with the signals. For yeast identification and evaluation of their sizes the segmentation editor was used choosing the free hand tool to select them. Statistics from these labeling were exported into Matlab and compared with values calculated from the respective 2D stack. Snapshots of the 3D reconstructions were saved.

2.8.3. MATLAB® - stack data quantification

A special MATLAB® R2010b (© 1994-2014 The MathWorks, Inc.) script for the quantification of the 2D stack LIVE/DEAD data was developed by Christian Westendorf at the University of Graz, Institute for Plant Sciences. Using the kmeans function (Statistics and Machine Learning Toolbox), first background and noise were subtracted from the image stack. Living bacteria were labelled in green, dead bacteria in red, signals appearing in both channels were labelled in orange. For the analysis first yeast and mucosal cells were detected semi-automated and subtracted from the binary mask of both corresponding confocal stacks. Then values from red, green and orange were calculated for each picture as a count of all non-zero pixels in the entire binarized confocal stack. As orange values could not exactly be assigned to one group, they were counted as dead bacteria and removed from further calculations. After that numbers of living and dead bacteria for each stack were summed up to 100%. Finally, survival curves were plotted using Python™ 2.7. (Python Software Foundation).

2.9. Pyrosequencing analysis

2.9.1. Sample preparation and DNA extraction

Oral biofilm on the enamel-dentin slabs was compared at two points in time: T0 – directly after extraction from the human mouth and T3 – after 48 hours under laboratory conditions in the biofilm reactor. To harvest the biofilm slabs were glued into the lids of 1.5 ml reaction vials with a two-component adhesive so that it covered all surfaces except the standardized one carrying the biofilm. Then 200 µl ultra-pure water were added together with DNA-free sterile glass beads. The biofilm was then shredded in a tissue lyser for 2 min with the highest step. The DNA was further extracted by Michael Bozic, Medical University of Graz, Institute of Hygiene, Microbiology and Environmental Medicine, mixing it with 380 µl MagNA Pure Bacterial Lysis Buffer (Roche Applied Science, Germany) and 20 µl proteinase K solution (20mg/ ml). Cell wall digestion at 65 °C for 10 minutes was terminated by a 10 minutes' heat inactivation at 95 °C. Solutions were transferred to MagNA Pure Compact Sample Tubes and DNA isolated on the MagNA Pure Compact instrument according to the manufacturer's instructions. MagnaPure LC DNA III Isolation Kit (Bacteria, fungi) and the bacterial purification protocol III were used (Roche Diagnostics, Germany). DNA was eluted in 50 µl elution buffer and stored at -20 °C until further processing.

2.9.2. Pyrosequencing preparation and FLX454 run

The Roche FLX 454 sequencer was used for the pyrosequencing analysis (Center for Medical Research Graz, Core Facility Molecular Biology). For the amplification of the 16S rRNA gene one way read fusion primers with the template specific sequences F27 3'-AGAGTTTGATCCTGGCTCAG-5' and R534 3'- ATTACCGCGGCTGCTGGC-5' were used (Lib-L kit, Primer A, Primer B, Roche 454 Life Science, Branford, CT, USA). These primers target the hypervariable regions V1-V3 (Baker et al. 2003; Watanabe et al. 2001). MIDs and adaptor sequences were assigned as shown in Table 2.

PCR was performed in triplicates (25 µl each) containing the Fast Start High Fidelity Buffer, 200 µm dNTPs, 1.25U High Fidelity Enzyme, PCR-grade water (all Roche Diagnostics, Mannheim, Germany), 0.4 µm of the barcoded primers (Eurofins MWG, Ebersberg, Germany) and 5 µl total genomic DNA. Negative controls were also prepared in triplets using PCR-grade water instead of the genomic DNA. PCR conditions were chosen as follows: initial denaturation at 95 °C for 3 minutes, 30-35 cycles denaturation at 95 °C for 45 seconds, annealing at 55 °C for 45 seconds and extension at 72 °C for 1 minute followed by a final extension at 72 °C for 7 minutes. Amplicons were then purified and collected using the WAVE apparatus, a denaturing HPLC (Transgenomic Inc., Omaha, NE, USA). A linear gradient (12-17%) of acetonitrile in 0.1M triethylammoniumacetate (TEAA) was used for 10 minutes at 50 °C. The DNA was purified via NucleoFast ® 96 PCR plates (Macherey-Nagel, Düren, Germany). A vacuum pump was used according to the protocol and elution was performed in 30 µl elution buffer (Qiagen, Hilden, Germany). Quant-iT^{TM} PicoGreen® dsDNA Assays were then used to measure DNA concentrations according to the manufacturer's instructions (Life Technologies, CA, USA). Thirty barcode labeled amplicons were then pooled equimolar. The Bio Analyzer 2100 was then used to analyze these pools using a DNA 7500 kit (Agilent Technologies, Waldbronn, Germany). For the FLX run emulsion PCR of the pooled samples was then performed with the GS Titanium MV emPCR Kit and method (Lib-L) (Roche 454 Life Science, Branford, CT, USA) according to manufacturer's instructions. Equimolar pools of the 30 samples were then sequenced on a 2/4 PTP using the GS FLX Titanium Sequencing Kit XLR70 (Roche 454 Life Science, Branford, CT, USA) according to manufacturer's instructions. All samples were run on one plate to minimize bias.

Table 2: Adapter and MID assignment for the FLX 454 run. Sample name composition: P, person; T0 -T3, time points 0-3; 01-26, consecutive sample numbering. Sample o bk was the respective negative control. Sample containing a W were the repeats of the respective samples. Sequences finally consisted of: Titanium A adaptor (CCATCTCATCCCTGCGTGTCTCCGAC), a four-bases key sequence (TCAG) and the eigth-bases barcode (MID). For the reverse primer, the Titanium B adaptor (CCTATCCCCTGTGTGCCTTGGCAGTC) was used similar as above but without the MID sequence.

Sample	MIDs	MID sequences [5'-3']	Target sequences [5'-3']	Tit. Adaptor sequence	Key
PT0_01	MID 1	ACGAGTGCGT	AGAGTTTGATCCTGGCTCAG	CCATCTCATCCCTGCGTGTCTCCGAC	TCAG
PT0_03	MID 2	ACGCTCGACA	AGAGTTTGATCCTGGCTCAG	CCATCTCATCCCTGCGTGTCTCCGAC	TCAG
PT0_05	MID 3	AGACGCACTC	AGAGTTTGATCCTGGCTCAG	CCATCTCATCCCTGCGTGTCTCCGAC	TCAG
PT0_06	MID 4	AGCACTGTAG	AGAGTTTGATCCTGGCTCAG	CCATCTCATCCCTGCGTGTCTCCGAC	TCAG
PT0_07	MID 5	ATCAGACACG	AGAGTTTGATCCTGGCTCAG	CCATCTCATCCCTGCGTGTCTCCGAC	TCAG
PT0_08	MID 6	ATATCGCGAG	AGAGTTTGATCCTGGCTCAG	CCATCTCATCCCTGCGTGTCTCCGAC	TCAG
PT0_09	MID 7	CGTGTCTCTA	AGAGTTTGATCCTGGCTCAG	CCATCTCATCCCTGCGTGTCTCCGAC	TCAG
PT0_10	MID 8	CTCGCGTGTC	AGAGTTTGATCCTGGCTCAG	CCATCTCATCCCTGCGTGTCTCCGAC	TCAG
PT0_12	MID 10	TCTCTATGCG	AGAGTTTGATCCTGGCTCAG	CCATCTCATCCCTGCGTGTCTCCGAC	TCAG
PT0_13	MID 11	TGATACGTCT	AGAGTTTGATCCTGGCTCAG	CCATCTCATCCCTGCGTGTCTCCGAC	TCAG
PT0_14	MID 13	CATAGTAGTG	AGAGTTTGATCCTGGCTCAG	CCATCTCATCCCTGCGTGTCTCCGAC	TCAG
PT0_15	MID 14	CGAGAGATAC	AGAGTTTGATCCTGGCTCAG	CCATCTCATCCCTGCGTGTCTCCGAC	TCAG
PT0_16	MID 15	ATACGACGTA	AGAGTTTGATCCTGGCTCAG	CCATCTCATCCCTGCGTGTCTCCGAC	TCAG
PT0_17	MID 16	TCACGTACTA	AGAGTTTGATCCTGGCTCAG	CCATCTCATCCCTGCGTGTCTCCGAC	TCAG
PT0_18	MID 17	CGTCTAGTAC	AGAGTTTGATCCTGGCTCAG	CCATCTCATCCCTGCGTGTCTCCGAC	TCAG
PT0_19	MID 18	TCTACGTAGC	AGAGTTTGATCCTGGCTCAG	CCATCTCATCCCTGCGTGTCTCCGAC	TCAG
PT0_20	MID 20	ACGACTACAG	AGAGTTTGATCCTGGCTCAG	CCATCTCATCCCTGCGTGTCTCCGAC	TCAG
PT0_21	MID 19	TGTACTACTC	AGAGTTTGATCCTGGCTCAG	CCATCTCATCCCTGCGTGTCTCCGAC	TCAG
PT0_22	MID 20	ACGACTACAG	AGAGTTTGATCCTGGCTCAG	CCATCTCATCCCTGCGTGTCTCCGAC	TCAG
PT0_23	MID 21	CGTAGACTAG	AGAGTTTGATCCTGGCTCAG	CCATCTCATCCCTGCGTGTCTCCGAC	TCAG
PT0_24	MID 22	TACGAGTATG	AGAGTTTGATCCTGGCTCAG	CCATCTCATCCCTGCGTGTCTCCGAC	TCAG
PT0_25	MID 26	ACATACGCGT	AGAGTTTGATCCTGGCTCAG	CCATCTCATCCCTGCGTGTCTCCGAC	TCAG
PT0_26	MID 24	TAGAGACGAG	AGAGTTTGATCCTGGCTCAG	CCATCTCATCCCTGCGTGTCTCCGAC	TCAG
PT1_26	MID 26	ACATACGCGT	AGAGTTTGATCCTGGCTCAG	CCATCTCATCCCTGCGTGTCTCCGAC	TCAG
PT2_26	MID 25	TCGTCGCTCG	AGAGTTTGATCCTGGCTCAG	CCATCTCATCCCTGCGTGTCTCCGAC	TCAG
PT3_01	MID 1	ACGAGTGCGT	AGAGTTTGATCCTGGCTCAG	CCATCTCATCCCTGCGTGTCTCCGAC	TCAG
PT3_03	MID 2	ACGCTCGACA	AGAGTTTGATCCTGGCTCAG	CCATCTCATCCCTGCGTGTCTCCGAC	TCAG
PT3_05	MID 3	AGACGCACTC	AGAGTTTGATCCTGGCTCAG	CCATCTCATCCCTGCGTGTCTCCGAC	TCAG
PT3_06	MID 4	AGCACTGTAG	AGAGTTTGATCCTGGCTCAG	CCATCTCATCCCTGCGTGTCTCCGAC	TCAG
PT3_07	MID 5	ATCAGACACG	AGAGTTTGATCCTGGCTCAG	CCATCTCATCCCTGCGTGTCTCCGAC	TCAG
PT3_08	MID 6	ATATCGCGAG	AGAGTTTGATCCTGGCTCAG	CCATCTCATCCCTGCGTGTCTCCGAC	TCAG
PT3_09	MID 7	CGTGTCTCTA	AGAGTTTGATCCTGGCTCAG	CCATCTCATCCCTGCGTGTCTCCGAC	TCAG
PT3_10	MID 8	CTCGCGTGTC	AGAGTTTGATCCTGGCTCAG	CCATCTCATCCCTGCGTGTCTCCGAC	TCAG
PT3_12	MID 10	TCTCTATGCG	AGAGTTTGATCCTGGCTCAG	CCATCTCATCCCTGCGTGTCTCCGAC	TCAG
PT3_13	MID 11	TGATACGTCT	AGAGTTTGATCCTGGCTCAG	CCATCTCATCCCTGCGTGTCTCCGAC	TCAG
PT3_14	MID 13	CATAGTAGTG	AGAGTTTGATCCTGGCTCAG	CCATCTCATCCCTGCGTGTCTCCGAC	TCAG
PT3_15	MID 14	CGAGAGATAC	AGAGTTTGATCCTGGCTCAG	CCATCTCATCCCTGCGTGTCTCCGAC	TCAG
PT3_16	MID 15	ATACGACGTA	AGAGTTTGATCCTGGCTCAG	CCATCTCATCCCTGCGTGTCTCCGAC	TCAG
PT3_17	MID 16	TCACGTACTA	AGAGTTTGATCCTGGCTCAG	CCATCTCATCCCTGCGTGTCTCCGAC	TCAG
PT3_18	MID 17	CGTCTAGTAC	AGAGTTTGATCCTGGCTCAG	CCATCTCATCCCTGCGTGTCTCCGAC	TCAG
PT3_19	MID 18	TCTACGTAGC	AGAGTTTGATCCTGGCTCAG	CCATCTCATCCCTGCGTGTCTCCGAC	TCAG
PT3_20	MID 19	TGTACTACTC	AGAGTTTGATCCTGGCTCAG	CCATCTCATCCCTGCGTGTCTCCGAC	TCAG
PT3_21	MID 21	CGTAGACTAG	AGAGTTTGATCCTGGCTCAG	CCATCTCATCCCTGCGTGTCTCCGAC	TCAG
PT3_22	MID 22	TACGAGTATG	AGAGTTTGATCCTGGCTCAG	CCATCTCATCCCTGCGTGTCTCCGAC	TCAG
PT3_23	MID 23	TACTCTCGTG	AGAGTTTGATCCTGGCTCAG	CCATCTCATCCCTGCGTGTCTCCGAC	TCAG
PT3_24	MID 24	TAGAGACGAG	AGAGTTTGATCCTGGCTCAG	CCATCTCATCCCTGCGTGTCTCCGAC	TCAG
PT3_25	MID 25	TCGTCGCTCG	AGAGTTTGATCCTGGCTCAG	CCATCTCATCCCTGCGTGTCTCCGAC	TCAG
PT3_26	MID 27	ACGCGAGTAT	AGAGTTTGATCCTGGCTCAG	CCATCTCATCCCTGCGTGTCTCCGAC	TCAG
PTW3_26	MID 28	ACTACTATGT	AGAGTTTGATCCTGGCTCAG	CCATCTCATCCCTGCGTGTCTCCGAC	TCAG
PWT0_26	MID 23	TACTCTCGTG	AGAGTTTGATCCTGGCTCAG	CCATCTCATCCCTGCGTGTCTCCGAC	TCAG

2.9.3. Analysis of the pyrosequencing data with QIIME

In a first step pyrosequencing amplicon raw reads were denoised using the Acacia software (Bragg et al. 2012). The parameter file used was:

```
FASTQ=FALSE
FILTER_N_BEFORE_POS=350
FLOW_CYCLE_STRING=TACG
FLOW_KEY=TCAG
MAXIMUM_MANHATTAN_DISTANCE=13
MAX_RECURSE_DEPTH=2
MAX_STD_DEV_LENGTH=2
MIN_FLOW_TRUNCATION=150
MIN_READ_REP_BEFORE_TRUNCATION=0.0
OUTPUT_DIR=D:\Users\klugba\HTI\DATA_PYROANALYSIS\acaciaresults\r1
OUTPUT_PREFIX=reg1
QUAL_LOCATION=D:\Users\klugba\HTI\Results_Pyro_HTI\fasta\1.TCA.454Reads.qual
REPRESENTATIVE_SEQUENCE=Mode
SIGNIFICANCE_LEVEL=-9
SPLIT_ON_MID=FALSE
TRIM_TO_LENGTH=
TRUNCATE_READ_TO_FLOW=
MID_OPTION=NO_MID
MID_FILE:
```

After this denoising, sequence data was further analyzed with QIIME pipeline version 1.9.1 as follows (Caporaso, Kuczynski, et al. 2010). Mapping files containing SampleID, BarcodeSequence, LinkerPrimerSequence and metadata as timepoint, PatientID and Descriptions were checked and merged using the commands **validate_mapping_file.py** and **merge_mapping_files.py**. As MIDs were used twice, two files were created. For barcode/sample assignment and filtering of low-quality reads **split_libraries.py** was used with a maximum sequence length of 600 bases and 0 maximum ambiguous bases. To concatenate data from both files again the command **cat** was used. Operational Taxonomic Units (OTUs) were then picked with **pick_de_novo_otus.py**. This command comprises several functions: A 97% similarity is used to group sequences into OTUs. Only one of these sequences is then used as representative for the respective OTU for further analysis with pyNAST based on the Greengenes 16S rRNA gene database (Caporaso, Bittinger, et al. 2010; DeSantis et al. 2006). Taxonomy is assigned with the RDP Classifier (Wang et al. 2007). The alignment was then filtered prior to tree building and positions with gaps deleted and specified with 0 in the lanemask. FastTree was then used for phylogenetic tree calculation and an OTU table was created (Price et al. 2009). ChimeraSlayer

implementation, **identify_chimeric_seqs.py**, identified chimera on the PyNAST-aligned representative sequences. The **filter_fasta.py** function then sorted out chimeria. **Filter_alignement.py** generated a tree based on the alignment against the template from PyNAST. After this filtering a phylogenetic tree related to the OTUs found in this study was produced using the **make_phylogeny.py** command. The numbers of UCLUST sorted OTUs were then listed using the respective taxonomy file and excluding the chimeric sequences found with ChimeraSlayer using **make_otu_table.py**. This table was subsequently converted into the biom file format with **biom summarize-table** for further applications. Finally, all singletons were removed with **filter_otus_from_otu_table.py**. All biofilm files created were also converted into text files with **biom convert**. Taxa were summarized through plots with **summarize_taxa_through_plots.py**. The alpha and beta diversity of the so produced data was then analyzed as follows. First an alpha rarefaction was performed with **alpha_rarefaction.py** using an upper limit of 100 for the rarefaction depth. Then alpha diversity was generated with **alpha_diversity.py** calculating chao1, PD_whole_tree, simpson, shannon, observed_otus and ace. Betadiversity was calculated using **beta_diversity.py** based on non-phylogenetic metrics as Euclidean, Bray-Curtis and Pearson and the phylogenetic metrics unweighted and weighted UniFrac (Lozupone et al. 2010). Finally, plots were created using **beta_diversity_through_plots.py** and **make_2d_plots.py**.

2.9.4. Analysis of the pyrosequencing data with SPSS, R and Matlab

SPSS 21.0 and R 3.3.0 and 3.3.1 were used for downstream analysis of the previously generated data on all hierarchical levels by Katharina Eberhard (CMR, Medical University of Graz). In SPSS normal distribution was tested with the Shapiro Wilk's Test before calculating median, 25^{th} and 75^{th} percentile. To compare T0 and T3 values Wilcoxon signed-rank test with Bonferroni correction for multiple comparison was used seeing all values with a $p < 0.05$ as statistically significant.

The analysis in R was performed with scripts written by Christian Westendorf. Heat maps based on relative abundances were plotted in R version 3.3.0 and the phyloseq package and plot_heatmap function within (McMurdie and Holmes 2012; Rajaram and Oono 2010). Further, correspondence analysis was performed in R 3.3.1 using the Vegan Package 2.4. To exclude bias, OTUs with zero counts at all points in time were

removed from the data file. The biplots are shown in site-specific scaling. Matlab R2016 was used to calculate the Log2fold change (log2FC). All OTUs being kingdom bacteria and having a relative abundance of over 2% were included. Then all species abundances were averaged per point in time. The log2FC was subsequently calculated using the formula: L2FC = $\log_2$(T3) – $\log_2$(T0) with the respective averages. All values equal to 0 were removed. Respective genera were finally plotted. Data from the absolute abundances of the heat map was used excluding 7 OTUs of which always one point in time had zero values.

3. Results

3.1. Dental splints

The palatal expanders examined in this study carried thick biofilm visible to the eye after four months in the oral cavity (Figure 15). The biofilm on top of the expanders reached a thickness of more than a millimeter. The red line in Figure 15 surrounds such a biofilm on a freshly removed palatal expander.

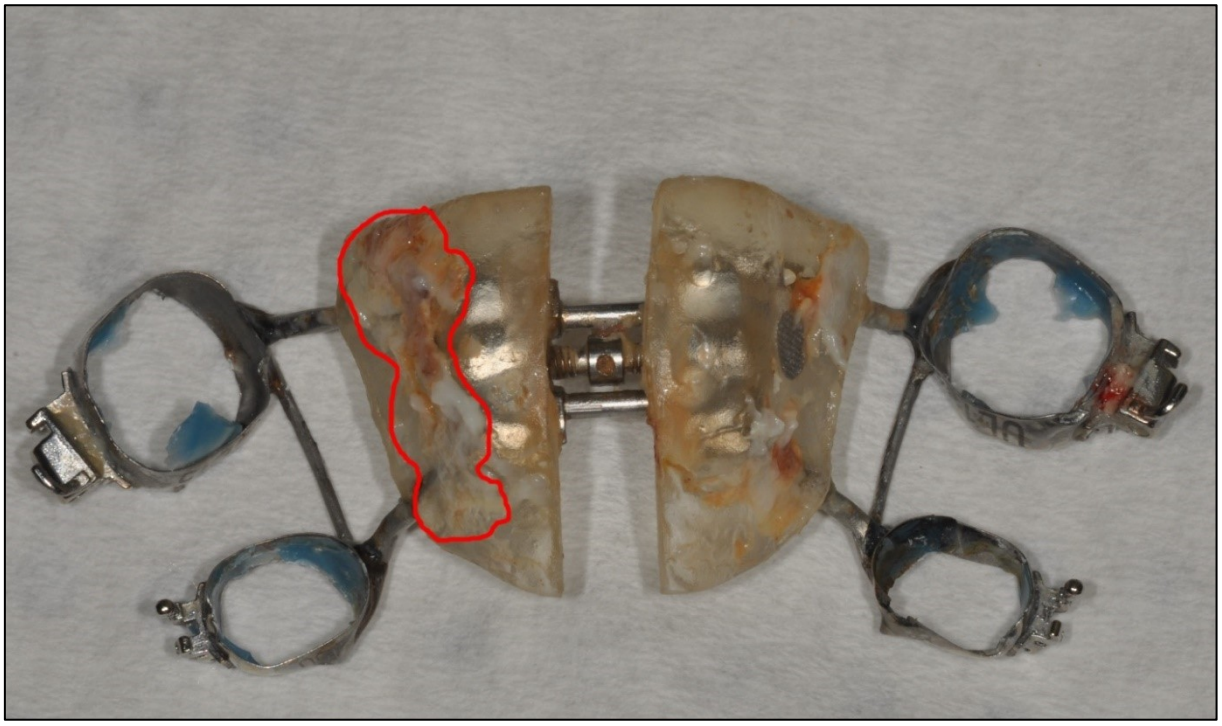

Figure 15: Palatal expander worn for four months with thick biofilm on top (red line).

The research splint developed in this study could be proven to work for *in vivo* biofilm growth. Easy transfer of the biofilm to a biofilm reactor was demonstrated. Disturbance of the biofilm was minimized through an easy handling design. Tooth slabs carrying the biofilm could be clipped out as shown in Figure 16 and transferred to BHI medium in seconds and without touching the biofilm.

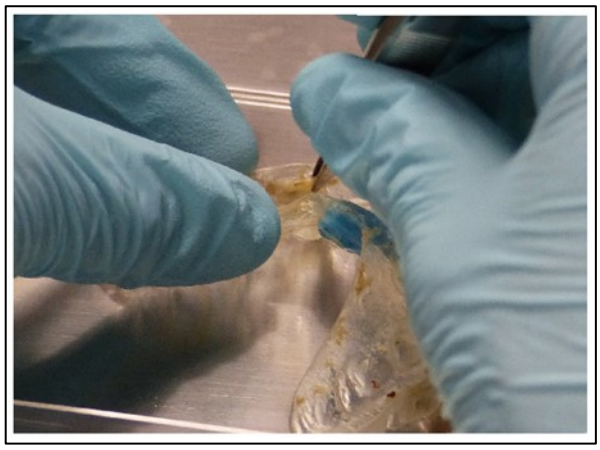

Figure 16: Clipping out the enamel-dentin slab from the research splint.

Also, the two sensors could quickly be removed to retrieve the logged data. The empty dental splint was discarded.

3.2. Analysis of the CLSM data

Several hundred Gigabyte of stack data were generated with CLSM using FISH- and the live/dead stained samples. All this data was evaluated qualitatively. Blurred images were removed before further analysis.

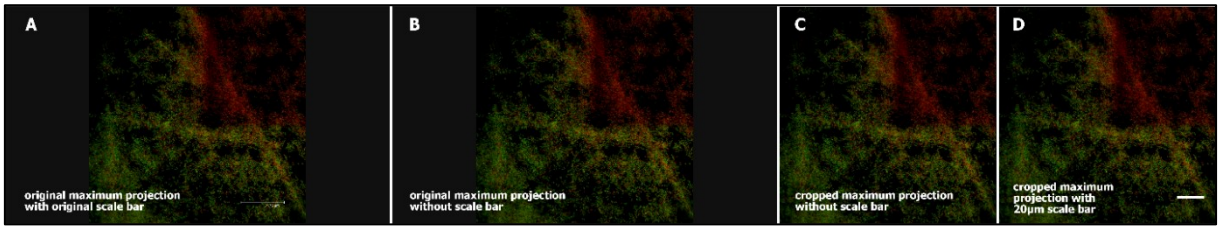

Figure 17: Processing of the CLSM maximum projections. A: original maximum projection showing the scale bar generated by the Leica software. B: The same maximum projection without the scale bar. C: Cropped maximum projection where grey frames were removed. D: Cropped maximum projection with new 20 µm scale bar.

Figure 17 shows how the maximum projections gained from the Leica software were processed. Panel A shows the original projection with the 31.75 µm scale bar inserted by the program. In panel B, the same picture is shown without the scale bar. This picture was then cropped as shown in panel C, taking off the grey margins left and right. Finally, a 20 or 40 µm scale bar was inserted (panel D).

3.2.1. Fluorescence *in situ* hybridization of oral biofilm on palatal expanders

FISH stained specific bacterial groups and also species on the palatal expanders and on the enamel-dentin slabs. The following figures show maximum projections of confocal stacks. Figure 18 shows a 2D overlay of CLSM stack data. The biofilm was stained with EUBmix, staining most bacteria (green), and LGCmix, staining all *Firmicutes* (yellow). Huge clusters of coccoid *Firmicutes* were found as the dominant phylum next to other bacteria.

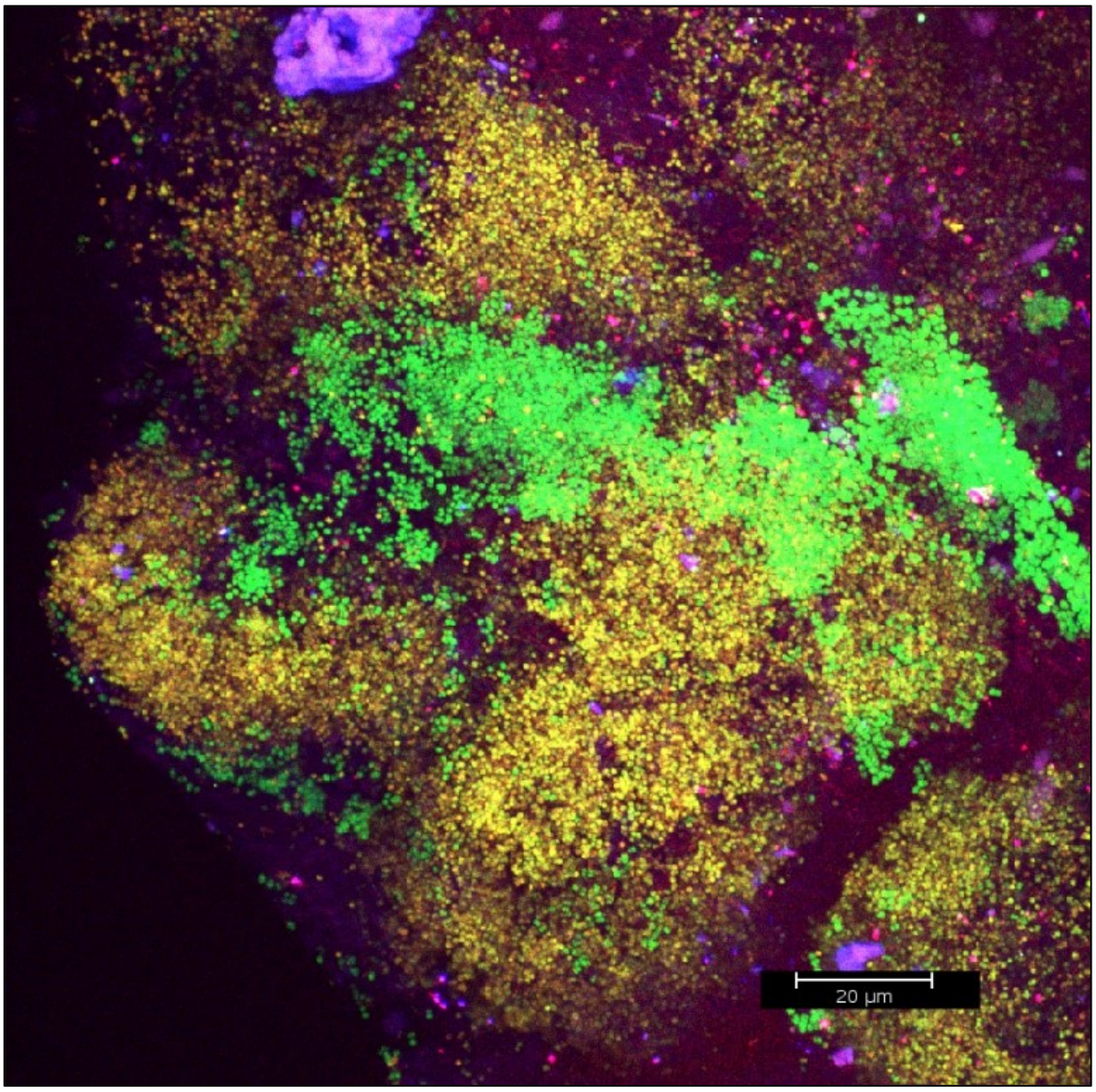

Figure 18: CLSM image: differentiation of a specific bacterial group. 2D overlay of 3D CLSM stack data. Biofilm stained with EUBmix (green, most bacteria) and LGCmix (yellow, *Firmicutes*). *Reproduced from Klug et al. 2011 with permission of JoVE.*

Using probe POGI, staining *Porphyromonas gingivalis*, a species known to be a periodontopathogen was found in rather high numbers in the biofilm (Figure 19, yellow dots). Also different morphologies can be found in Figure 19. In the left lower corner a bunch of big bacteria forming groups of four can be found beside the smaller cocci.

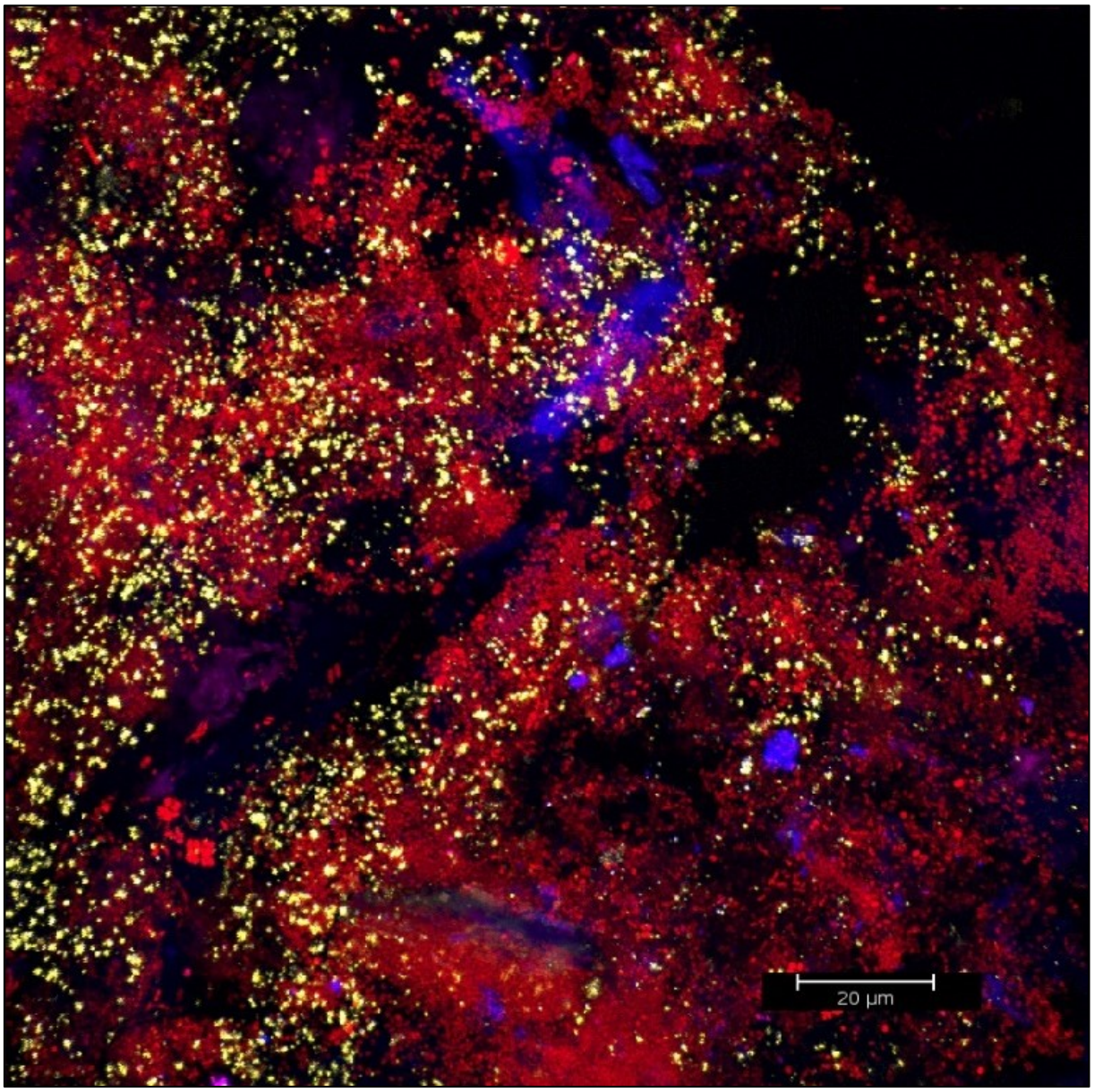

Figure 19: CLSM image: differentiation of a specific bacterial group. 2D overlay of 3D CLSM stack data. Biofilm stained with EUBmix (red, most bacteria), Bac303 (blue, *Bacteroidetes*) and POGI (yellow, *Porphyromonas gingivalis*). *Reproduced from Klug et al. 2011 with permission of JoVE*.

Figure 20 shows large clusters of coccoid bacteria in green, protruding from the biofilm surface. These clusters showed a typical mushroom structure as described before.

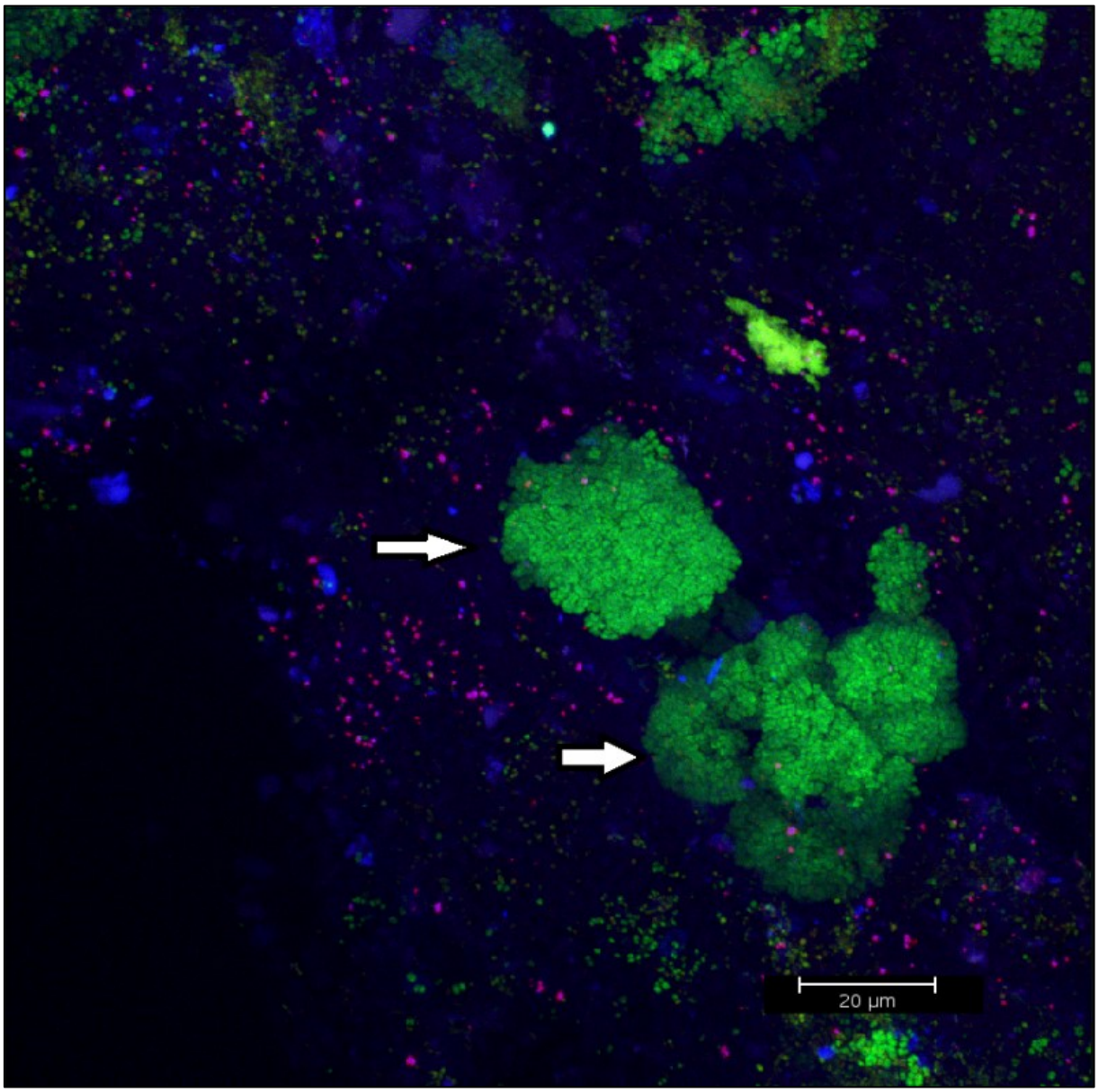

Figure 20: CLSM image: differentiation of specific morphologies. 2D overlay of 3D CLSM stack data. Biofilm stained with EUBmix (green, most bacteria). Large clusters of coccoid bacteria (arrows). *Reproduced from Klug et al. 2011 with permission of JoVE*.

Also, in Figure 21 these clusters of coccoid bacteria (red), probably *Streptococcus*, can be found. These clusters exhibit diameters of over 40 µm.

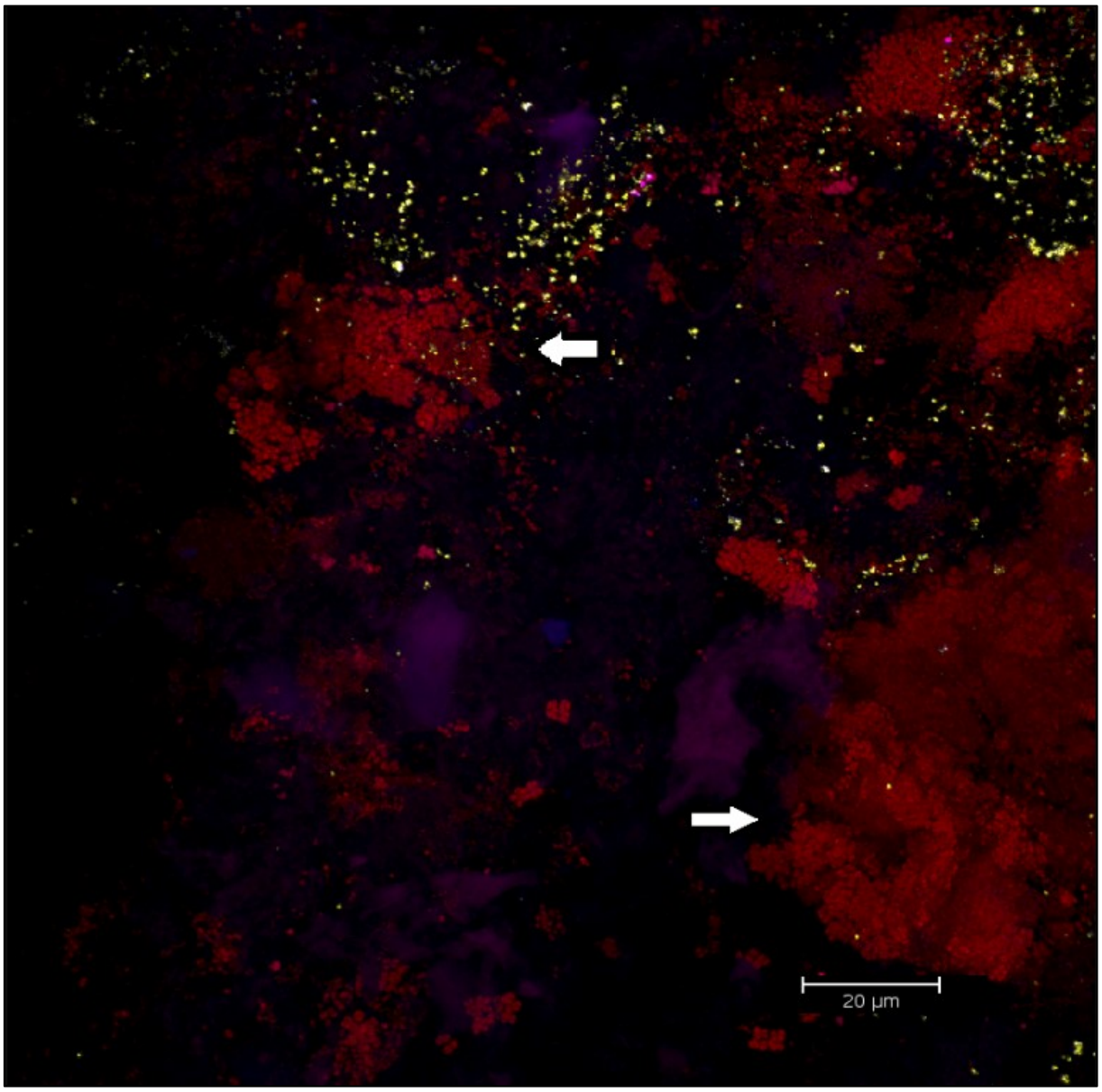

Figure 21: CLSM image: differentiation of specific morphologies. 2D overlay of 3D CLSM stack data. Biofilm stained with EUBmix (red, most bacteria). Large clusters of coccoid bacteria (arrows). *Reproduced from Klug et al. 2011 with permission of JoVE*.

In Figure 22 different bacterial morphologies can be found in the clusters. Coccoid bacteria there lie next to rods (all in red). Big red species, yeast respectively, are lying in between (left to the scale bar). Due to their autofluorescence they are here found in the same excitation range as EUBmix stained bacteria.

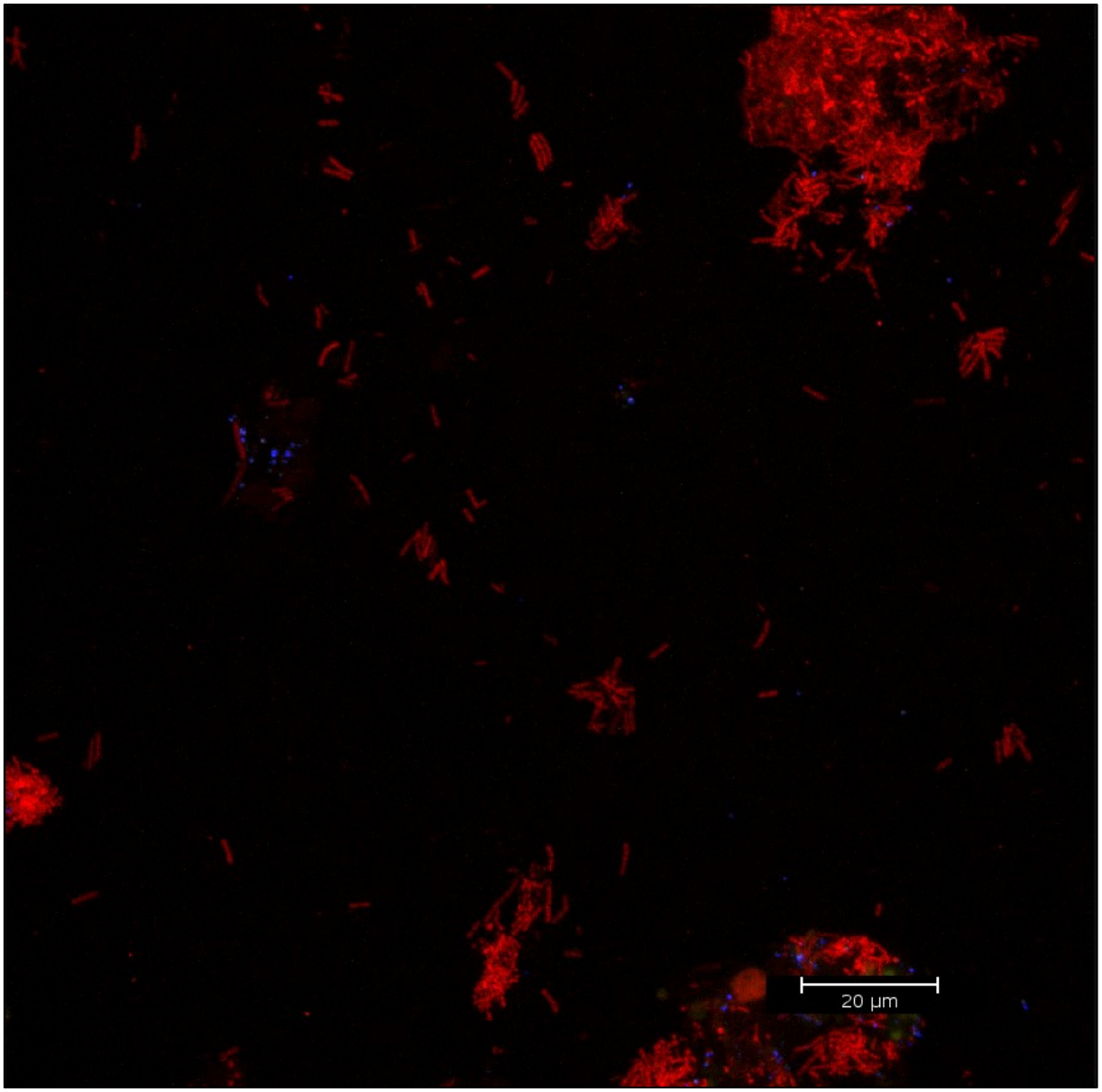

Figure 22: CLSM images: differentiation of specific morphologies. 2D overlay of 3D CLSM stack data. Biofilm stained with EUBmix (red, most bacteria). Coccoid (arrow below) and filamentous bacteria (arrow above) can be distinguished. *Reproduced from Klug et al. 2011 with permission of JoVE*.

FISH and CLSM showed different types of bacteria and huge clusters of the same morphotypes right next to each other on the palatal expanders. Also, on the enamel-dentin slabs used in the research splint, different taxonomic groups could be found with FISH.

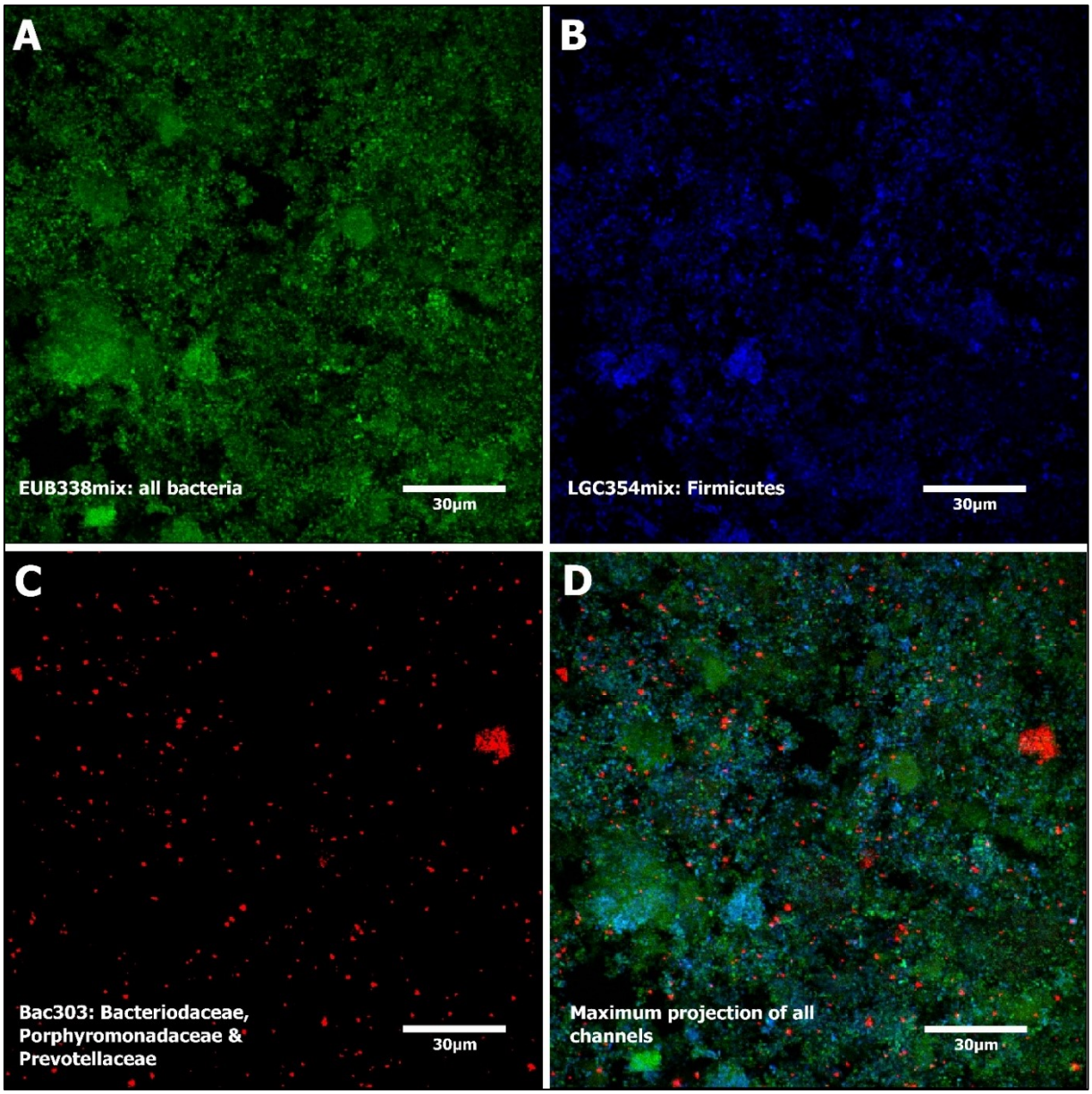

Figure 23: FISH staining of oral biofilm on enamel-dentin slabs. A: most bacteria stained in green (EUB338mix), B: Firmicutes stained in blue (LGC354mix), C: Bacteroidaceae, Porphyromonadaceae and Prevotellaceae stained in red (Bac303) and D: a maximum projection of all channels. *Reproduced from Klug et al. 2016 with permission of Frontiers.*

Figure 23 shows biofilm stained with EUB388mix (most bacteria), LGC354mix (*Firmicutes*) and Bac303 (*Bacteroidaceae*, *Porphyromonadaceae* and *Prevotellaceae*). Panel A to C show the certain bacterial species stained with the respective probes. Panel D presents the maximum projection of all three channels showing *Firmicutes* in turquois as they are stained by EUB388mix and LGC354mix. Also, on these enamel-dentin slabs the bacteria formed clusters similar in appearance and size to the ones found on the palatal expanders, before, best shown in panel A. The dominant phylum in this biofilm was *Firmicutes* was shown in panel B and in the

maximum projection. All green bacteria in the maximum projection belong to phyla other than the *Firmicutes*.

3.3. Live/dead staining

More than 104Gb of confocal stack data was generated with CLSM of the live/dead stained biofilms. Besides the information on the bacterial survival, live/dead staining also allows for analysis of the biofilm composition in respect to different bacterial morphotypes and the cells we assume to be yeast.

Figure 24 highlights the most prominent structures found during CLSM analysis of live/dead stained biofilm. In the first row, panel A and B show yeast cells, big red structures, lying in and around the bacterial biofilm (indicated by the white arrows). Due to their autofluorescence, they appear in red. Also, different sizes of bacteria can be found in A. Bigger dead cells (red) are surrounded by smaller living cells (green) in the huge cluster on the left. Small rods form their own cluster left of the big coccoid one. The panels C and D present very long chains of coccoid bacteria. Here living and dead bacteria seem to stay directly connected. At T3 such structures could reach lengths of more than 200 µm. In E and F different bacterial morphotypes are found right next to each other. Rods and coccoid bacteria form dense clusters with each other. In F clusters of dead bacteria seem to be overgrown by living bacteria.

3.3.1. CLSM analysis of the live/dead staining

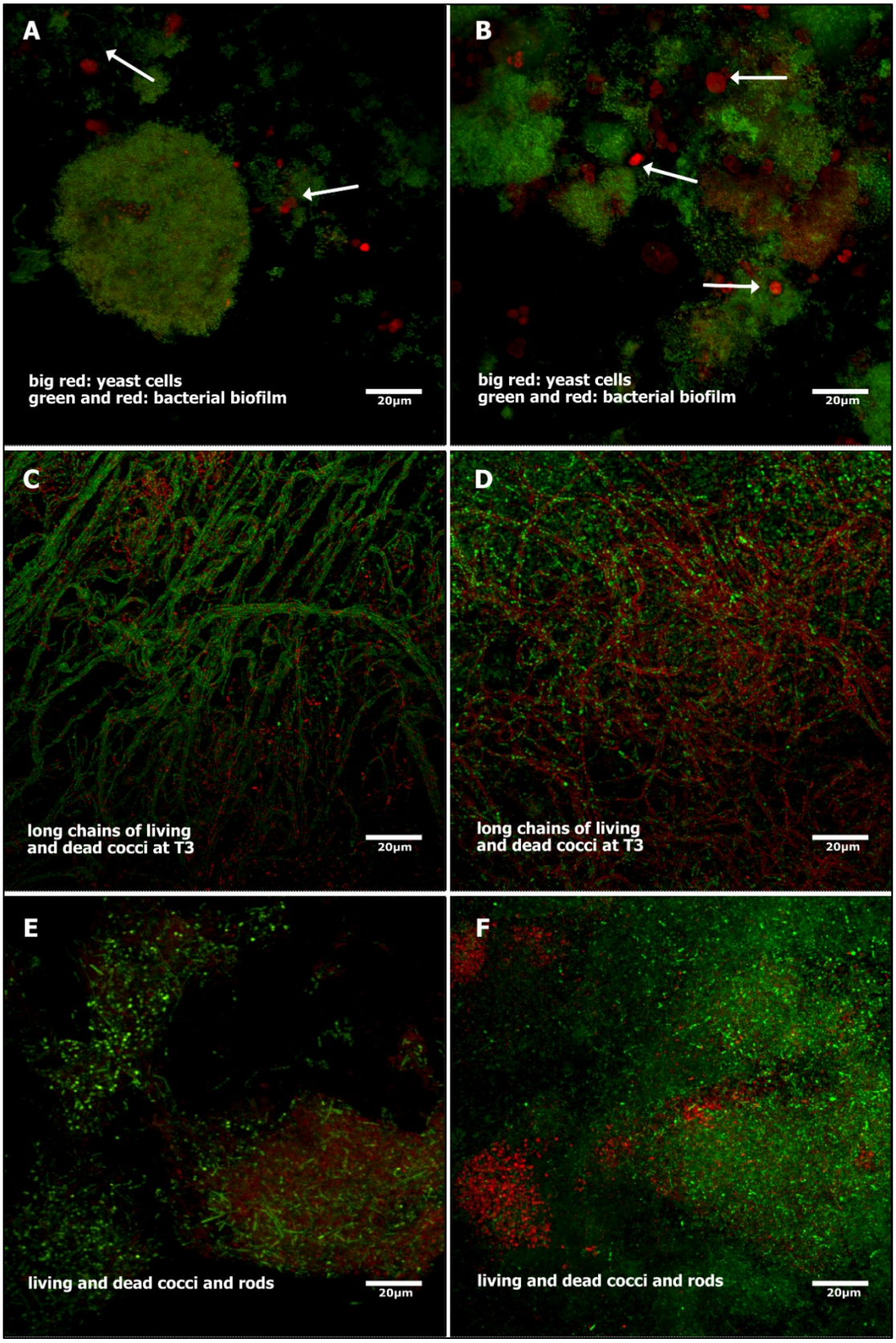

Figure 24: Biofilm structures found with live/dead staining. Living bacteria appear in green, dead in red. White arrows in A and B indicate yeast (big red structures) lying in the middle of huge clusters of variably sized coccoid bacteria. C and D: long chains of coccoid bacteria at T3. E and F: rods and coccoid bacteria lying next to each other in the biofilm.

Before analyzing the measured proportions of living and dead bacteria on the enamel-dentin slabs used in the research splint, yeast (big red) and double stained bacterial cells (orange) were excluded from further evaluations.

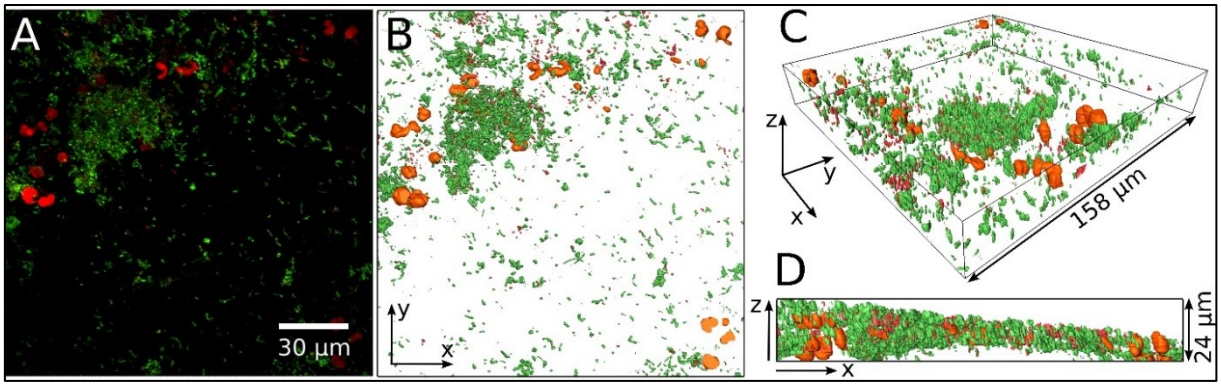

Figure 25: Example of yeast cells embedded in the bacterial biofilm. Maximum projection of the entire confocal stack of a life/dead stained biofilm (A). Green, living bacteria; red, dead bacteria and yeast. The prominent red cells are probably yeast cells and are visualized in orange in a 3D reconstruction of the biofilm (B–D). (B) Gives the top view while (C, D) show side views of the 3D reconstruction. *Reproduced from Klug et al. 2016 with permission of Frontiers.*

In Figure 25 large round yeast cells (red) lie in between the bacterial biofilm (green, living bacteria and red, dead bacteria). Showing the same emission spectrum as dead cells, their signals had to be removed before calculating live/dead ratios.

Figure 26 shows exemplarily the structure and composition of the oral biofilm on an enamel-dentin slab over time. All points in time (T0-T3) represent a time series of the same subject. Panels A show maximum projection of the respective confocal stack (green, living bacteria; red, dead bacteria). Panels B to D show 3D reconstructions of the respective confocal stack in the same coloring. A top view is presented in B, C and D show side views.

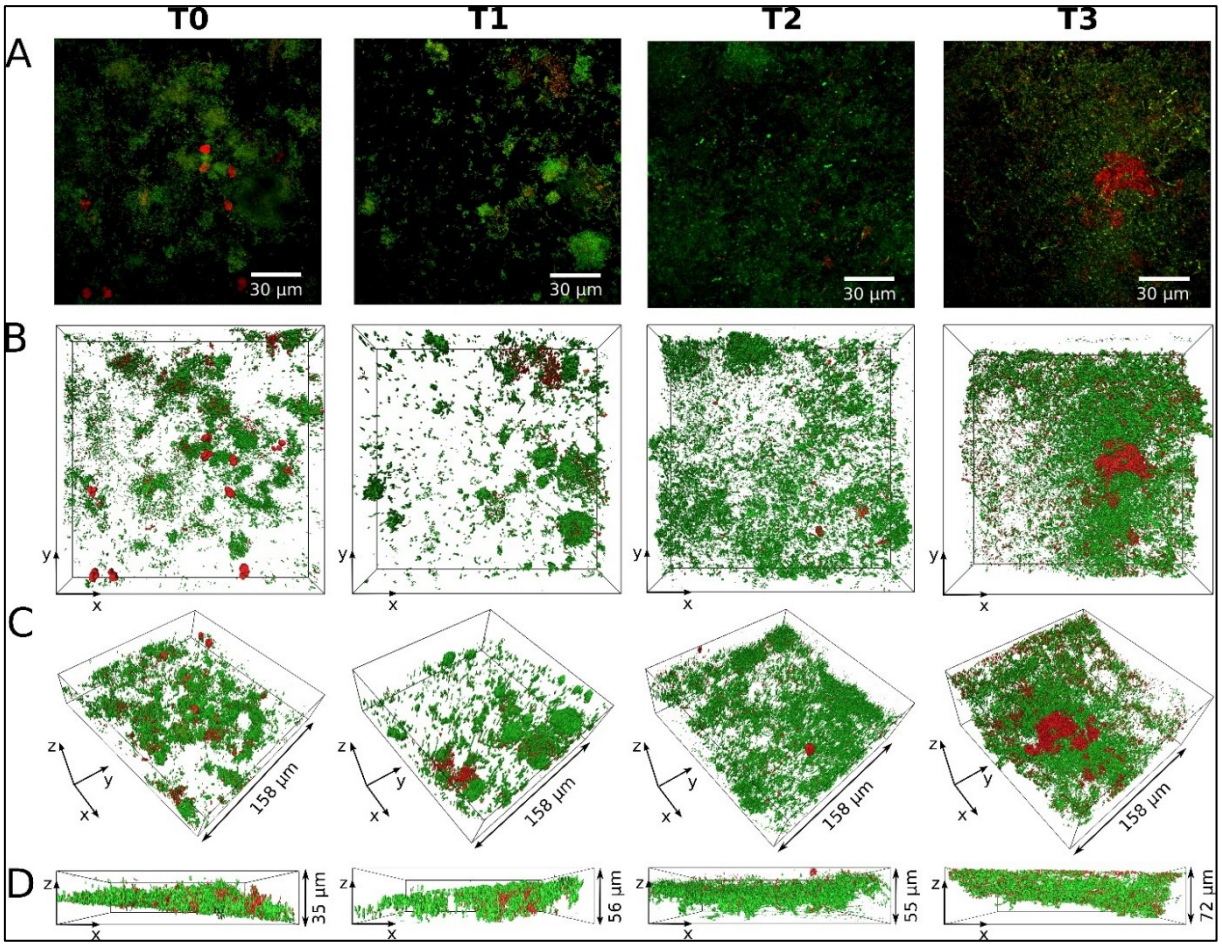

Figure 26: Structure and composition of the biofilm over time. Life/dead stained biofilms from one subject (S21) for all points in time (T0–T3) are shown. (A) Maximum projections of the respective confocal stacks with living bacteria stained in green and dead bacteria stained in red. The 3D reconstructions are displayed in (B–D) with the same coloring as in (A). (B) Top view of the 3D reconstruction. (C, D): Side views of the 3D reconstruction. *Image taken from Klug et al. 2016.*

The live/dead ratio calculated from these confocal stacks over all four points in time were then evaluated, results are shown below.

3.3.2. Quantification and statistical analysis of the live/dead CLSM data

After removal of blurred data and subjects with missing data points, biofilms from 17 subjects could be evaluated in live/dead analysis. For each subject mean values of the living bacteria are given in Figure 27. Higher numbers of living bacteria are presented in darker blue. Darker orange numbers instead show a low number of living bacteria. Grey panels represent values of 48-52% living bacteria. Standard deviations are given below the respective mean value.

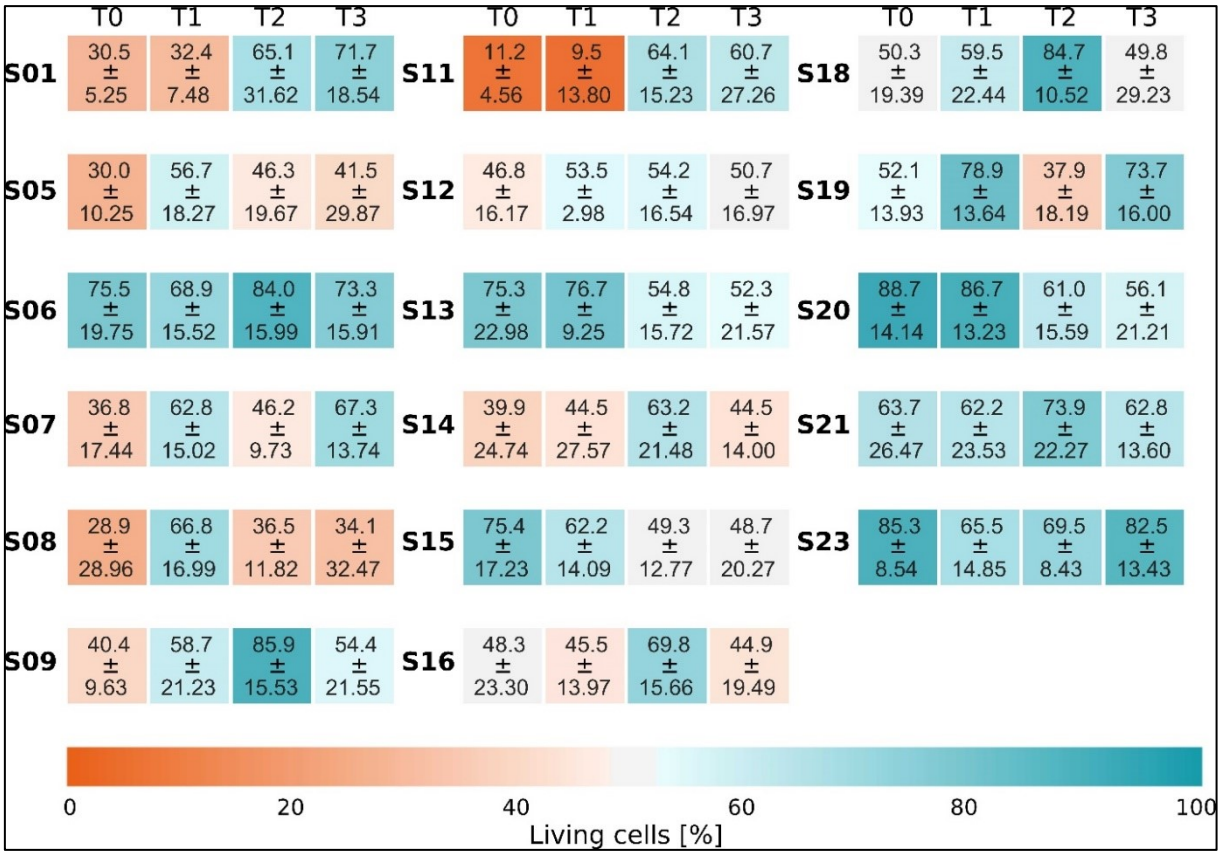

Figure 27: Life/Dead ratio. Each time series displays the fraction of living bacteria at each point in time and belongs to one individual subject. Each subject is labeled by a running number (SXX) on the left of the respective time series. The different sampling points in time are displayed by four panels (T0, T1, T2, T3). Values are the average over the fractions of living bacteria ± the sample standard deviation. *Reproduced from Klug et al. 2016 with permission of Frontiers.*

In all cases having more than 50% living bacteria at T0, also the subsequent points in time showed survival numbers of over 50%. In some case, T0 and T3 varied strongly. S01 i.e. shows an increase of living bacteria of over 40%. S20 instead lost over 30% living cells. The standard deviations varied from 2.98% to 31.47%.

Figure 28 presents the data given above as survival curves. Living bacteria are given in blue with the respective standard deviation as light blue shadow. The dead bacteria are shown in orange with a light orange shadow showing again the standard deviations. Survival curves are presented as single plots as the single experiments were independent from each other and could not be merged.

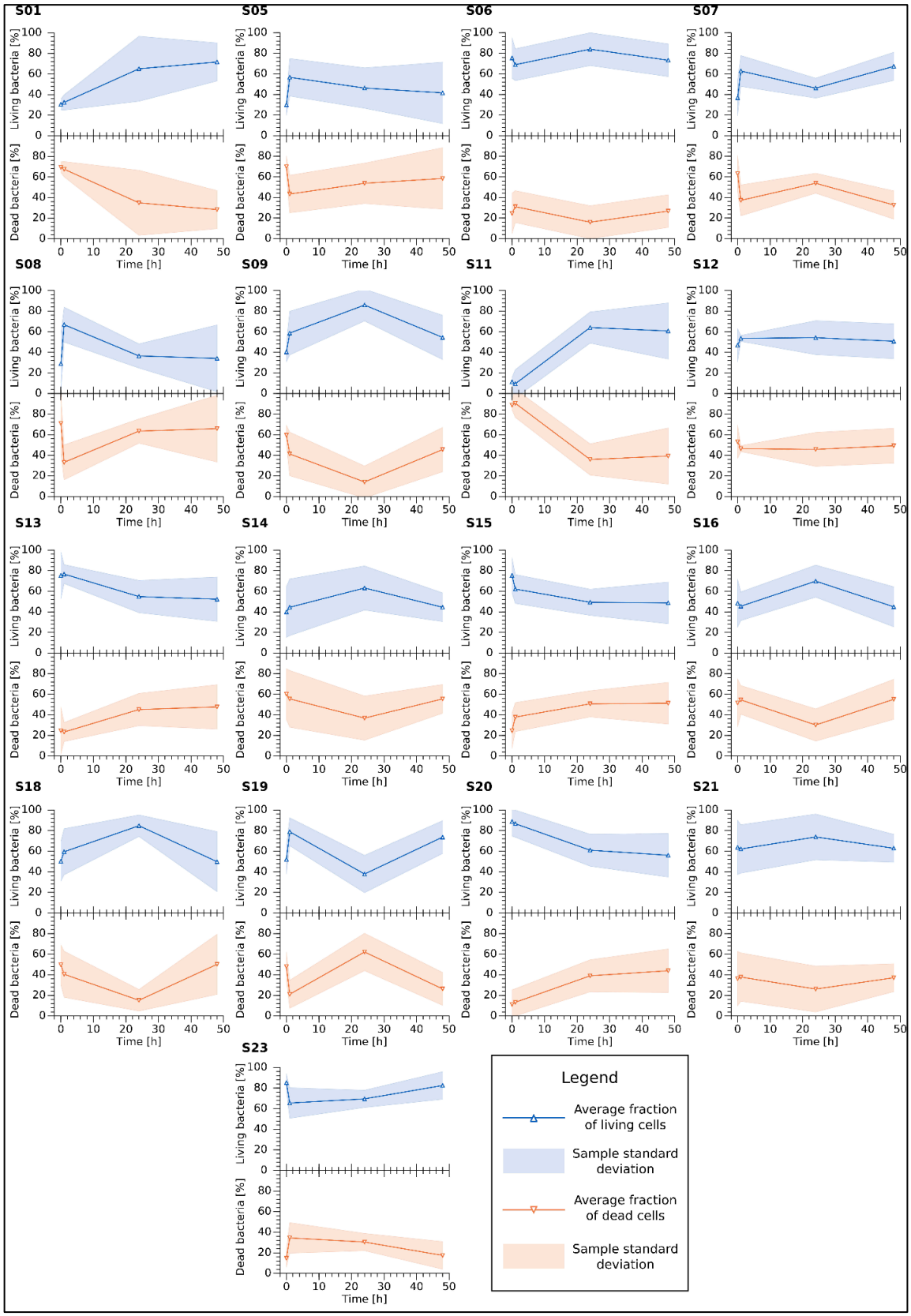

Figure 1: Development of the Life/Dead Ratio over time. Each individual plot displays the evolution of the fractions of living and dead bacteria over time. Each plot belongs to one subject and the running number (SXX) is given on the top left corner. Within an individual plot, each data point represents the mean over all fractions of living (top plot) and dead bacteria (bottom plot) at the particular point in time. The colored region gives the sample standard deviation. *Image taken from Klug et al. 2016.*

Variable courses of bacterial survival were found in the single subjects as already described above. Though no complete loss of living fractions was found. The biggest shift towards more living or more dead bacteria was found at T2. Most curves reached around T0 values at T3.

3.4. Analysis of the pyrosequencing data

A total count number of 139,303 sequences was produced with 454-pyrosequencing. After quality filtering, trimming, denoising and cleaning the data from chimera and singletons 119733 sequences remained for further analysis.

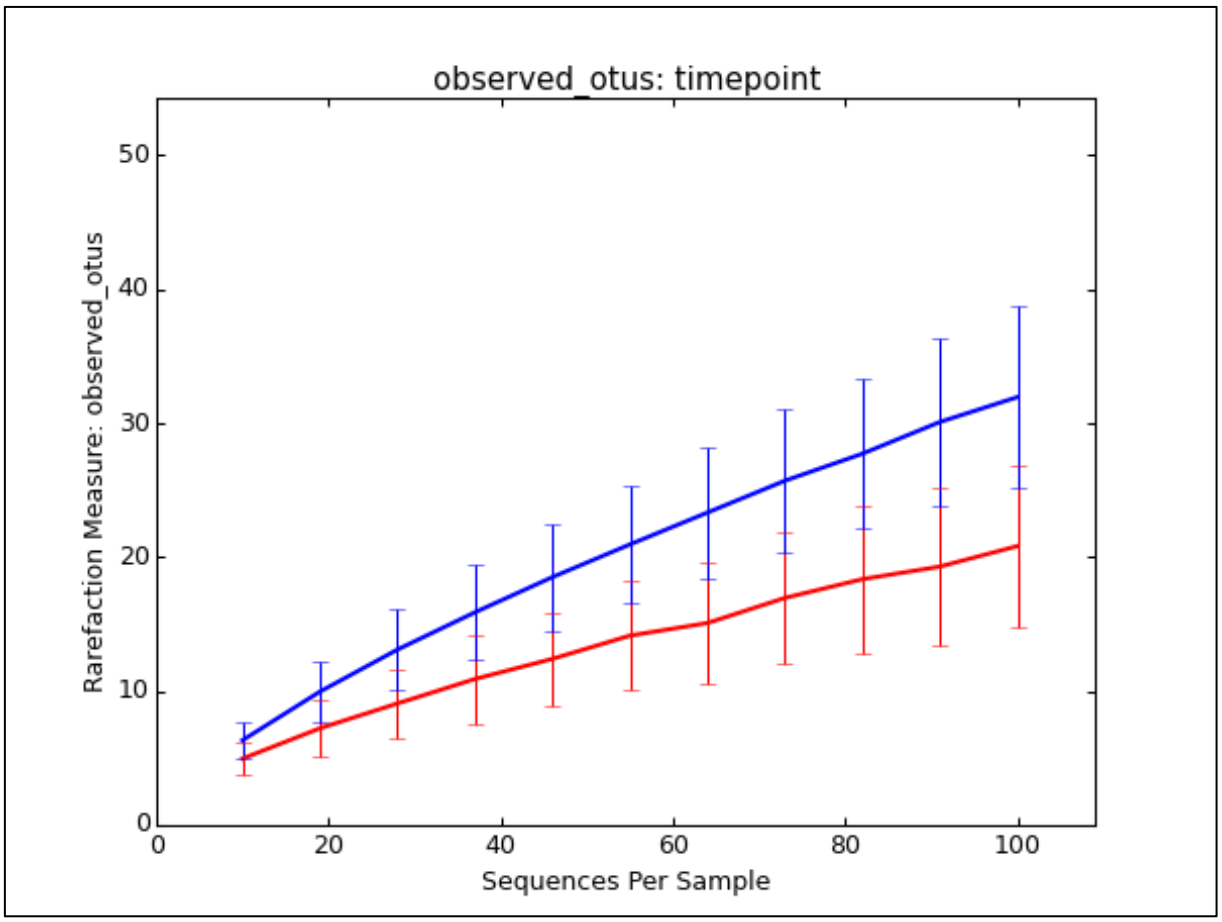

Figure 29: Rarefaction curves. Alpha-diversity of the observed OTUs. Blue line timepoint 0, red line timepoint 3.

Figure 29 gives an overview on the Alpha-diversity comparing T0 (blue) and T3 (red) plotted as rarefaction curve of the observed OTUs. The number of observed OTUs of T3 here generally lies below the one of T0.

Table 3: Alpha-diversity comparison of T0 and T3. SubjectID explanation: P = person, T = timepoint (0 or 3). XX = number of the subject.

SubjectID	Chao1	PD_whole_tree	Simpson	Shannon	observed_otus	ACE
PT0.01	177.44	3.84	0.52	1.62	88	220.19
PT3.01	358.91	8.89	0.81	3.85	185	402.56
PT0.03	335.04	7.76	0.80	3.69	180	331.00
PT3.03	514.40	13.16	0.87	4.75	257	530.99
PT0.05	346.68	8.29	0.75	3.51	203	386.40
PT3.05	417.89	11.52	0.91	4.87	230	444.41
PT0.06	476.17	7.96	0.80	3.95	236	495.08
PT3.06	439.52	11.97	0.89	4.87	246	489.87
PT0.07	427.11	8.30	0.59	2.85	193	457.37
PT3.07	453.08	11.27	0.83	4.27	229	528.72
PT0.08	203.32	4.27	0.79	3.37	151	242.90
PT3.08	296.35	12.05	0.91	4.73	199	325.16
PT0.09	288.00	5.71	0.87	3.96	159	298.46
PT3.09	465.89	11.36	0.93	5.16	230	488.23
PT0.10	271.53	9.32	0.80	3.38	170	308.16
PT3.10	536.95	14.39	0.90	5.11	265	566.56
PT0.12	292.25	6.22	0.82	3.47	147	343.81
PT3.12	440.20	15.10	0.89	5.00	284	491.94
PT0.13	278.37	3.61	0.53	1.93	143	341.52
PT3.13	371.22	11.45	0.82	4.20	238	395.18
PT0.14	243.28	7.12	0.75	3.26	162	278.69
PT3.14	294.81	8.54	0.43	2.19	164	334.49
PT0.15	449.34	8.65	0.77	3.50	199	480.57
PT3.15	403.15	9.75	0.95	5.45	229	434.24
PT0.16	234.04	5.55	0.77	3.04	126	291.79
PT3.16	358.45	10.24	0.92	5.01	212	403.71
PT0.17	364.03	6.96	0.71	2.99	175	467.48
PT3.17	381.33	10.57	0.89	4.58	198	366.44
PT0.18	413.20	8.22	0.81	4.08	206	432.79
PT3.18	555.50	15.07	0.86	5.11	314	591.38
PT0.19	360.78	7.91	0.73	3.11	170	390.45
PT3.19	379.57	11.73	0.70	3.51	220	439.04
PT0.20	571.25	11.62	0.59	2.97	211	561.04
PT3.20	231.58	9.79	0.65	3.02	136	267.95
PT0.21	390.75	10.75	0.77	3.33	199	458.64
PT3.21	344.66	9.71	0.92	5.12	224	388.36
PT0.22	428.73	13.80	0.93	5.27	254	483.45
PT3.22	441.12	13.91	0.71	3.86	251	511.40
PT0.23	245.56	5.79	0.79	3.29	140	317.27
PT3.23	429.52	10.21	0.85	4.42	236	495.67
PT0.24	299.65	3.85	0.37	1.71	137	348.66
PT3.24	506.23	13.62	0.85	4.24	259	561.06
PT0.25	421.47	10.71	0.62	3.27	238	467.00
PT3.25	281.10	4.89	0.61	2.83	158	311.55

Table 3 presents a comparison of the alpha diversity. The sample names are explained by: P (Pyrosequencing), T0 and T3 (points in time) and the sample IDs (1-25). One subject's samples are presented below each other.

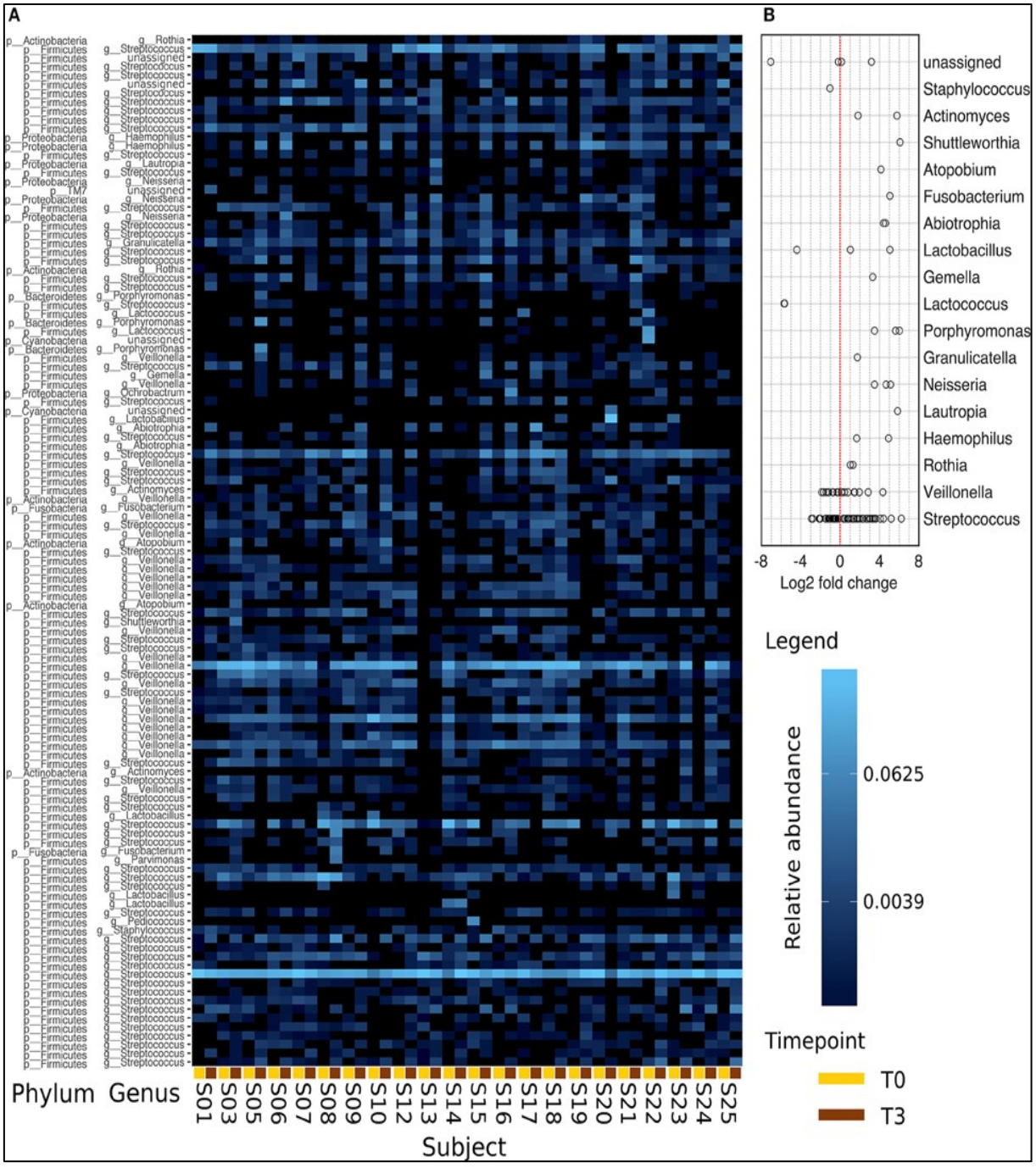

Figure 30: Comparison of the abundances between T0 and T3. Data is derived from the 117 most abundant OTUs found in all samples. Panel (A) presents a heat map of this data assigned to the respective genera with a relative abundance >2%. T0 and T3 of each subject are positioned next to each other (line below: T0, yellow; T3, brown). The color scaling is logarithmic. In (B), the log2 fold change calculated on the absolute abundances data of (A) is plotted. Seven OTUs were excluded as their average abundance in one of the points in time was equal to 0. *Reproduced from Klug et al. 2016 with permission of Frontiers*

The overall diversity is low as demonstrated by relatively low Simpson values. More OTUs were mostly found at T3. Higher Chao1 values at T3 suggest that these higher OTU counts are mainly rare species (Table 3).

The relative abundance of the 117 most abundant OTUs found in all samples is presented in Figure 30A assigned to their respective genera. The points in time are shown in yellow (T0) and brown (T3). One subject's samples lie next to each other. Light blue colors stand for a high relative abundance. Dark blue colours stand for a low relative abundance. Signatures of *Streptococcus* and *Veillonella* here show the strongest signals. Lactobacilli instead appear in very small numbers. The single subjects have a strong individuality although patterns seem to resemble each other in the biggest groups. Figure 30B presents the log2FC analysis of the 18 OTUs presented in the heat map. Excluding the unassigned genera, *Lactococcus* have lost the most showing a log2FC of almost 6. Also, Staphylococci lost in relative abundance. *Veillonella*, *Streptococcus* and lactobacilli showed loss and gain in relative abundance relatively equal with *Streptococcus* showing a higher positive log2FC. *Rothia*, *Granulicatella*, and *Gemella* present groups with a log2FC of one to three. All *Actinomyces*, *Shuttleworthia*, *Atopobium*, *Fusobacterium*, *Abiotrophia*, *Porphyromonas*, *Neisseria*, *Lautropia* and *Haemophilus* show a log2FC of 4 to 7.

Figure 31 shows a comparison of T0 and T3 on genus level. PCoA and CA were applied to find different or similar patterns of the two points in time. In the Panels A – C PCoA is shown in the three dimensions explaining the highest variations. In A, PC2 is plotted against PC1 with 9.29% and 14.32% variation explained respectively. In B, PC2 is shown against PC3 explaining 9.29 and 5.77% of the variation. Panel C shows PC3 versus PC1 together explaining 20.09% of the variation. In Panel A and C T0 and T3 cluster in two groups. The third dimension (panel B) does not confirm this as T0 and T3 are equally distributed.

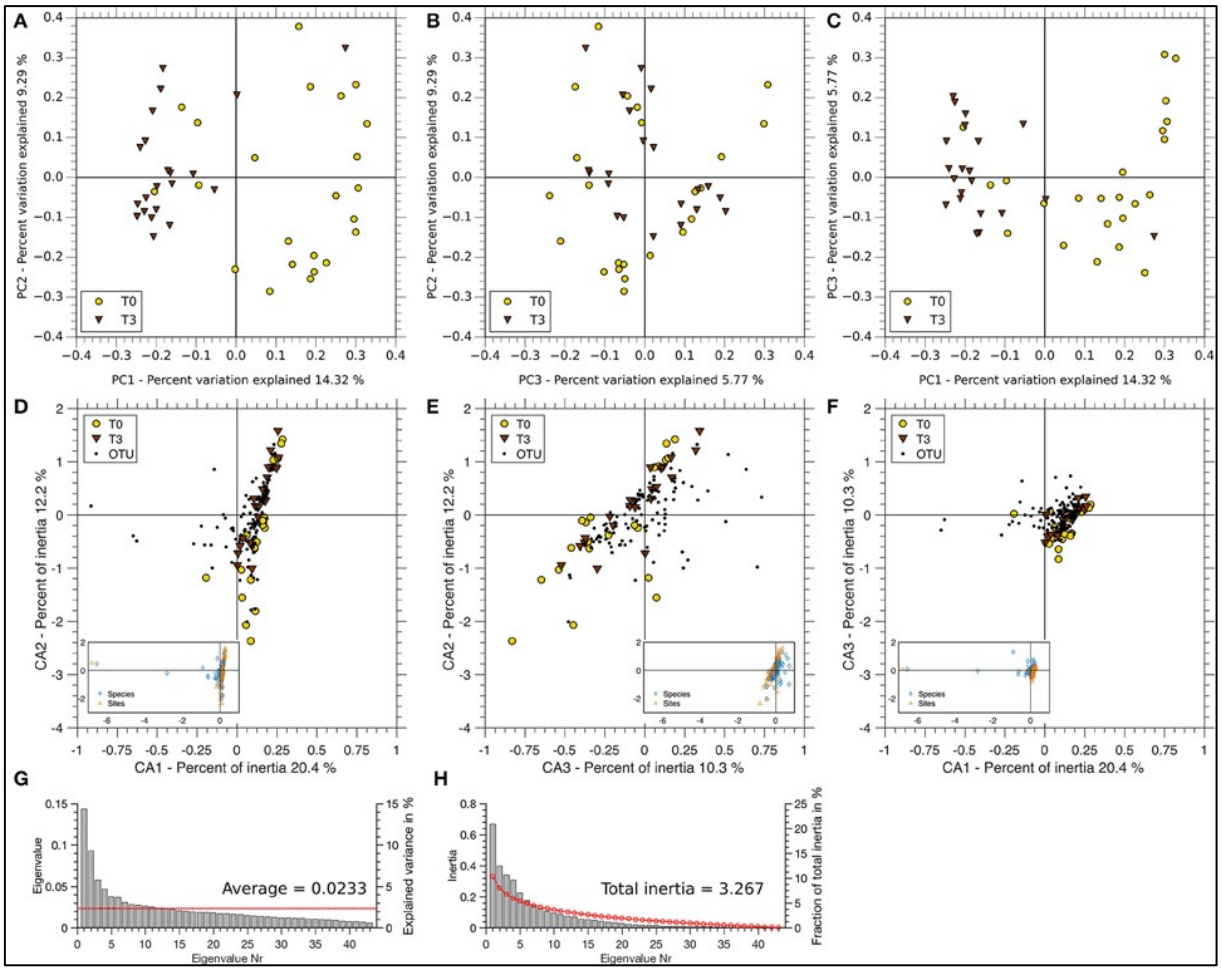

Figure 31: PCoA and CA comparison of T0 and T3 on genus level. (A–C) Variance of T0 (yellow) and T3 (brown) pyrosequencing data is shown in the three coordinates (PC1, PC2, PC3) with the highest support (summing up to 29.38%). (A) PC1 vs. PC2, (B) PC3 vs. PC2, and (C) PC1 vs. PC3. (D, F) Biplots of OTUs and samples are ordinated by correspondence analysis. (D) Axis 1 vs. Axis 2, (E) Axis 3 vs. Axis 2, and (F) Axis 1 vs. Axis 3. Full plots are shown in the respective small panels of each plot. All plots were scaled with respect to the sites (points in time). (G) Scree plot of the Eigenvalues derived by PCoA. The red line indicates the mean over all Eigenvalues. (H) Scree plot of the Eigenvalues derived by the CA. The red line shows the broken stick distribution. *Reproduced from Klug et al. 2016 with permission of Frontiers*.

The CA results can be found in the panels D to F. In D CA2 is shown against CA1, together explaining 32,6% of the variance found. Panel E presents CA2 against CA3 with 12.2% and 10.3% inertia respectively. Panel F finally shows CA3 against CA1 explaining the variance with a total of 20.7%. In all three plots, T0, T3 and the OTUs cluster together. The plots are scaled with respect to the points in time.

Figure 32 shows a comparison of T0 (top) and T3 (bottom) on genus level. A slight decrease in the number of Firmicutes (*Veillonella* and *Streptococcus*) is found in T3. In return the diversity increases over the 48 hours, meaning that smaller groups grew to a measurable size, in the biofilm reactor as has also been shown in Figure 30.

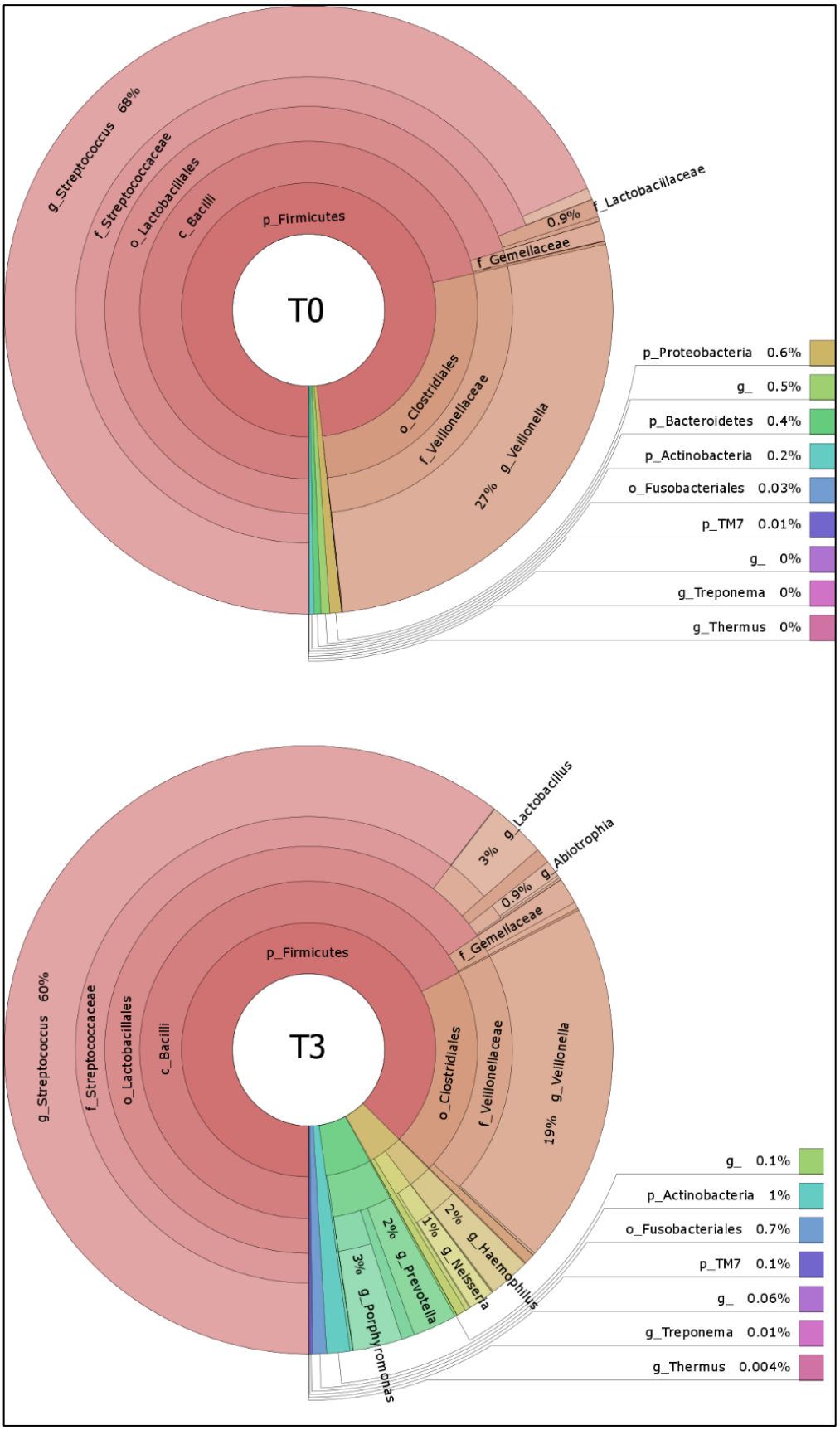

Figure 32: Hierarchy plot: comparison of T0 and T3. Rings from inside out: kingdom, phylum, class, order, family and genus level.

3.5. Statistical analysis on all taxonomic levels

The differences found through plotting the pyrosequencing data were statistically analyzed to find significant changes. Table 4 - Table 8 present this data. If data could not be assigned to a certain phylogenetic level, the next higher level is given in parenthesis.

Table 4: Statistical comparison of the pyrosequencing data on phylum level. A $p < 0.05$ was considered significant after Bonferroni correction. *Reproduced from Klug et al. 2016 with permission of Frontiers.*

Taxon Bacteriae	Time point 1 [%]			Time point 3 [%]			Wilcoxon signed-rank test	Wilcoxon signed-rank test (Bonferroni corr.)
Phylum	**25th**	**Median**	**75th**	**25th**	**Median**	**75th**	**p-value[#]**	**p-value adj.[##]**
Other	0.70	1.07	1.28	1.36	1.69	1.99	.0007	.0042
Actinobacteria	0.00	0.11	0.32	0.38	0.99	2.37	.0001	.0007
Bacteroidetes	0.00	0.01	0.77	0.70	3.20	8.91	.0000	.0002
Firmicutes	97.23	98.67	99.30	82.94	87.71	92.29	.0001	.0007
Fusobacteria	0.00	0.00	0.01	0.15	0.26	0.74	.0000	.0000
Proteobacteria	0.00	0.00	0.07	0.38	2.06	4.74	.0019	.0115

Statistical analysis on phylum level revealed significant changes in the relative abundance in all phyla (Table 4).

Table 5: Statistical comparison of the pyrosequencing data on class level. A $p < 0.05$ was considered significant after Bonferroni correction. *Reproduced from Klug et al. 2016 with permission of Frontiers.*

Taxon: Bacteriae	Time point 1 [%]			Time point 3 [%]			Wilcoxon signed-rank test	Wilcoxon signed-rank test (Bonferroni corr.)
Phylum/Class	**25th**	**Median**	**75th**	**25th**	**Median**	**75th**	**p-value[#]**	**p-value adj.[##]**
Other								
Other	0.70	1.07	1.28	1.36	1.69	1.99	.001	.006
Actinobacteria								
Actinobacteria	0.00	0.05	0.23	0.19	0.57	1.06	.001	.006
Coriobacteriia	0.00	0.00	0.01	0.00	0.15	0.29	.001	.006
Bacteroidetes								
Bacteroidia	0.00	0.01	0.75	0.45	3.15	8.85	.000	.000
Flavobacteriia	0.00	0.00	0.01	0.04	0.05	0.16	.002	.015
Firmicutes								
Bacilli	55.12	68.13	95.94	63.30	70.13	80.11	.235	1.000
Clostridia	3.48	27.18	42.81	7.01	14.85	27.29	.222	1.000
Fusobacteria								
Fusobacteriia	0.00	0.00	0.01	0.15	0.26	0.74	.000	.000
Proteobacteria								
Gammaproteobacteria	0.00	0.00	0.07	0.30	0.87	2.29	.004	.034

Looking at the class level, *Flavobacteriia* (*Bacteroidetes*) and the two classes with the highest relative abundance, *Bacilli* and *Clostridia* (both *Firmicutes*), did not change significantly over time (Table 5).

Table 6: Statistical comparison of the pyrosequencing data on order level. A $p < 0.05$ was considered significant after Bonferroni correction. *Reproduced from Klug et al. 2016 with permission of Frontiers*.

Taxon: Bacteriae	Time point 1 [%]			Time point 3 [%]			Wilcoxon signed-rank test	Wilcoxon signed-rank test (Bonferroni corr.)
Phylum/Order	**25th**	**Median**	**75th**	**25th**	**Median**	**75th**	**p-value**[#]	**p-value adj.**[##]
Other								
Other	0.70	1.07	1.28	1.36	1.69	1.99	.001	.008
Actinobacteria								
Actinomycetales	0.00	0.05	0.23	0.19	0.57	1.06	.001	.008
Coriobacteriales	0.00	0.00	0.01	0.00	0.15	0.29	.001	.008
Bacteroidetes								
Bacteroidales	0.00	0.01	0.75	0.45	3.15	8.85	.000	.000
Flavobacteriales	0.00	0.00	0.01	0.04	0.05	0.16	.002	.020
Firmicutes								
Other	0.00	0.01	0.06	0.00	0.04	0.10	.487	1.000
Bacillales	0.00	0.01	0.19	0.00	0.06	0.18	.417	1.000
Gemellales	0.00	0.00	0.07	0.12	0.77	1.42	.030	.355
Lactobacillales	54.76	67.99	90.88	62.02	67.11	78.17	.210	1.000
Clostridiales	3.48	27.18	42.81	7.01	14.85	27.29	.222	1.000
Fusobacteria								
Fusobacteriales	0.00	0.00	0.01	0.15	0.26	0.74	.000	.000
Proteobacteria								
Pasteurellales	0.00	0.00	0.03	0.30	0.80	2.29	.004	.051

Table 6 presents changes on order level. Here again the orders with the highest relative abundance belonging to the phylum Firmicutes did not change significantly. Also, *Pasteurellales* from the phylum Proteobacteria did not show a significant loss or gain. Still, single orders do show a change, although values are not significant.

Table 7: Statistical comparison of the pyrosequencing data on family level. A $p < 0.05$ was considered significant after Bonferroni correction. *Reproduced from Klug et al. 2016 with permission of Frontiers.*

Taxon: Bacteriae	Time point 1 [%]			Time point 3 [%]			Wilcoxon signed-rank test	Wilcoxon signed-rank test (Bonferroni corr.)
Phylum/Family	**25th**	**Median**	**75th**	**25th**	**Median**	**75th**	**p-value[#]**	**p-value adj.[##]**
Other								
Other	0.70	1.07	1.28	1.36	1.69	1.99	.001	.010
Actinobacteria								
Actinomycetaceae	0.00	0.04	0.13	0.06	0.27	0.86	.006	.094
Micrococcaceae	0.00	0.00	0.05	0.00	0.13	0.28	.008	.115
Coriobacteriaceae	0.00	0.00	0.01	0.00	0.15	0.29	.001	.010
Bacteroidetes								
Prevotellaceae	0.00	0.01	0.22	0.14	1.13	2.73	.001	.013
Firmicutes								
Other	0.00	0.01	0.06	0.00	0.04	0.10	.487	1.000
Staphylococcaceae	0.00	0.01	0.12	0.00	0.06	0.18	.369	1.000
Gemellaceae	0.00	0.00	0.07	0.12	0.77	1.42	.030	.444
Other	0.00	0.00	0.04	0.00	0.16	1.53	.004	.064
Carnobacteriaceae	0.09	0.23	0.37	0.61	1.56	2.19	.002	.025
Lactobacillaceae	0.00	0.00	1.28	0.00	0.00	0.06	.470	1.000
Streptococcaceae	54.57	65.96	88.78	47.97	61.05	75.04	.074	1.000
Lachnospiraceae	0.00	0.00	0.03	0.02	0.11	0.28	.000	.002
Veillonellaceae	3.43	27.17	42.78	6.80	13.99	27.23	.137	1.000
Proteobacteria								
Pasteurellaceae	0.00	0.00	0.03	0.30	0.80	2.29	.004	.064

On Family level *Prevotellaceae* (*Bacteroidetes*), *Coriobacteriaceae* (*Actinobacteria*), *Carnobacteriaceae* and *Lachnospiraceae* (both *Firmicutes*) changed significantly gaining in relative abundance (Table 7).

Finally, analyzing genus level, *Rothia* (*Actinomyces*), *Prevotella* (*Bacteroidetes*), *Granulicatella* (*Firmicutes*) and *Haemophilus* (*Proteobacteria*) changed significantly (Table 8). They again all gained in relative abundance over the 48 hours incubation *in vitro*. All other changes on genus level were not statistically significant.

Table 8: Statistical comparison of the pyrosequencing data on genus level. A $p < 0.05$ was considered significant after Bonferroni correction. *Reproduced from Klug et al. 2016 with permission of Frontiers.*

Taxon: Bacteriae	Time point 1 [%]			Time point 3 [%]			Wilcoxon signed-rank test	Wilcoxon signed-rank test (Bonferroni corr.)
Phylum/Genus	**25th**	**Median**	**75th**	**25th**	**Median**	**75th**	**p-value[#]**	**p-value adj.[##]**
Other								
Other	0.70	1.07	1.28	1.32	1.63	1.93	.000	.005
Actinobacteria								
Actinomyces	0.00	0.04	0.13	0.06	0.30	0.97	.001	.021
Rothia	0.00	0.00	0.05	0.00	0.13	0.32	.001	.009
Bacteroidetes								
Prevotella	0.00	0.01	0.22	0.15	1.02	2.44	.000	.006
Firmicutes								
Other (Bacilli)	0.00	0.01	0.06	0.00	0.04	0.10	.706	1.000
Staphylococcus	0.00	0.01	0.12	0.00	0.07	0.17	.548	1.000
(Gemellaceae)	0.00	0.00	0.07	0.12	0.77	1.24	.005	.091
(Lactobacillales)	0.00	0.00	0.04	0.00	0.12	1.50	.004	.073
Granulicatella	0.09	0.23	0.37	0.64	1.59	2.28	.000	.003
Lactobacillus	0.00	0.00	0.18	0.00	0.00	0.04	.700	1.000
Other (Streptococcaceae)	0.00	0.04	0.13	0.00	0.10	0.19	.768	1.000
(Streptococcaceae)	0.04	0.10	0.23	0.12	0.37	0.69	.005	.083
Streptococcus	53.42	61.96	88.38	48.44	60.83	73.97	.055	.930
Other (Lachnospiraceae)	0.00	0.00	0.01	0.00	0.00	0.11	.003	.058
Dialister	0.00	0.00	0.04	0.00	0.00	0.04	.240	1.000
Veillonella	3.43	27.15	42.78	6.69	13.38	27.05	.157	1.000
Proteobacteria								
Haemophilus	0.00	0.00	0.03	0.31	0.84	2.38	.000	.008

3.6. Temperature oscillations in the oral cavity

Temperature measurements performed with the two sensors Star Oddi® DST nano-T and TheraMon® Microsensor resulted in mean values around 35 °C during the 48 hours in the oral cavity. The minimum temperature lay below 10 °C, the maximum temperature reached 42 °C. Figure 33 shows eight temperature curves measured with the Star Oddi® DST nano-T during 48 hours in the oral cavity. The insertion and removal of the research splint carrying the sensor can clearly be seen at the beginning and the end of the measurement where all temperature curves rise from and drop again below 25 °C. The mean temperatures lay around 35 °C.

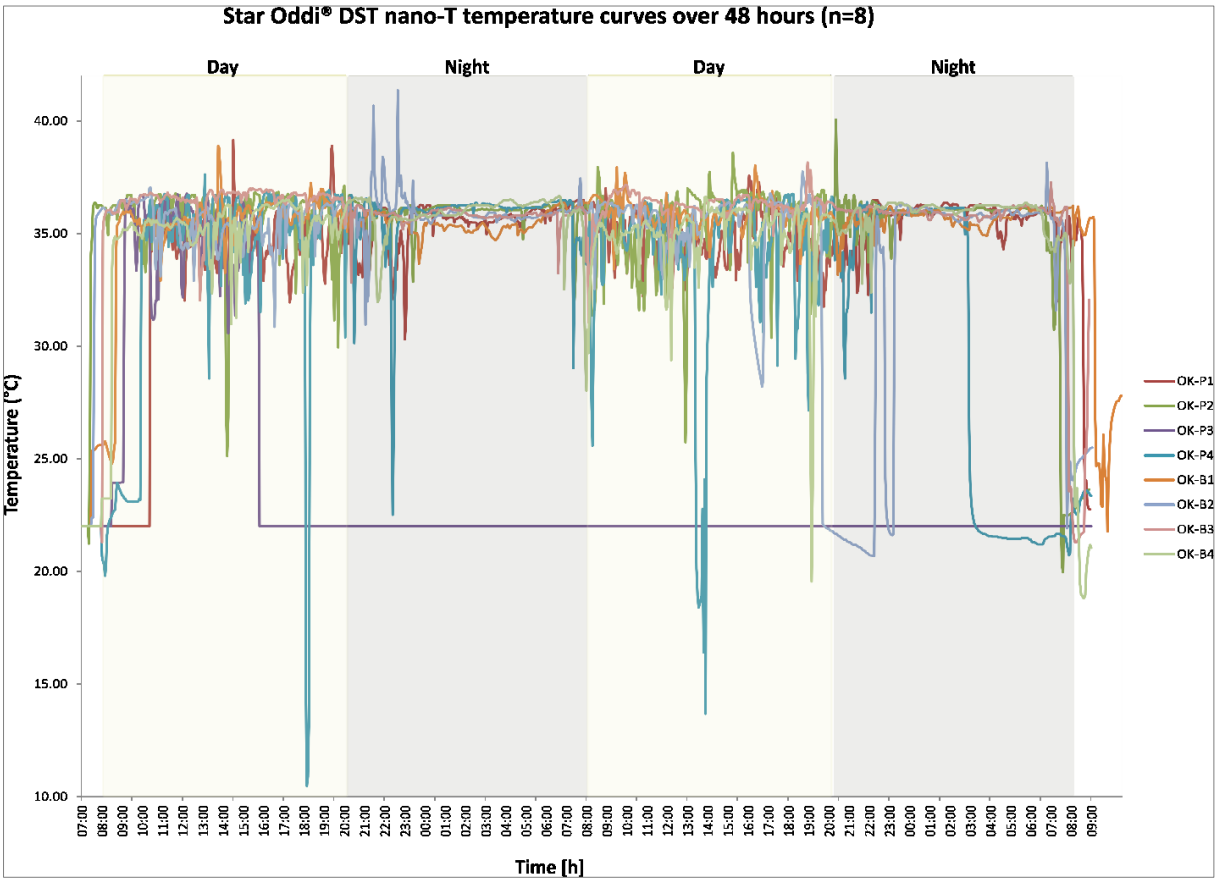

Figure 33: Temperature curves measured with the Star Oddi® DST nano-T. Data from 8 individual measurements are shown. Day and night phases are marked in yellow and grey. Lilac line (OK-P3) shows a premature termination of the measurements after 8 hours.

The curves show strong perturbations during the day phases but almost none during the night phases. OK-P3 presents a preterm removal of the splint after only five hours of wearing due to discomfort. In OK-P4 very low values down to 10 °C were found. The explanation therefore was found in the respective nutrition protocol that was included in this study and evaluated by Heidrun Frankl in her diploma thesis (diploma thesis data, Heidrun Frankl, Medical University of Graz, 2013). She found, that this volunteer ate ice cream at the respective point in time. Temperature elevation were in contrast to decreases less extreme. Only some peaks over 37 °C can be found in all curves. The maximum value only reached 42 °C although all volunteers also ate warm food.

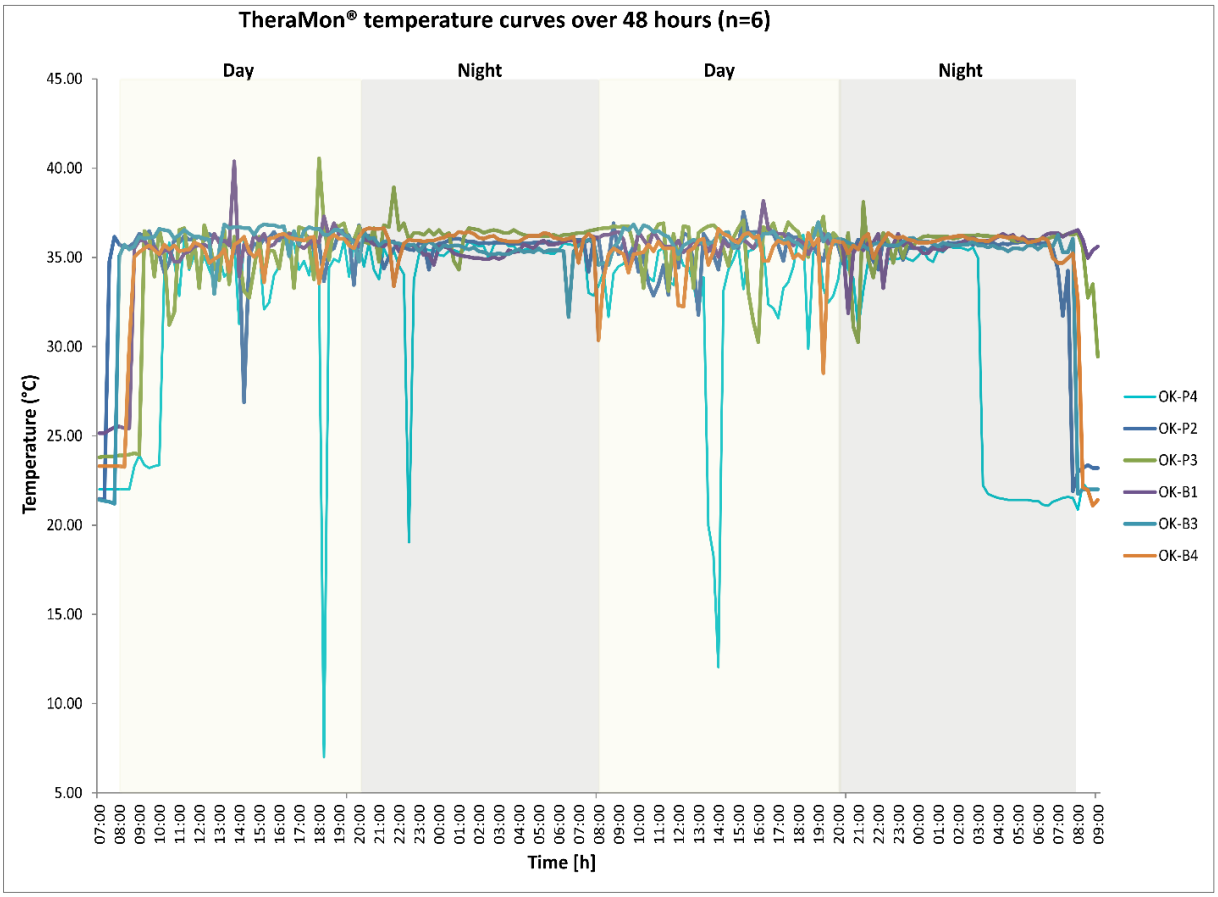

Figure 34: Temperature curves measured with the TheraMon® Microsensor. Six measurements are presented, logged in 15 minutes intervals.

Figure 34 shows the temperature curves measured with the TheraMon® Microsensor intraorally for 48 hours. Values here were logged in 15 minutes intervals. Two curves had to be excluded due to technical issues. This microsensor also logged the day and night differences in the temperature oscillations. The “calmer” night phases logged with the Star Oddi® DST nano-T were also found with this sensor. Also, the ice-cream peaks can be retrieved in curve OK-P4. Due to the longer interval the perturbations here seem to be weaker than measured by the Star Oddi® DST nano-T.

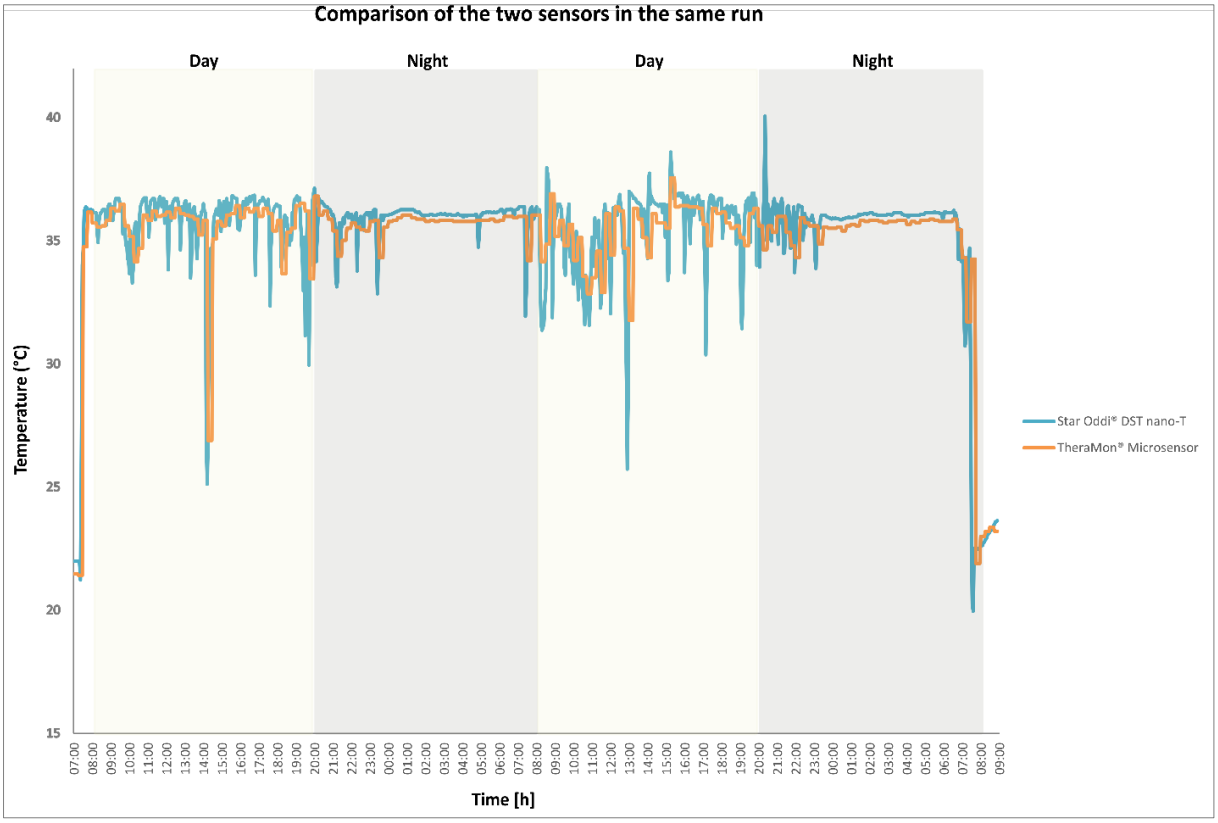

Figure 35: Comparison of the two sensor measurements in the same run. Star Oddi® DST nano-T in blue, TheraMon® Microsensor in orange. The TheraMon® values were multiplied by five for the comparison.

Comparing the two sensors it can be shown that the Star Oddi® DST nano-T is more sensitive to temperature perturbations due to the much smaller logging interval. Thus, the temperature oscillations are stronger if monitored with this logger. The values of the TheraMon® Microsensor were multiplied by five for a better comparison of the two measurements.

Summarizing the results, several methods were adapted to create a new combined *in vivo – in vitro* biofilm model. The according workflow and material adaptations allow intraoral (*in vivo*) microbiota growth and offer the possibility for its transfer to and further analysis in an *in vitro* test system. Molecular staining methods as FISH and live-dead staining enable visualization of the structural and compositional changes as well as bacterial survival with CLSM during the test phase. Next generation sequencing technologies can breakdown microbiome composition to genus level. Logging the temperature additionally includes an environmental factor in the analysis.

4. Discussion

The oral microbiome still keeps a lot of secrets which have to be unraveled. We still only begin to understand the microbiome variations during our life span and further the differences in microbiome compositions in health and disease. This study has developed a new combined *in vivo* – *in vitro* biofilm model system for a more sophisticated analysis of native bacterial biofilm in the human oral cavity.

4.1. Defining a healthy oral microbiome

In this thesis two methods for the analysis of native oral microbiota were established. First, the composition and structure of biofilm grown on palatal expanders was visualized with FISH and CLSM for the first time. Second, a method for the *in vivo* growth of native oral biofilm, its transfer to an *in vitro* setting and the monitoring of live/dead ratios and compositional changes over time in a biofilm reactor was developed. These two methods enabled new insights into the oral microbiome composition on artificial and natural surfaces in healthy children and adults. With this a further step in the discussion of how to define a “healthy core microbiome” was made confirming earlier results (Marsh 2010; Griffen et al. 201; Cho and Blaser 2012; Solbiati and Frias-Lopez 2018; Zarco et al. 2012). But they also offered new insights leading to new questions. Zijnge presented Firmicutes as the primary colonizers of the sub-, and supragingival regions before (Zijnge et al. 2010). Our FISH and CLSM analysis reflect these results, also showing a strong domination of Firmicutes (including *Streptococcus*) in the biofilm grown on the palatal expanders. Further, phyla as Bacteroidetes were found in clusters in our analysis. Even the periodontopathogen *Porphyromonas gingivalis* (PG), related to periodontal disease so far, was visualized in this biofilm. Further studies need to be done to prove a possible role of PG as a belonging to the healthy “core microbiome”. Zaura et al. tried to define that healthy “core microbiome” meaning a group of bacteria common to all samples taken with 454-pyrosequencing. They found up to 500 “species-level” phylotypes per person in up to 104 higher taxa (genus level and above). Predominant taxa were *Firmicutes* (36% of all reads), *Proteobacteria* (22%), *Actinobacteria* (25%), *Bacteroidetes* (11%) and *Fusobacteria* (5%). Three individuals compared with each other shared 26% of the unique sequences, 47% of the OTUs and 72% of the higher taxa. This also means that the rest of the sequences/OTUs or taxa seem to represent up the individuality of a persons’ microbiome (Zaura et al. 2009). This individuality was also found in our results

were only 117 OTUs were common to all samples while around 1800-3800 OTUs were found per person.

But not only the strong interpersonal variations complicate finding a core microbiome definition, also intrapersonal variations are found. When sampling the same human being over a fixed period of time, significant changes in the microbial composition were found. Hall et al. compared samples from tongue, saliva and supragingival plaque over 90 days (Hall et al. 2017). They found 26 core OTUs classified within the genera *Streptococcus*, *Fusobacterium*, *Haemophilus*, *Neisseria*, *Prevotella* and *Rothia* present in 95% of the samples and accounting for ~65% of the total sequence data. The overall microbial composition here stayed very stable within the individuals over time. But they found high variance in the composition of rare microorganisms. Also, the inter-individual variations were high. Further, tongue and saliva samples cluster together while supragingival plaque seems to be significantly different. During this thesis, also a strong inter-individuality of the oral microbiome was found. Further great variation in the abundances of the 117 most abundant OTUs found in all samples, reflects a strong personalization in the microbiota of the respective participants.

This individuality was also found in the biofilm samples on the dental appliances microscopied in this study. Seeing these differences in the composition in healthy people makes it even harder to define a disease baseline. Alcaraz compared samples from healthy and dental caries sites with 454-pyrosequencing (Alcaraz et al. 2012). Based on their results, not only the definition of healthy microbiome, but also the cause of diseases has to be reconsidered. They propose to see dental caries as a polymicrobial disease rather than being started by a single species. Further, they conclude that also the probiotic treatment approaches will need to include more species, based on this information.

4.2. Oral biofilms and dental materials

The mouth is the location in the human body where the most artificial materials are introduced for restauration (e.g. fillings, crowns, implants, bridges or dentures) (Auschill et al. 2002; Chin et al. 2006; Buser et al. 2017; Veitz-Keenan and Keenan 2017; de Waal et al. 2014; Größner- Schreiber et al. 2009; Busscher et al. 2010). This creates surfaces having other properties than the human tissues. Bacterial adhesion to oral tissues depends on the properties of both, the substratum surface and the properties of the bacterial cells. Surface roughness here is a major factor. Increased

surface roughness of the substratum and surface free energy of the bacterial cell wall, facilitate microbial adhesion (Subramani et al. 2009). Other factors as substrate hydrophobicity play major roles in biofilm formation in stagnant regions such as subgingival pockets (Ren et al. 2014). Palatal expanders as investigated in this work, thus present a large new artificial habitat for oral microbiota, fixed in the oral cavity for months. Such dental splints are often one of the first materials fixed in the oral cavity, often long before first fillings, crowns or other materials appear. It is still unclear to which extend fixed orthodontic treatment is a potential risk of periodontal disease due to microbiota changes introduced by the surface colonization.

Palatal expanders as the HAAS expander used in this study are tools for the expansion of the upper jaw during orthodontic treatment. The expanders used here were fixed in the oral cavity for four months. During this time, biofilm developed undisturbed on the acrylic surface lying in the upper jaw. The palatal expander itself served as a kind of wall against shear forces through tongue, food and drinks. At the same time, the biofilm was well nourished by the nutrients solved in saliva and waste products were washed away. Such biofilms on top of these palatal expanders in the four months grew to a size that can be seen with the naked eye (Klug et al. 2011). The results of the FISH and CLSM analysis of the biofilm performed in this thesis suggests further studies on the influence of theses microbiota on the native oral biofilm. For more information on the impact of this biofilms, different locations in the oral cavity need to be sampled and analyzed during the time of orthodontic treatment and further during the months and years after the treatment has ended. It should be of high interest for dentistry to find out more on the influence of the changes in the oral microbiota due to orthodontic treatments.

4.3. Combined *in vivo* and *in vitro* biofilm models

All data on the second part of this thesis (oral biofilm modelling) were published in (Klug et al. 2016).

The second approach in oral microbiome research is the analysis via models. The models discussed in this work exclude all forms of animal models and concentrate on the combination of intraoral (in humans) and laboratory assays. The molecular analysis of the oral biofilm in the context of dental research, nowadays exceeds simple analysis of samples taken intraorally. To find out more about the *in vivo* way of life of oral biofilm, it is important to be able to reconstruct *in vitro* it, but this is a challenging task as many

factors play various roles. We can mainly distinguish between microbiota-prone factors and factors coming from the “environment” as the surfaces in the oral cavity, human immune system, food, smoking, and many more. Most of these factors are so far only little understood. Especially in the onset of disease, we are only beginning to understand the complexity. This thesis has concentrated on the microbiota-prone factors as they were spatiotemporal presence of oral bacteria and their survival over time. Biofilm composition is a crucial factor in disease. Old hypothesis mostly saw single species as the trigger of disease – mostly due to technological limitations in the biofilm analysis. These theses are nowadays more and more replaced by new explanations seeing the disease as an interplay of a multitude of species and their interaction with the human host. Aruni et al. wrote that one of the most prominent oral diseases, periodontitis, is considered a multifactorial disease nowadays. Its diverse clinical features cannot be explained by the etiologic role of a single bacterium (Aruni et al. 2015). Several research teams also suggest caries as a multispecies disease much more than only caused by *Streptococcus mutans* (Gross et al. 2012; Jiang et al. 2016; Nyvad et al. 2012; Peterson et al. 2011). Keeping this in mind, research on single species biofilms only leads to limited information on the real nature of multispecies biofilms. This is also true looking into dental material research. The behavior of a biofilm containing only three different species will not efficiently mirror real life conditions. Thus, models of native oral biofilm need to be established to make a next step in this important research branch. With the second part of this work, we have tried to step into the new age of a combined *in vivo/in vitro* biofilm modeling where native oral biofilm is derived directly from the human mouth and transferred to an *in vitro* setting. Its natural composition after 48 hours in the mouth and its survival and compositional changes during and after 48 hours in the *in vitro* setting were monitored (Klug et al. 2016). For an easy biofilm growth and transfer a research splint was produced.

4.3.1. Research splint

The development of a research splint as a tool for the intraoral biofilm growth is not new. Different groups have developed dental splints carrying various carrier materials for oral biofilm sampling. Hannig et al. fixed individually fitted splints in the upper jaw (Hannig et al. 2007). These splints contained bovine enamel discs as biofilm carriers. The discs were colonized by *Streptococcus* already three minutes after insertion.

Takeshita et al. used hydroxyapatite discs on removable resin splints to monitor biofilm growth over 7 days (Takeshita et al. 2015). They also found a predominance of *Streptococcus* as was in this thesis. Some of the *Streptococcus* than lost in relative abundance during the 7 days, *Streptococcus gordonii* in the contrary gained. Other OTUs related to bacteria known as secondary and late colonizers such as *Veillonella parvula*, *Fusobacterium periodonticum*, *Neisseria flavescens*, *Granulicatella adiacens* or *Gemella haemolysans* strongly gained in relative abundance until day 7. This goes along with our results also showing a strong increase of *Fusobacteria*, *Actinomyces*, *Granulicatella*, *Neisseria*, *Lautropia* and *Gemella*. Al-Ahmad et al. used fixed enamel slabs in dental splints (Al-Ahmad et al. 2009). The enamel slabs were prepared from bovine incisors and ground with abrasive paper with a 400-4000 grit. They disinfected the slabs in 70% ethanol for 3 minutes and washed and stored them then in distilled water. The human enamel-dentin slabs used in this study were prepared in a similar way except that we autoclaved them for sterilization and kept them in 0.9% NaCl for storage. We produced enamel-dentin slabs with a standardized size of 2 x 4 x 6mm. This was best possible using molars as they had the largest surfaces. Handling these slabs was uncomplicated and they could be removed from the dental splint without touching the biofilm on top.

Different to previous studies, we did not remove the dental splint for eating and drinking. Once fixed in the mouth, they stayed there for 48 hours. So, the problem of storage during the extraoral time was circumvented. We assumed that taking out the dental splint for eating, drinking and dental hygiene would disturb and even destroy the biofilm. Here not only mechanic shear forces would work on the biofilm, but also temperature changes over a longer period (e.g. eating for 15 minutes) and a storage medium different to saliva would alter biofilm formation. Further drinking alcohol, tooth brushing or swimming in chlorinated water were prohibited during this time. All these factors have been neglected in earlier studies. Also different to other studies as the ones of Hannig et al., Al-Ahmad et al. and Jung et al. in this study the enamel-dentin slabs were inserted inside the splint directly facing the human teeth (Al-Ahmad et al. 2009; Jung et al. 2010; Hannig et al. 2007). Consequently, they were protected from shear forces as derived from the cheeks or tongue. New in this field was the insertion of the two sensors. This allowed the gain of information on temperature oscillation being natural for the oral biofilm in parallel to it growing. With the Star Oddi® DST

nano-T and the TheraMon® Microsensor two sensors were chosen that were small enough in order not to lead to strong discomfort in the carrier. This was important as we needed to ensure that the volunteers had normal eating and drinking behavior. The temperature monitoring with these two sensors further also revealed the study compliance of the carriers. As the splints were removable, non-compliance appeared as temperature decreases to room temperature. In one case a preliminary termination of the carrying was thus shown through a temperature drop down as further discussed below.

4.4. *In vitro* survival of native oral biofilm

Factors influencing *in vitro* survival of biofilms are limited. The laboratory setup such facilitates the analysis of single parameters. Choosing constant growing parameters as: medium, temperature, oxygen concentration and removal of waste, makes it easier to compare results to other studies and standardize the system for e.g. dental material tests. For the development of more complex biofilm models, it is necessary to analyze biofilm survival under such standardized circumstances. The respective results can show if native biofilm can survive under *in vitro* conditions in its natural complexity at all.

Using the enamel-dentin slabs as biofilm carriers, made it easy to transfer the natively grown biofilm to the biofilm reactor. Mechanical disturbances, extreme temperature drops and an “oxygen shock” could thus be avoided. The bacteria showed a strong growth in the first hour of incubation comparing T0 and T1. This can be explained by the rich BHI medium used for these experiments. Based on Standar et al., this medium is similar to sulcus fluid (Standar et al. 2010). First attempts to use sterilized human saliva treated with 2.5 mM dithiothreitol (Foster and Kolenbrander 2004) could not satisfyingly be standardized. This resulted in a complete loss of viability in most attempts.

LIVE/DEAD staining directly on the slabs and using water immersible lenses for microscopy allowed for analysis of biofilm survival in *in vitro* settings. The biofilm on top of the slabs such was not damaged through transferring, pipetting or other staining actions. Survival of the biofilm members was shown in all assays over 48 hours *in vitro*. Interestingly after the first growth of the biofilm (T0-T1), after the 48 hours (T3), the proportions of living and dead bacteria reached the initial level measured at T0 (Klug et al. 2016). Native oral biofilm thus seems to stay vital for at least 48 hours *in vitro*.

For the evaluation of the CLSM stack data generated with the LIVE/DEAD stained samples, a computer program was written by Christian Westendorf using Matlab and Python. In a first step, unambiguously stained cells (red + green = orange) were excluded from further analysis. This problem appears when natural biofilms are stained with SYTO 9 and PI and there is no explanation for the phenomenon at this moment. Still Netuschil et al. presented these two stains to work best on a mixture of different bacteria (Netuschil et al. 2014). As mentioned in (Klug et al. 2016) this can lead to an underestimation of living bacteria. After this step huge round cells, presumably yeast cells, were also excluded, as they would suggest a much higher number of dead bacterial cells as really there. This finally led to a dataset of only red and green bacterial cells numbers. Including the exclusion of “falsely” stained bacteria and structures that could not be bacteria (size exclusion), were the advantages of this in-house created program we used for the analysis. Other commercially available programs and also freeware, were not able to deliver the same results and were thus not used.

4.5. Compositional shifts of the oral microbiota through the transfer to *in vitro* settings

The compositional shift of the oral microbiota through living in the biofilm reactor for 48 hours was published in Klug et al. 2016 as the following discussion:

“In our analysis of the biofilm composition, the phylum *Firmicutes*—and here *Streptococcus* (facultative anaerobes) and *Veillonella* (anaerobes)—appear to be the primary colonizers forming a “base” on which other bacteria can dock (Rickard et al. 2003; Zijnge et al. 2010). *Streptococcus* spp. and *Veillonella spp*. have been reported to show a strong co-occurrence and co-aggregation in native oral biofilm and to interact in *in vitro* tests (Egland et al. 2004; Palmer et al. 2006; Chalmers et al. 2008). They also showed a similar behavior over the 48 h of incubation as demonstrated in the log2 fold change analysis. This leads us to the assumption that those two genera further interact in our *in vivo* system. We also found that *Streptococcus* made up the biggest bacterial group with around 60% of the population. These did not change significantly in number after 48 h of *in vitro* incubation. Interestingly, other genera like *Actinomyces* (mainly anaerobic growth), *Prevotella* (obligate anaerobes) and *Rothia* (facultative anaerobes) increased significantly. Kolenbrander et al. showed co-aggregation of *Actinomyces naeslundii T14V* with *Streptococcus*, *Prevotella* (obligate anaerobes), and *Capnocytophaga* strains (Kolenbrander et al. 2006). These genera play an

important role in the “pre-organization” phase of the biofilm which is the period in biofilm development lasting between 18 h and up to 4 days (Jakubovics 2015). Together with *Streptococcus* and *Veillonella* they also tended to remain the predominant microorganisms although their relative abundance stagnated (Diaz et al. 2006). This increase after several days has been previously shown *in vivo* by (Takeshita et al. 2015). The growing numbers seen in the other genera, i.e., facultative and obligate anaerobes, prove that our *in vitro* model using the BHI medium works without an anaerobic chamber. The ability to keep these genera alive over several generations is a good foundation for further assays. This is also supported by a heat map analysis on OTU level. The α-diversity calculated with PD-whole tree is higher across all samples at T3. Sterility was proven for the biofilm reactor system, so we can argue that the reason for higher values at T3 is a relative abundance at T0 which was too low to be detected by 454 pyrosequencing. As the biofilm sampling is discontinuous due to two different slabs used for T0 and T3, bacteria found at T3 can also derive from this.

PCoA explaining around 30% of the variance due to time shows a clustering of the points in time in two dimensions, no clustering can be found in the third dimension. To be able to better interpret this environmental data, correspondence analysis was used to model the change between T0 and T3 and the OTU distributions based on the same data as PCoA. The CA shows a clear proximity of the samples at T0 and T3 with around 40% of total inertia. OTUs appear in high abundance at both points in time reflected through the data points shown in strong vicinity to the sample points. Correspondence analysis thus supports our hypothesis that there is no difference between T0 and T3.

To get more information on cell viability and to confirm the biofilm composition found by pyrosequencing, we also performed the FISH analysis. FISH probes that only bind to viable cells prove that our biofilm is not only vital, but still able to live. Based on the strong signals gained, we conclude that the biofilm is also vital. LGCmix, staining Firmicutes, represented the main group also in FISH analysis. This is consistent with our pyrosequencing data showing Firmicutes as the largest group. Furthermore, signals were recorded from Bac303 staining most *Bacteroidaceae* and *Prevotellaceae*, and some *Porphyromonadaceae*. This result goes along with previous findings that detected these groups in healthy adults (Aas et al. 2005).

Our “mouth to model” system allows for native oral biofilm growth *in vivo*, a simple transfer of this biofilm to laboratory setups and further growth *in vitro* in biofilm reactors.

Our setup can be easily reconstructed and settings used in miscellaneous studies. With this setup the biofilm stays alive and diverse over 48 h of *in vitro* incubation. This is an important outcome making our study a sound basis for a new biofilm model to be used in (phyto-) pharmacological assays or dental materials research. Further investigations and validation of the appropriate conditions for *in vitro* cultivation of native oral biofilms could facilitate the study of all biofilm-induced diseases".

4.6. Temperature oscillations in the oral cavity

With the here presented research splint, intraoral temperature recordings are possible at the same time as the biofilm grows intraorally. In earlier studies different methods were applied for temperature measurements. Longman et al. tested intraoral temperature variations in four subjects. They suggest a "normal" oral temperature of 2-4 °C below the so far supposed 37 °C (Longman and Pearson 1987). Some years later, Volchansky et his colleagues used a Bailey Instruments' digital thermometer with a fine thermocouple point of 0.3 mm diameter to measure sublingual and mucosal temperatures in different assays. They found sublingual temperatures around 35.5 for posterior teeth and 34.6 °C for anterior teeth. This group further showed that bone is cooler than overlying mucosa (Volchansky and Cleaton- Jones 1994). Barclay et al. used miniature bead thermistors at various sites in the oral cavity inserted in vacuum formed splints. They found temperatures between 1.56 °C and 65.61 °C drinking cold and warm drinks. Interestingly the temperature differences between upper and lower jaws and buccal and lingual positions could clearly be seen (Barclay et al. 2005).

Regarding only the results from these studies, we decided to introduce thermo-loggers into our research splints in order to find out more about the natural temperature oscillations. A clear differentiation between night and day could be made from the temperature curves plotted. During night (sleep), the oscillations were only minimal. Temperature differences there were no larger than 5 °C lying around 36 °C. In contrary to that strong oscillations were found during daytime ranging from under 10 °C to over 40 °C. Different to Barclays drinking experiments, we did not find values above 45 °C although all participants ate and drank warm food and drinks (dietary records were collected, data not shown). These differences could be due to the fact, that the sensors were placed facing the palate. Measuring directly at the front teeth, could lead to higher maximum temperatures. But usage of the same sensors would lead to a major discomfort for the volunteers.

For further models, these highly specific temperature oscillations will surely need to be considered. Questions remaining open are: 1) how long does it take until a biofilm reacts on temperature changes, 2) how big do these changes have to be, 3) can we measure temperature changes throughout the whole biofilm, or only at the top layers, 4) how important is the minimal-temperature-change-sleeping phase and many more. Going deeper into research on the temperature-microbiota interplay even further question will appear. Considering natural temperature oscillations in future microbiome modelling is highly recommended by this data.

5. Conclusion

In this thesis a method was developed for the FISH and CLSM analysis of bacteria grown on orthodontic appliances fixed in the oral cavity for several months. This method could also be used for other dental materials and appliances. Secondly, a model for the native oral biofilm growth in the oral cavity and its transfer it into a laboratory set up for a further *in vitro* growth was created. In this system the biofilm stays alive and in a stable composition over a 48 hours incubation. Including small sensors in research splints, temperature measurements even during night are made possible without disturbance of the daily routine of the person wearing it. The normal oral temperature shows a strong oscillation during the day but stays quite stable during night. There is a strong need for the improvement of established biofilm models as they are outdated. Such models should include many more factors as variable temperature, variably nourishment, stress through human immune response factors and native oral biofilm. And there are surely many more factors that can be included. These model systems will then enable native oral microbiome analysis during material tests as well as tests of new pharmaceutical compounds.

6. Bibliography

Aas, J., Paster, B., Stokes, L., Olsen, I. and Dewhirst, F. 2005. Defining the Normal Bacterial Flora of the Oral Cavity. *Journal of Clinical Microbiology* 43(11), pp. 5721–5732.

Al-Ahmad, A., Follo, M., Selzer, A.-C., Hellwig, E., Hannig, M. and Hannig, C. 2009. Bacterial colonization of enamel *in situ* investigated using fluorescence *in situ* hybridization. *Journal of medical microbiology* 58(Pt 10), pp. 1359–66.

Alcaraz, L.D., Belda-Ferre, B., Cabrera-Rubio, R., Romero, H., Simón-Soro, Á., Pignatelli, M., and Mira, A. 2012. Identifying a healthy oral microbiome through metagenomics. *Clinical Microbiology and Infection* 18(s4), pp. 54–57.

Apel, S., Apel, C., Morea, C., Tortamano, A., Dominguez, G. and Conrads, G. 2009. Microflora associated with successful and failed orthodontic mini implants. *Clinical Oral Implants Research* 20(11), pp. 1186–1190.

Aruni, A., Dou, Y., Mishra, A. and Fletcher, H. 2015. The Biofilm Community: Rebels with a Cause. *Current Oral Health Reports* 2(1), pp. 48–56.

Auschill, T., Arweiler, N., Brecx, M., Reich, E., Sculean, A. and Netuschil, L. 2002. The effect of dental restorative materials on dental biofilm. *European Journal of Oral Sciences* 110(1), pp. 48–53.

Baker, G.C., Smith, J.J. and Cowan, D.A. 2003. Review and re-analysis of domain-specific 16S primers. *Journal of Microbiological Methods* 55(3).

Baker, J.L., Bor, B., Agnello, M., Shi, W. and He, X. 2017. Ecology of the Oral Microbiome: Beyond Bacteria. *Trends in microbiology*.

Barclay, C., Spence, D. and Laird, W. 2005. Intra-oral temperatures during function. *Journal of Oral Rehabilitation* 32(12), pp. 886–894.

Belibasakis, G. and Thurnheer, T. 2014. Validation of antibiotic efficacy on *in vitro* subgingival biofilms. *Journal of periodontology* 85(2), pp. 343–8.

Bikel, S., Valdez-Lara, A., Cornejo-Granados, F., Rico, K., Canizales-Quinteros, S., Soberón, X., Del Pozo-Yauner, L. and Ochoa-Leyva, A. 2015. Combining metagenomics, metatranscriptomics and viromics to explore novel microbial interactions: towards a systems-level understanding of human microbiome. *Computational and structural biotechnology journal* 13, pp. 390–401.

Ter Braak, C. 1985. Correspondence analysis of incidence and abundance data: properties in terms of a unimodal response model. *Biometrics*.

Bragg, L., Stone, G., Imelfort, M., Hugenholtz, P. and Tyson, G. 2012. Fast, accurate error-correction of amplicon pyrosequences using Acacia. *Nature Methods* 9(5), pp. 425–426.

Bray, JR and Curtis, JT 1957. An ordination of the upland forest communities of southern Wisconsin. *Ecological monographs*.

Buser, D., Sennerby, L. and Bruyn, H. 2017. Modern implant dentistry based on osseointegration: 50 years of progress, current trends and open questions. *Periodontology 2000* 73(1), pp. 7–21.

Busscher, H.J., Rinastiti, M., Siswomihardjo, W. and van der Mei, H.C. 2010. Biofilm formation on dental restorative and implant materials. *Journal of dental research* 89(7), pp. 657–65.

Caporaso, G., Bittinger, K., Bushman, F., DeSantis, T., Andersen, G. and Knight, R. 2010. PyNAST: a flexible tool for aligning sequences to a template alignment. *Bioinformatics* 26(2), pp. 266–267.

Caporaso, G., Kuczynski, J., Stombaugh, J., Bittinger, K., Bushman, F., Costello, E., Fierer, N., Peña, A., Goodrich, J., Gordon, J., Huttley, G., Kelley, S., Knights, D., Koenig, J., Ley, R., Lozupone, C., McDonald, D., Muegge, B., Pirrung, M., Reeder, J., Sevinsky, J., Turnbaugh, P., Walters, W., Widmann, J., Yatsunenko, T., Zaneveld, J. and Knight,

R. 2010. QIIME allows analysis of high-throughput community sequencing data. *Nature Methods* 7(5), pp. 335–336.
Cardinale, M., de Castro, J., Müller, H., Berg, G. and Grube, M. 2008. *In situ* analysis of the bacterial community associated with the reindeer lichen Cladonia arbuscula reveals predominance of Alphaproteobacteria. *FEMS Microbiology Ecology* 66(1), pp. 63–71.
Chalmers, N., Palmer, R., Cisar, J. and Kolenbrander, P. 2008. Characterization of a Streptococcus sp.-Veillonella sp. community micromanipulated from dental plaque. *Journal of bacteriology* 190(24), pp. 8145–54.
Chen, Y., Wong, R., Seneviratne, Hägg, U., Mcgrath, C., Samaranayake and Kao, R. 2011. The antimicrobial efficacy of Fructus mume extract on orthodontic bracket: A monospecies-biofilm model study *in vitro*. *Archives of Oral Biology* 56(1), p. 1621.
Chin, M., Busscher, H., Evans, R., Noar, J. and Pratten, J. 2006. Early biofilm formation and the effects of antimicrobial agents on orthodontic bonding materials in a parallel plate flow chamber. *The European Journal of Orthodontics* 28(1), pp. 1–7.
Cho, I. and Blaser, M. 2012. The human microbiome: at the interface of health and disease. *Nature Reviews Genetics* 13(4), pp. 260–270.
Cole, J.R., Chai, B., Farris, R.J. and Wang, Q. 2005. The Ribosomal Database Project (RDP-II): sequences and tools for high-throughput rRNA analysis. *Nucleic acids ….*
Cole, J.R., Wang, Q., Cardenas, E. and Fish, J 2009. The Ribosomal Database Project: improved alignments and new tools for rRNA analysis. *Nucleic acids ….*
Costerton, J.W., Geesey, G.G. and Cheng, K.J. 1978. How bacteria stick. *Scientific American* 238(1), pp. 86–95.
Costerton, J.W., Stewart, P.S. and Greenberg, E.P. 1999. Bacterial biofilms: a common cause of persistent infections. *Science (New York, N.Y.)* 284(5418), pp. 1318–22.
Crielaard, W., Zaura, E., Schuller, A., Huse, S., Montijn, R. and Keijser, B. 2011. Exploring the oral microbiota of children at various developmental stages of their dentition in the relation to their oral health. *BMC Medical Genomics* 4(1), p. 22.
Darrene, L.-N.N. and Cecile, B. 2016. Experimental Models of Oral Biofilms Developed on Inert Substrates: A Review of the Literature. *BioMed research international* 2016, p. 7461047.
DeSantis, T.Z., Hugenholtz, P., Larsen, N., Rojas, M., Brodie, E.L., Keller, K., Huber, T., Dalevi, D., Hu, P. and Andersen, G.L. 2006. Greengenes, a chimera-checked 16S rRNA gene database and workbench compatible with ARB. *Applied and environmental microbiology* 72(7), pp. 5069–5072.
Diaz, P.I., Chalmers, N.I., Rickard, A.H., Kong, C., Milburn, C.L., Palmer R.J.Jr., and Kolenbrander, P.E. 2006. Molecular Characterization of Subject-Specific Oral Microflora during Initial Colonization of Enamel. *Applied and Environmental Microbiology* 72(4), pp. 2837–2848.
Diaz, P.I., Hong, B.-Y., Dupuy, A. and Strausbaugh, L. 2016. Mining the oral mycobiome: Methods, components, and meaning. *Virulence* 8(3) pp. 313-323.
Dupuy, A., David, M., Li, L., Heider, T., Peterson, J., Montano, E., Dongari-Bagtzoglou, A., Diaz, P. and Strausbaugh, L. 2014. Redefining the Human Oral Mycobiome with Improved Practices in Amplicon-based Taxonomy: Discovery of Malassezia as a Prominent Commensal. *PLoS ONE* 9(3) :e90899.
Eckert, R., He, J., Yarbrough, D.K., Qi, F., Anderson, M.H., and Shi, W. 2006. Targeted Killing of Streptococcus mutans by a Pheromone-Guided 'Smart' Antimicrobial Peptide. *Antimicrobial Agents and Chemotherapy* 50(11), p. 36513657.
Egland, P., Palmer, R. and Kolenbrander, P. 2004. Interspecies communication in *Streptococcus gordonii–Veillonella atypica* biofilms: Signaling in flow conditions

requires juxtaposition. *Proceedings of the National Academy of Sciences of the United States of America* 101(48), pp. 16917–16922.
Elvers, K.T., Leeming, K. and Lappin-Scott, H.M. 2002. Binary and mixed population biofilms: Time-lapse image analysis and disinfection with biocides. *Journal of Industrial Microbiology and Biotechnology* 29(6), p. 331338.
Exterkate, R.A, Zaura, E., Brandt, B.W., Buijs, M.J., Koopman, J.E., Crielaard, W. and ten Cate, J.M. 2014. The effect of propidium monoazide treatment on the measured bacterial composition of clinical samples after the use of a mouthwash. *Clinical Oral Investigations* 19(4), pp. 813-22
Faith, D.P. 1992. Conservation evaluation and phylogenetic diversity. *Biological conservation* 61 pp. 1-10.
Foster, J.S. and Kolenbrander, P.E. 2004. Development of a Multispecies Oral Bacterial Community in a Saliva-Conditioned Flow Cell. *Applied and Environmental Microbiology* 70(7):4340-8.
De Freitas, A., Marquezan, M., da Nojima, M., Alviano, D. and Maia, L. 2014. The influence of orthodontic fixed appliances on the oral microbiota: A systematic review. *Dental Press Journal of Orthodontics* 19(2).
Garcez, A., Suzuki, S., Ribeiro, M., Mada, E., Freitas, A. and Suzuki, H. 2011. Biofilm retention by 3 methods of ligation on orthodontic brackets: a microbiologic and optical coherence tomography analysis. *American journal of orthodontics and dentofacial orthopedics : official publication of the American Association of Orthodontists, its constituent societies, and the American Board of Orthodontics* 140(4), pp. e193–8.
Gest, H. 2004. The discovery of microorganisms by Robert Hooke and Antoni Van Leeuwenhoek, fellows of the Royal Society. *Notes and records of the Royal Society of London* 58(2), pp. 187–201.
Ghannoum, M., Jurevic, R., Mukherjee, P., Cui, F., Sikaroodi, M., Naqvi, A. and Gillevet, P. 2010. Characterization of the Oral Fungal Microbiome (Mycobiome) in Healthy Individuals. *PLoS Pathogens* 6(1).
Goeres, D., Hamilton, M., Beck, N., Buckingham-Meyer, K., Hilyard, J., Loetterle, L., Lorenz, L., Walker, D. and Stewart, P. 2009. A method for growing a biofilm under low shear at the air–liquid interface using the drip flow biofilm reactor. *Nature Protocols* 4(5), pp. 783–788.
Gomez, A. and Nelson, K. 2016. The Oral Microbiome of Children: Development, Disease, and Implications Beyond Oral Health. *Microbial Ecology* 73(2), pp. 492–503.
Griffen, A., Beall, C., Campbell, J., Firestone, N., Kumar, P., Yang, Z., Podar, M. and Leys, E. 2011. Distinct and complex bacterial profiles in human periodontitis and health revealed by 16S pyrosequencing. *The ISME Journal* 6(6), pp. 1176–1185.
Gross, E., Beall, C., Kutsch, S., Firestone, N., Leys, E. and Griffen, A. 2012. Beyond Streptococcus mutans: Dental Caries Onset Linked to Multiple Species by 16S rRNA Community Analysis. *PLoS ONE* 7(10), p. e47722.
Größner-Schreiber, B., Teichmann, J., Hannig, M., Dörfer, C., Wenderoth, D. and Ott, S. 2009. Modified implant surfaces show different biofilm compositions under *in vivo* conditions. *Clinical Oral Implants Research* 20(8), pp. 817–826.
Guggenheim, M., Shapiro, S., Gmür, R., and Guggenheim, B. 2001. Spatial Arrangements and Associative Behavior of Species in an *In vitro* Oral Biofilm Model. *Applied and Environmental Microbiology* 67(3), p. 13431350.
Hall, M., Singh, N., Ng, K., Lam, D., Goldberg, M., Tenenbaum, H., Neufeld, J., Beiko, R. and Senadheera, D. 2017. Inter-personal diversity and temporal dynamics of dental, tongue, and salivary microbiota in the healthy oral cavity. *npj Biofilms and Microbiomes* 3(1), p. 2.

Hannig, C., Hannig, M., Rehmer, O., Braun, G., Hellwig, E. and Al-Ahmad, A. 2007. Fluorescence microscopic visualization and quantification of initial bacterial colonization on enamel *in situ*. *Archives of Oral Biology* 52(11), pp. 1048–1056.

Hansen, M., Palmer, R. and White, D. 2000. Flowcell culture of Porphyromonas gingivalis biofilms under anaerobic conditions. *Journal of Microbiological Methods* 40(3), p. 233239.

Howe, M.-S. 2017. Implant maintenance treatment and peri-implant health. *Evidence-Based Dentistry* 18(1), pp. 8–10.

Hug, L.A., Baker, B.J., Anantharaman, K., Brown, C.T., Probst, A.J., Castelle, C.J., Butterfield, C.N., Hernsdorf, A.W., Amano, Y., Ise, K., Suzuki, Y., Dudek, N., Relman, D.A., Finstad, K.M., Amundson, R., Thomas, B.C. and Banfield, J.F. 2016. A new view of the tree of life. *Nature microbiology* 1, p. 16048.

Huse, S., Ye, Y., Zhou, Y. and Fodor, A. 2012. A Core Human Microbiome as Viewed through 16S rRNA Sequence Clusters. *PLoS ONE* 7(6).

Ireland, A.J, Soro, V., Sprague, S.V., Harradine, N.W., Day, C., Al-Anezi, S., Jenkinson, H.F., Sherriff, M., Dymock, D. and Sandy J.R. 2014. The effects of different orthodontic appliances upon microbial communities. *Orthodontics & Craniofacial Research* 17(2), pp. 115–123.

Jakubovics, N. 2015. Intermicrobial Interactions as a Driver for Community Composition and Stratification of Oral Biofilms. *Journal of Molecular Biology* 427(23) pp. 3662-75.

Jiang, S., Gao, X., Jin, L. and Lo, E. 2016. Salivary Microbiome Diversity in Caries-Free and Caries-Affected Children. *International Journal of Molecular Sciences* 17(12), p. 1978.

Jung, D., Al-Ahmad, A., Follo, M., Spitzmüller, B., Hoth-Hannig, W., Hannig, M. and Hannig, C. 2010. Visualization of initial bacterial colonization on dentin and enamel *in situ*. *Journal of microbiological methods* 81(2), pp. 166–74.

Kent, A.D., Yannarell, A.C., Rusak, J.A., Triplett, E.W. and McMahon, K.D. 2007. Synchrony in aquatic microbial community dynamics. *The ISME journal* 1(1), pp. 38–47.

Kim, K., Heimisdottir, K., Gebauer, U. and Persson, R. 2010. Clinical and microbiological findings at sites treated with orthodontic fixed appliances in adolescents. *American journal of orthodontics and dentofacial orthopedics : official publication of the American Association of Orthodontists, its constituent societies, and the American Board of Orthodontics* 137(2), pp. 223–8.

Kistler, J.O., Booth, V., Bradshaw, D.J. and Wade, W.G. 2013. Bacterial community development in experimental gingivitis. *PLoS One* 8(8), p. e71227.

Klug, B., Rodler, C., Koller, M., Wimmer, G., Kessler, H.H., Grube, M. and Santigli, E. 2011. Oral biofilm analysis of palatal expanders by fluorescence in-situ hybridization and confocal laser scanning microscopy. *Journal of visualized experiments* (56).

Klug, B., Santigli, E., Westendorf, C., Tangl, S., Wimmer, G. and Grube, M. 2016. From Mouth to Model: Combining *in vivo* and *in vitro* Oral Biofilm Growth. *Frontiers in microbiology* 7, p. 1448. eCollection 2016

Kolenbrander, P., Palmer, R., Rickard, A., Jakubovics, N., Chalmers, N. and Diaz, P. 2006. Bacterial interactions and successions during plaque development. *Periodontology 2000* 42(1), pp. 47–79.

Krom, B.P., Kidwai, S. and ten Cate, J.M. 2014. Candida and other fungal species: forgotten players of healthy oral microbiota. *Journal of dental research* 93(5), pp. 445–51.

Lamfon, H., Al-Karaawi, Z., McCullough, M., Porter, S. and Pratten, J. 2005. Composition of *in vitro* denture plaque biofilms and susceptibility to antifungals. *FEMS Microbiology Letters* 242(2), pp. 345–351.

Lebeaux, D., Chauhan, A., Rendueles, O. and Beloin, C. 2013. From *in vitro* to *in vivo* Models of Bacterial Biofilm-Related Infections. *Pathogens* 2(2), pp. 288–356.
Lee, H.-J., Park, H.-S., Kim, K.-H., Kwon, T.-Y. and Hong, S.-H. 2011. Effect of garlic on bacterial biofilm formation on orthodontic wire. *The Angle Orthodontist* 81(5).
Lee, Y., Zimmerman, J., Custodio, W., Xiao, Y., Basiri, T., Hatibovic-Kofman, S. and Siqueira, W. 2013. Proteomic Evaluation of Acquired Enamel Pellicle during *In vivo* Formation. *PLoS ONE* 8(7).
Ling, Z., Kong, J., Jia, P., Wei, C., Wang, Y., Pan, Z., Huang, W., Li, L., Chen, H. and Xiang, C. 2010. Analysis of Oral Microbiota in Children with Dental Caries by PCR-DGGE and Barcoded Pyrosequencing. *Microbial Ecology* 60(3), pp. 677–690.
Liu, Y., Zhang, Y., Wang, L., Guo, Y. and Xiao, S. 2013. Prevalence of Porphyromonas gingivalis four rag locus genotypes in patients of orthodontic gingivitis and periodontitis. *PloS one* 8(4), p. e61028.
Longman, C.M. and Pearson, G.J. 1987. Variations in tooth, surface temperature in the oral cavity during fluid intake. *Biomaterials* 8(5), pp. 411–414.
Loy, A., Maixner, F., Wagner, M. and Horn, M. 2007. probeBase—an online resource for rRNA-targeted oligonucleotide probes: new features 2007. *Nucleic Acids Research* 35(suppl 1), pp. D800–D804.
Lozupone, C., Lladser, M., Knights, D., Stombaugh, J. and Knight, R. 2010. UniFrac: an effective distance metric for microbial community comparison. *The ISME Journal* 5(2), pp. 169–172.
Ly, M., Abeles, S.R., Boehm, T.K., Robles-Sikisaka, R., Naidu, M., Santiago-Rodriguez, T. and Pride, D.T. 2014. Altered oral viral ecology in association with periodontal disease. *mBio* 5(3), pp. e01133–14.
Mager, D.L., Ximenez-Fyvie, L.A., Haffajee, A.D. and Socransky, S.S. 2003. Distribution of selected bacterial species on intraoral surfaces. *Journal of clinical periodontology* 30(7), pp. 644–54.
Marsh, P.D. 2010. Microbiology of dental plaque biofilms and their role in oral health and caries. *Dental clinics of North America* 54(3), pp. 441–54.
McMurdie, P. and Holmes, S. 2012. Phyloseq: a bioconductor package for handling and analysis of high-throughput phylogenetic sequence data. *Pacific Symposium on Biocomputing. Pacific Symposium on Biocomputing*, pp. 235–46.
Mei, L., Busscher, H., Mei, H., Chen, Y., Vries, J. and Ren, Y. 2009. Oral bacterial adhesion forces to biomaterial surfaces constituting the bracket–adhesive–enamel junction in orthodontic treatment. *European Journal of Oral Sciences* 117(4), pp. 419–426.
Moter, A. and Göbel, U. 2000. Fluorescence *in situ* hybridization (FISH) for direct visualization of microorganisms. *Journal of Microbiological Methods* 41(2).
Do Nascimento, C., Issa, J., Watanabe, E. and Ito, I. 2006. DNA Checkerboard Method for Bacterial Pathogen Identification in Oral Diseases. *International Journal of Morphology* 24(4).
Netuschil, L., Auschill, T., Sculean, A. and Arweiler, N. 2014. Confusion over live/dead stainings for the detection of vital microorganisms in oral biofilms - which stain is suitable? *BMC Oral Health* 14(1), p. 2.
Nobbs, A.H., Jenkinson, H.F. and Jakubovics, N.S. 2011. Stick to Your Gums. *Journal of Dental Research* 90(11), pp. 1271–1278.
Nyvad, B., Crielaard, Mira, Takahashi and Beighton 2012. Dental Caries from a Molecular Microbiological Perspective. *Caries Research* 47(2), pp. 89–102.
Obata, J., Takeshita, T., Shibata, Y., Yamanaka, W., Unemori, M., Akamine, A. and Yamashita, Y. 2014. Identification of the Microbiota in Carious Dentin Lesions Using 16S rRNA Gene Sequencing. *PLoS ONE* 9(8): e103712.

Palmer, R., Diaz, P. and Kolenbrander, P. 2006. Rapid Succession within the Veillonella Population of a Developing Human Oral Biofilm *In situ*. *Journal of Bacteriology* 188(11), pp. 4117–4124.
Pan, S., Liu, Y., Zhang, L., Li, S., Zhang, Y., Liu, J., Wang, C. and Xiao, S. 2017. Profiling of subgingival plaque biofilm microbiota in adolescents after completion of orthodontic therapy. *PLOS ONE* 12(2), p. e0171550.
Paster, B.J., Olsen, I., Aas, J.A. and Dewhirst, F.E. 2006. The breadth of bacterial diversity in the human periodontal pocket and other oral sites. *Periodontology 2000* 42, pp. 80-7.
Peterson, S., Snesrud, E., Schork, N. and Bretz, W. 2011. Dental caries pathogenicity: a genomic and metagenomic perspective. *International Dental Journal* 61(s1), pp. 11–22.
Price, M., Dehal, P. and Arkin, A. 2009. FastTree: Computing Large Minimum Evolution Trees with Profiles instead of a Distance Matrix. *Molecular Biology and Evolution* 26(7), pp. 1641–1650.
Rajaram, S. and Oono, Y. 2010. NeatMap - non-clustering heat map alternatives in R. *BMC Bioinformatics* 11(1), pp. 1–9.
Ramette, A. 2007. Multivariate analyses in microbial ecology. *FEMS Microbiology Ecology* 62(2), pp. 142–160.
Rams, T., Degener, J. and Winkelhoff, A. 2014. Antibiotic resistance in human peri-implantitis microbiota. *Clinical Oral Implants Research* 25(1), pp. 82–90.
Rath, H., Stumpp, S. and Stiesch, M. 2017. Development of a flow chamber system for the reproducible *in vitro* analysis of biofilm formation on implant materials. *PLOS ONE* 12(2), p. e0172095.
Ren, Y., Jongsma, M., Mei, L., van der Mei, H. and Busscher, H. 2014. Orthodontic treatment with fixed appliances and biofilm formation—a potential public health threat? *Clinical Oral Investigations* 18(7), p. 17111718.
Rickard, A., Gilbert, P., High, N., Kolenbrander, P. and Handley, P. 2003. Bacterial coaggregation: an integral process in the development of multi-species biofilms. *Trends in Microbiology* 11(2).
Rogers, J.D., Palmer, R.J. Jr., Kolenbrander, P.E. and Scannapieco, F.A. 2001. Role of Streptococcus gordonii Amylase-Binding Protein A in Adhesion to Hydroxyapatite, Starch Metabolism, and Biofilm Formation. *Infection and Immunity* 69(11), p. 70467056.
Rudney, J.D., Chen, Lenton, Li, Li, Jones, R.S., Reilly, Fok, A.S. and Aparicio 2012. A reproducible oral microcosm biofilm model for testing dental materials. *Journal of Applied Microbiology* 113(6), pp. 1540–1553.
Salek, M., Jones, S. and Martinuzzi, R. 2009. The influence of flow cell geometry related shear stresses on the distribution, structure and susceptibility of Pseudomonas aeruginosa 01 biofilms. *Biofouling* 25(8), pp. 711–25.
Santigli, E., Leitner, E., Wimmer, G., Kessler, H., Feierl, G., Grube, M., Eberhard, K. and Klug, B. 2016. Accuracy of commercial kits and published primer pairs for the detection of periodontopathogens. *Clinical Oral Investigations* 20(9), pp. 2515–2528.
Santigli, E., Trajanoski, S., Eberhard, K. and Klug, B. 2017. Sampling Modification Effects in the Subgingival Microbiome Profile of Healthy Children. *Frontiers in Microbiology* 7.
Santos, O., Lindh, L., Halthur, T. and Arnebrant, T. 2010. Adsorption from saliva to silica and hydroxyapatite surfaces and elution of salivary films by SDS and delmopinol. *Biofouling* 26(6), pp. 697–710.
Sbordone, L. and Bortolaia, C. 2003. Oral microbial biofilms and plaque-related diseases: microbial communities and their role in the shift from oral health to disease. *Clinical Oral Investigations* 7(4), pp. 181–188.

Schmidt, B., Kuczynski, J., Bhattacharya, A., Huey, B., Corby, P., Queiroz, et al. 2014. Changes in Abundance of Oral Microbiota Associated with Oral Cancer. *PLoS ONE* 9(6):e98741.

Schwartz, K., Stephenson, R., Hernandez, M., Jambang, N. and Boles, B. 2010. The use of drip flow and rotating disk reactors for Staphylococcus aureus biofilm analysis. *Journal of visualized experiments : JoVE* (46).

Schwieger, F. and Tebbe, C.C. 1998. A new approach to utilize PCR-single-strand-conformation polymorphism for 16S rRNA gene-based microbial community analysis. *Applied and environmental microbiology* 64(12), pp. 4870–6.

Segata, N., Haake, S., Mannon, P., Lemon, K., Waldron, L., Gevers, D., Huttenhower, C. and Izard, J. 2012. Composition of the adult digestive tract bacterial microbiome based on seven mouth surfaces, tonsils, throat and stool samples. *Genome biology* 13(6), p. R42.

Socransky, S.S., Smith, C., Martin, L., Paster, B.J., Dewhirst, F.E. and Levin, A.E. 1994. 'Checkerboard' DNA-DNA hybridization. *BioTechniques* 17(4), pp. 788–92.

Solbiati, J. and Frias-Lopez, J. 2018. Metatranscriptome of the Oral Microbiome in Health and Disease. *Journal of Dental Research*, p. 002203451876164.

Standar, K., Kreikemeyer, B., Redanz, S., Münter, W., Laue, M. and Podbielski, A. 2010. Setup of an *In vitro* Test System for Basic Studies on Biofilm Behavior of Mixed-Species Cultures with Dental and Periodontal Pathogens. *PLoS ONE* 5(10).

Subramani, K., Jung, R.E., Molenberg, A. and Hammerle, C.H. 2009. Biofilm on dental implants: a review of the literature. *The International journal of oral & maxillofacial implants* 24(4), pp. 616–26.

Sunde, P., Olsen, I., Göbel, U., Theegarten, D., Winter, S., Debelian, G., Tronstad, L. and Moter, A. 2003. Fluorescence *in situ* hybridization (FISH) for direct visualization of bacteria in periapical lesions of asymptomatic root-filled teeth. *Microbiology* 149(5), pp. 1095–1102.

Svendsen, I.E. and Lindh, L. 2009. The composition of enamel salivary films is different from the ones formed on dental materials. *Biofouling* 25(3), pp. 255–61.

Takeshita, T., Yasui, M., Shibata, Y., Furuta, M., Saeki, Y., Eshima, N. and Yamashita, Y. 2015. Dental plaque development on a hydroxyapatite disk in young adults observed by using a barcoded pyrosequencing approach. *Scientific reports* 5, p. 8136.

Tian, Y., He, X., Torralba, M., Yooseph, S., Nelson, K.E., Lux, R., McLean, J.S., Yu, G. and Shi, W. 2010. Using DGGE profiling to develop a novel culture medium suitable for oral microbial communities. *Molecular Oral Microbiology* 25(5), pp. 357–367.

Veerachamy, S., Yarlagadda, T., Manivasagam, G. and Yarlagadda, P.K. 2014. Bacterial adherence and biofilm formation on medical implants: A review. *Proceedings of the Institution of Mechanical Engineers, Part H: Journal of Engineering in Medicine* 228(10), pp. 1083–1099.

Veitz-Keenan, A. and Keenan, J. 2017. Implant outcomes poorer in patients with history of periodontal disease. *Evidence-Based Dentistry* 18(1), pp. 5–5.

Volchansky, A. and Cleaton-Jones, P. 1994. Variations in oral temperature. *Journal of Oral Rehabilitation* 21(5), pp. 605–611.

De Waal, Y., Winkel, E., Meijer, H., Raghoebar, G. and van Winkelhoff, A. 2014. Differences in Peri-Implant Microflora Between Fully and Partially Edentulous Patients: A Systematic Review. *Journal of Periodontology* 85(1), p. 6882.

Walker, C. and Sedlacek, M.J. 2007. An *in vitro* biofilm model of subgingival plaque. *Oral Microbiology and Immunology* 22(3), pp. 152–161.

Wang, Q., Garrity, G., Tiedje, J. and Cole, J. 2007. Naïve Bayesian Classifier for Rapid Assignment of rRNA Sequences into the New Bacterial Taxonomy. *Applied and Environmental Microbiology* 73(16), pp. 5261–5267.

Watanabe, K., Kodama, Y. and Harayama, S. 2001. Design and evaluation of PCR primers to amplify bacterial 16S ribosomal DNA fragments used for community fingerprinting. *Journal of Microbiological Methods* 44(3), pp. 253–262.

Watnick, P. and Kolter, R. 2000. Biofilm, city of microbes. *Journal of bacteriology* 182(10), pp. 2675–9.

Whittaker, R.H. 1972. Evolution and Measurement of Species Diversity. *Taxon* 21(2/3), pp. 213 – 251.

Whittaker, R.H. 1960. Vegetation of the Siskiyou Mountains, Oregon and California. *Ecological Monographs* 30(3), pp. 279 – 338.

Zarco, M.F., Vess, T.J. and Ginsburg, G.S. 2012. The oral microbiome in health and disease and the potential impact on personalized dental medicine. *Oral Diseases* 18(2), pp. 109–120.

Zaura, E., Keijser, B., Huse, S. and Crielaard, W. 2009. Defining the healthy 'core microbiome' of oral microbial communities. *BMC Microbiology* 9(1), p. 259.

Zhou, Y., Gao, H., Mihindukulasuriya, K., Rosa, P., Wylie, K., Vishnivetskaya, T., Podar, M., Warner, B., Tarr, P., Nelson, D., Fortenberry, D., Holland, M., Burr, S., Shannon, W., Sodergren, E. and Weinstock, G. 2013. Biogeography of the ecosystems of the healthy human body. *Genome Biology* 14(1), p. R1.

Zijnge, V., van Leeuwen, B., Degener, J., Abbas, F., Thurnheer, T., Gmür, R. and Harmsen, H. 2010. Oral biofilm architecture on natural teeth. *PloS one* 5(2), p. e9321.

Øgaard, B. 2008. White Spot Lesions During Orthodontic Treatment: Mechanisms and Fluoride Preventive Aspects. *Seminars in Orthodontics* 14(3), pp. 183–193.

7. Appendix

7.1. Disclosures

Data for this thesis was published in the original articles 1 and 2 below.

1. **Klug, B., Rodler, C., Koller, M., Wimmer, G., Kessler, H.H., Grube, M. and Santigli, E.** 2011. Oral biofilm analysis of palatal expanders by fluorescence *in-situ* hybridization and confocal laser scanning microscopy. Journal of visualized experiments (56).
2. **Klug, B., Santigli, E., Westendorf, C., Tangl, S., Wimmer, G. and Grube, M**. 2016. From Mouth to Model: Combining *in vivo* and *in vitro* Oral Biofilm Growth. Frontiers in microbiology 7, p. 1448.

Article 2 was also published in the book: Moissl-Eichinger, C., Berg, G., Grube, M., eds. (2018). Microbiome Interplay and Control. Lausanne: Frontiers Media. doi: 10.3389/978-2-88945-505-8

The Co-authors in these publications were:

1. Univ.-Ass. Mag.phil. Dr.med.dent. Dr.med.univ. **Elisabeth Santigli**. Department of Dental Medicine and Oral Health, Division of Oral Surgery and Orthodontics, Medical University of Graz, Graz, Austria
2. Dr. **Christian Westendorf**. Institute of Plant Sciences, University of Graz, Graz, Austria
3. Mag.rer.nat. **Stefan Tangl**. Karl Donath Laboratory for Hard Tissue and Biomaterial Research, Department of Oral Surgery, Medical University of Vienna, Vienna, Austria
   and Austrian Cluster for Tissue Regeneration, Vienna, Austria
4. Univ.-Ass. Priv.-Doz. Dr.med.univ. **Gernot Wimmer**. Department of Dental Medicine and Oral Health, Division of Preventive and Operative Dentistry, Periodontology, Prosthodontics and Restorative Dentistry, Medical University of Graz, Graz, Austria
5. Univ.-Prof. Mag. Dr.rer.nat. **Martin Grube**. Institute of Plant Sciences, University of Graz, Graz, Austria
6. Sen.Lecturer Dr.med.dent. **Martin Koller**. Department of Prosthodontics, Restorative Dentistry, Periodontology and Implantology, Medical University of Graz

7. Dr.med.dent. **Claudia Rodler**. Department of Orthodontics and Maxillofacial Orthopedics, Medical University of Graz.
8. Univ.-Prof. Dr.med.univ. **Harald H. Kessler**. Institute of Hygiene, Microbiology and Environmental Medicine, Medical University of Graz, Graz

All co-authors were contacted for their permission to use the data in this thesis. They all agreed to the use in written statements that were sent to the organizational unit study management of the Medical University of Graz.
The further publications listed were published during the time this thesis was made with my contribution. Their context is related to and methods partially used in this thesis. Respective sections are cited throughout the text.

1. Santigli, E., Leitner, E., Wimmer, G., Kessler, H., Feierl, G., Grube, M., Eberhard, K. and Klug, B. 2016. Accuracy of commercial kits and published primer pairs for the detection of periodontopathogens. Clinical Oral Investigations 20(9), pp. 2515–2528.

2. Santigli, E., Trajanoski, S., Eberhard, K. and Klug, B. 2017. Sampling Modification Effects in the Subgingival Microbiome Profile of Healthy Children. Frontiers in Microbiology 7.

3. Santigli, E., Koller, M., Klug, B. 2017. Oral Biofilm Sampling for Microbiome Analysis in Healthy Children. J. Vis. Exp. (130), e56320, doi:10.3791/56320

7.2. Copyright statements

In the following copyright statements of all journals which contained figures reused in this thesis are listed:

1) *Copyright © 2016 Klug, Santigli, Westendorf, Tangl, Wimmer and Grube. This is an open-access article distributed under the terms of the Creative Commons Attribution License (CC BY). The use, distribution or reproduction in other forums is permitted, provided the original author (s) or licensor are credited and that the original publication in this journal is cited, in*

accordance with accepted academic practice. No use, distribution or reproduction is permitted which does not comply with these terms.

(Citation: Klug B, Santigli E, Westendorf C, Tangl S, Wimmer G and Grube M (2016) From Mouth to Model: Combining *in vivo* and *in vitro* Oral Biofilm Growth. Front. Microbiol. 7:1448. doi: 10.3389/fmicb.2016.01448.).

2) Copyright © 2017 Santigli, Trajanoski, Eberhard and Klug. This is an open-access article distributed under the terms of the Creative Commons Attribution License (CC BY). The use, distribution or reproduction in other forums is permitted, provided the original author (s) or licensor are credited and that the original publication in this journal is cited, in accordance with accepted academic practice. No use, distribution or reproduction is permitted which does not comply with these terms.

(Citation: Santigli E, Trajanoski S, Eberhard K and Klug B (2017) Sampling Modification Effects in the Subgingival Microbiome Profile of Healthy Children. *Front. Microbiol*. 7:2142. doi: 10.3389/fmicb.2016.02142

3) Statement for JoVE

Dear Barbara,

You have our permission to use the images from your JoVE article "Klug, B., Rodler, C., Koller, M., Wimmer, G., Kessler, H. H., Grube, M., et al. Oral Biofilm Analysis of Palatal Expanders by Fluorescence In-Situ Hybridization and Confocal Laser Scanning Microscopy. J. Vis. Exp. (56), e2967, doi:10.3791/2967 (2011)" in your thesis as requested.

Please be sure to cite the article accordingly and consider this email as approval. Do not hesitate to email me with any other questions and have a great day.

Best Regards,

Alycia

Alycia Bittner, PhD

Manager of Journal Writing & Review

JoVE

617.674.1401 Ext. 204|Fax 1.866.381.2236

Follow us: Facebook | Twitter | LinkedIn

About JoVE

4) Statement for the reuse of Figure 1

This Agreement between Barbara Klug ("You") and Elsevier ("Elsevier") consists of your license details and the terms and conditions provided by Elsevier and Copyright Clearance Center.

License Number 4442380597947

License date Oct 05, 2018

Licensed Content Publisher Elsevier

Licensed Content Publication Journal of Molecular Biology

Licensed Content Title Intermicrobial Interactions as a Driver for Community Composition and Stratification of Oral Biofilms

Licensed Content Author Nicholas S. Jakubovics

Licensed Content Date Nov 20, 2015

Licensed Content Volume 427

Licensed Content Issue 23

Licensed Content Pages 14

Start Page 3662

End Page 3675

Type of Use reuse in a thesis/dissertation

Portion figures/tables/illustrations

Number of figures/tables/illustrations 2

Format both print and electronic

Are you the author of this Elsevier article? No

Will you be translating? No

Original figure numbers Figure 2

Title of your thesis/dissertation "Molecular analysis of oral biofilm"

Expected completion date Jan 2019

Estimated size (number of pages) 150